NTNU – Trondheim
Norwegian University of
Science and Technology

Reactive Power and Voltage Control of Offshore Wind Farms

Anders Jerkø

Master of Energy and Environmental Engineering
Submission date: June 2014
Supervisor: Kjetil Uhlen, ELKRAFT

Norwegian University of Science and Technology
Department of Electric Power Engineering

Problem Description

The number of offshore wind farms is increasing, both in Norway and the rest of Europe. Transmitting the produced power from these wind farms is a challenge, due to large reactive power production in the cables for long distances. The regulations published by the Transmission System Operator (TSO), which define grid codes with requirements concerning reactive power compensation and voltage regulations for new wind power installations, have to be followed.

The main objective of this Master's thesis is to evaluate some of the challenges concerning the use of HVAC transmission from an offshore wind farm to shore. The main focus will be on reactive power and voltage control.

By utilising the simulation tool DIgSILENT© PowerFactory, a model will be made to investigate different reactive power compensation possibilities. Various design criteria will be incorporated in the model, including the location of the reactive compensation devices, the coordination between load tap changers and a static var compensator, and loss reduction by applying an SVC in the system.

Preface

This Master's thesis is written in coordination with Statkraft at the Department of Electric Power Engineering as the final part of the 5th year Master of Science program at the Norwegian University of Science and Technology. The Master's thesis is a continuation of the project specialisation thesis, written autumn 2013, which contained static analysis of the same objective.

Offshore wind power has been a subject of great interest to me, making it easy to stay motivated during the work on this thesis.

Many people have helped me with the Master's thesis. First of all, I would like to thank my supervisor, Professor Kjetil Uhlen, for his advice and guidance, and Jarle Eek for making an interesting topic for me to investigate. I appreciate the assistance from my co-supervisor, PhD student Traian Nicolae Preda, who has helped me a lot with his expertise in the simulation software DIgSILENT© PowerFactory. Gratitude is also extended to Professor Olimpo Anaya-Lara for his help in the start-up period and to Vegard Bekkeseth for general guidance in PowerFactory during the work on the specialisation thesis. Finally I acknowledge several professors at NTNU for giving me the technical background necessary to write this Master's thesis.

I would also like to extend a special thanks to my class mates, especially Sondre Heen Brovold and Jørn Frøysa Hole, my girlfriend Emma Woldseth Brørs, and my sister Marte Jerkø, for their help, support and many laughs.

Trondheim, June 2014

Anders Jerkø

Abstract

There are several challenges related to reactive power and voltage control of HVAC transmission from offshore wind farms to the main grid, which need to be addressed when designing wind farms. One challenge is the variation of wind speeds and thereby also power production, which can make it difficult to operate the system within the grid code requirements. This Master's thesis focuses on finding beneficial operating strategies to solve these challenges. Various locations of a static var compensator (SVC) are tested in addition to local regulation on the turbines through voltage source converters (VSCs).

To investigate different operational strategies, a simulation model of a system connecting an offshore wind farm to the main grid has been developed in DIgSILENT© PowerFactory. A comprehensive examination of the behaviour of the dynamic voltage control devices has been performed to ensure the desired functionality of the model. Two different approaches for controlling the output of the wind farm have been examined; P-Q operation controls the active and reactive power output, whilst P-V control mode determines the active power and the voltage at the connected node. For these two scenarios, a static var compensator has been implemented on both sides of the transmission cables. Coordination between load tap changers (LTCs) and the static var compensator has been examined, and the active power losses for operating the system with an SVC offshore have been estimated.

Simulation results show that the most beneficial operational strategy for the wind farm in both P-Q and P-V control mode is to use an SVC located offshore. This operational strategy provides better voltage control and lower cable currents than the other analysed system structures. Thus, a longer distance to shore is possible without exceeding maximum cable currents. Cable losses are also lower with the SVC implemented offshore. The SVC was barely affected by the taps from LTCs, and coordination issues between these two dynamic components can be considered negligible.

Sammendrag

Det er mange utfordringer knyttet til reaktiv effektkompensering og spenningsregulering av HVAC-overføring fra vindparker til sentralnettet som må tas hensyn til når vindparker designes. En av utfordringene er variasjon i vindhastigheter og dermed også kraftproduksjon. Dette kan føre til problemer med å drifte systemet innenfor reguleringene gitt i såkalte grid codes. I denne masteroppgaven er hovedfokuset å finne de beste driftsstrategiene for å løse de nevnte utfordringene ved å kontrollere spenningene i systemet med en static var compensator (SVC) på forskjellige steder med lokal regulering i vindturbinene gjennom voltage source converters (VSCs).

For å undersøke forskjellige driftsstrategier har en simuleringsmodell av et system som kobler en offshore vindpark til sentralnettet blitt utviklet i DIgSILENT© PowerFactory. En omfattende analyse av de dynamiske spenningsregulerende komponentenes atferd har blitt utført for å bekrefte ønsket modellfunksjonalitet. To forskjellige tilnærminger til drift av vindparken har blitt sett på for å analysere ulike driftssituasjoner. P-Q-drift kontrollerer aktiv og reaktiv effekt, mens P-V-kontroll fastsetter den aktive effekten og spenningen ved den tilkoblede noden. For disse to scenarioene har en static var compensator blitt implementert både på onshore- og offshoresiden av overføringskablene. Eventuelle koordinasjonsproblemer mellom LTCene og SVCen har blitt analysert. I tillegg har aktivt effekttap ved å benytte en SVC offshore, sammenlignet med ikke å ha noen spenningsregulerende komponenter, blitt estimert.

Konklusjonen er at den beste driftsstrategien for vindparken både i P-Q- og P-V-modus kan oppnås med en SVC plassert offshore. Denne driftssituasjonen bidrar til bedre spenningskontroll og lavere kabelstrøm enn de andre scenarioene som har blitt analysert. Dette fører til at er lengre kabellengder mulig uten å overgå maksimumsgrensen for kabelstrømmen. De aktive tapene i kablene ble også lavere med SVCen offshore. Koordinasjonsproblemer mellom SVCen og LTCene ble konkludert med å være neglisjerbare.

Table of Contents

List of Figures

List of Tables

Nomenclature

Parameter	Explanation
ϕ	Phase angle
z	Impedance
r	Resistance
x	Reactance
g	Shunt conductance
L	Inductance
C	Capacitance
l	Length
y	Shunt admittance
γ	Propagation constant
δ	Voltage angle
I_C	Charging current
L_C	Critical length
Z_C	Characteristic impedance
V_n	Rated voltage
P_{SIL}	Surge impedance load
S	Apparent power
Q	Reactive power
V	Voltage
I	Current
T_{A+}, T_{A-}	Transistors
D_{A+}, D_{A-}	Diodes
i_0	AC current
V_d	Input DC voltage
$v_{control}$	Sinusoidal control signal given by the PWM
v_{tri}	Triangular control signal given by the PWM
V_{A0}	Line-to-midpoint voltage for phase A
$\tilde{V}$	Peak voltage amplitudes
f_s	Synchronous frequency
m_a	Modulation ratio
ω	Pulsation, equal to 2πf
V_{phase}	Single phase voltage
V_{DC}	DC voltage
Q_{cap}	Reactive capability
S_n	Nominal power
E	Generated voltage of the VSC
V	Line voltage of the transmission line
X	Reactance
U	Applied voltage
N	Number of electrical turns
B_{max}	Maximum susceptance value
e_S, e_P	Induced voltage on, respectively, secondary and primary side
N_P, N_S	Number of coils on, respectively, secondary and primary side
E_k	Kinetic energy
m	Mass
v	Air velocity
$\dot{m}$	Mass flux

Nomenclature

Parameter	Explanation
ρ	Air density
A	Rotor swept area
C_p	Power coefficient
ω	Angular speed
λ	Tip speed ratio
n	Synchronous speed
f	Frequency
P	Number of poles
$\overline{P_w}$	Average wind turbine power
$P_W(U)$	Power output compared to wind speed
$p(U)$	Probability density function of U
n	Number of observations
σ_U	Standard deviation
G	Skewness
$F(U)$	Cumulative distribution function
ρ	Resistivity of conducting material
k	Shape parameter
c	Scale parameter
k	Temperature coefficient
S_{SC}	Short circuit power level
S_r	Rated turbine power level
I_{SC}	Short circuit current
r_{SC}	Short circuit resistance
t	Time in seconds
U_B	Desired voltage level
ΔU	Allowed voltage level
T	Time delay
V_C, R_C, X_C	Compensator voltage, resistance and reactance
$\tilde{V}$, $\tilde{I}$	Measured phasor voltage and current at the transformer secondary side
R_{base}	Rated reactive power of the SVC
K	Proportional gain
Γ	Gamma function
I_B, V_B, S_B, Z_B	Base quantities of current, voltage, apparent power and impedance
Z_Ω	Impedance with the unit Ω
P_{ij}, Q_{ij}	Active and reactive power flowing from bus i to bus j
R_{ij}	Resistance between bus i and bus j
$P_{loss,\ ij}$	Active power losses on the line between bus i and bus j
ϑ	Admittance angle
J	Jacobian matrix
P_{spec}, Q_{spec}	Initial values for active and reactive power
i_d	Current, direct axis
i_q	Current, quadratic axis
i_0	Current, zero sequence
i_a, i_b, i_c	Currents in phase a, b and c, respectively

Chapter 1

1 Introduction

1.1 Motivation

Generating enough energy to sustain the increasing global population, while simultaneously minimizing environmental impacts associated with energy extraction and consumption is a global concern of great importance. Wind power is a renewable energy source which could help ameliorate these concerns, and today the number of installed wind power turbines in the world is increasing rapidly [1]. Wind power has been utilised for a long period of time, but thus far mostly onshore. There are, however, several reasons for installing wind power farms offshore instead of onshore. Firstly, the wind out in the ocean usually has a more consistent and high wind speed because of the lack of obstacles stopping the wind. Secondly, wind power offshore does not affect the local areas in the same way as onshore wind does since the visibility and noise issues can be avoided [2].

The technical perspectives of producing offshore wind power are more complex than for onshore wind power production. Offshore wind power is still in the development stage and there are countless different strategies and philosophies for how offshore wind farms should be designed.

In a power system, almost all equipment used is designed for a rated voltage. Deviations from the rated voltage level can cause reduced performance and shorter life expectancy for the components. By controlling the voltages in the grid, these issues can be avoided. The reactive power flow in the system is dependent on the voltage and vice versa. By controlling the voltage, the reactive power flows can be controlled and the losses caused by reactive power flows can be reduced [3].

1.2 Research Objective

In this Master's thesis, some of the challenges with respect to the integration of offshore wind power into the main grid is discussed and shown using the simulation software DIgSILENT© PowerFactory. In offshore systems, the distance from the production units to shore is usually large, which causes issues with the transmission of active power due to losses and reactive power flows circulating in the cables. Long AC cables produce a substantial amount of reactive power which contributes to less active power transmitted. An important part of this thesis is to determine when reactive power compensation is necessary and to review possible scenarios for power transmission from the wind power production units. The variability in wind velocities makes it difficult to forecast the production and the transmission system needs to be able to handle these challenges.

In the simulations performed in this thesis, HVAC transmission is chosen. The motivation behind this choice is to review how new technologies using power electronics can improve the results using a well-explored and widespread technology such as HVAC transmission. The distance between the offshore wind park and shore is crucial for the power transmission, which will be examined. A lot of research has been performed on offshore wind power transmission earlier. However, there are many unanswered questions regarding coordination of several control devices to determine the most beneficial operational strategies for specific model designs.

The main objective is to build a model in PowerFactory to determine the effect of applying an SVC in the system. The SVC will be tested both offshore and onshore to determine the most beneficial solution. The annual production and active power losses for a given scenario will be analysed both with and without the SVC to establish the gain of utilising an SVC in the system. The voltage source converters in the turbines will be tested in different control modes, and transformer tap changers will be added to examine their contributions to the system. Dynamic simulations for coordination between load tap changers and a static var compensator will be performed to analyse their interactions.

1.3 Report Outline

A brief introduction of the structure of this report is presented to provide an overview of the contents to the reader.

Chapter 2, 3 and 4 provides the theoretical background to the thesis. Chapter 2 explains HVAC cable transmission and reactive power and voltage control, while Chapter 3 describes the fundamentals of wind power and wind power statistics. Chapter 4 presents the regulations and framework of a functional operation of the electric system, given in grid codes published by Statnett and ENTSO-E.

In Chapter 5 and 6 the methodology used is described. Chapter 5 presents a description of the simulation software PowerFactory, and an overview of the model design is given in Chapter 6.

The results obtained by the simulations are presented in Chapter 7. Chapter 8 discusses the results and general problems within the scope of the thesis. In Chapter 9, the conclusions are presented. Ideas for further development of the topic and the simulation model are exposed in Chapter 10.

An extensive number of scenarios performed leads to a lengthy report.

Chapter 2

2 Reactive Power and Voltage Control

An introduction to the theoretical basis for HVAC transmission, reactive power, voltage control devices and transformers will be presented in this section.

2.1 HVAC Transmission Technology

High voltage alternating current (HVAC) cable transmission is the most used transmission technology in the power system today for offshore and submarine applications. This technology is straight forward, and some of the advantages of using HVAC transmission is the ease of interconnection, installation, maintenance, operational reliability and cost effectiveness [4].

2.1.1 Overhead lines

A transmission power line is divided into several components and it is a complex system whose goal is to transmit the produced power to the load demanding consumers. The distributed parameters in Equation 2.1 and 2.2 determine the basis of the line. z is the series impedance and y is the shunt admittance of the line per unit length per phase. In these equations r is the series resistance, L is the series inductance, g is the shunt conductance and C is the shunt capacitance [5] [6].

$$z = r + j\omega L \quad (2.1)$$

$$y = g + j\omega C \quad (2.2)$$

The parameters $x_L = \omega L$ and $b = \omega C$ represent the reactance and the susceptance of the line, respectively. For series parameters, the resistance r represents the heating loss and L is dependent on the partial flux-linkages within the one conductor and between the conductors. The shunt conductance g represents corona loss and the leakage currents on the insulators. The capacitance C is a product of the potential difference between the lines. The following figure shows a simplified equivalent circuit of a power line.

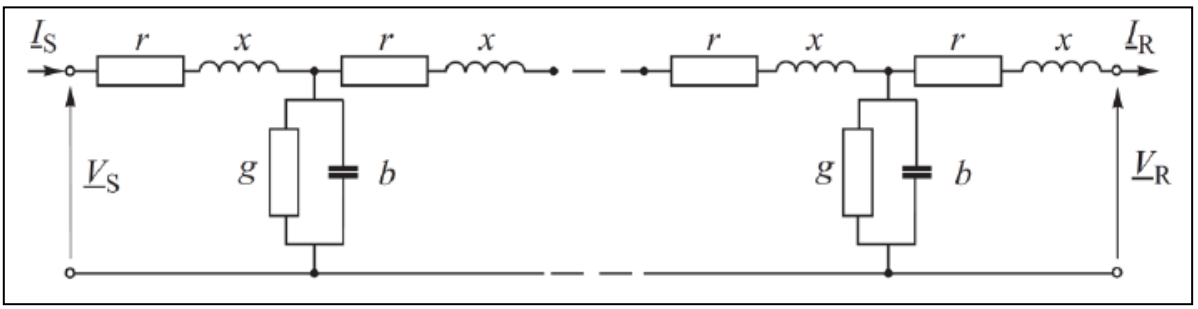

Figure 1: Single-phase equivalent circuit of a transmission line with distributed parameters [6].

The equations can be solved by different methods considering the length of the line. If the line is short, the charging current and the capacitance C may be neglected. Equation 2.3 and 2.4 show the set of equations used to calculate the voltages and currents of a long line, where S stands for sending end and R is the receiving end.

$$V_S = cosh\gamma l * V_R + Z_C sinh\gamma l * I_R \quad 2.3$$

$$I_s = \frac{sinh\gamma l}{Z_C} * V_R + cosh\gamma l * I_R \quad 2.4$$

In this set of equation, the propagation constant γ is equal to $\sqrt{zy}$ and Z_C, which is the characteristic impedance of the line, given in Equation 2.9 and 2.10.

The real and reactive power transmission can be derived from a full π-equivalent model of the line or cable in focus. Equation 2.5 gives the active power transmission.

$$P_R = \frac{V_S V_R}{X} sin\delta_{SR} \quad 2.5$$

In the previous equation, V_S and V_R are the voltages in two nodes, δ is the angle between their phasors, X is the total inductive reactance between the nodes and P is the active power flowing.

If one considers a simplified line model where δ_{SR} is kept small, implying that $\cos(\delta_{SR})\approx 1$, and thus the active power $P_R=0$, the reactive power transmission can be expressed by the following equation:

$$Q_R = \frac{V_R(V_S - V_R)}{X} \quad 2.6$$

2.1.2 Cable systems

The main difference between cables and transmission lines are the different parameter values for the series impedance and shunt admittance. In cables, the conductors are closer to each other and they are surrounded by metallic screens, which combined gives a higher shunt susceptance than in transmission lines [5]. Thus, charging currents in the AC cables arise, and the maximum distance of transmission has a limit. When the cable length increases, the capacitance (causing production of reactive power) increases and compensation is necessary.

The charging current is calculated using the following equation:

$$I_C = \omega C U \cdot 10^{-6} \text{ [A/km]} \quad 2.7$$

I_C = Charging current (A/km)
ω = 2πf, f=system frequency[Hz]
C = Capacitance per unit length (μF/km)
U = Applied voltage

The charging currents generate heat losses in cables. This can be a problem, especially in long cables, since the capacitance and charging current increases linearly with the length of the cables. The "critical length" is the length of a cable at which its thermal capacity is consumed by charging current and it is calculated as follows [7]:

$$L_C = \frac{I\sqrt{3}}{\omega C U} 10^3 km \qquad 2.8$$

U = Line (phase to phase) voltage (kV)
I = Phase current (A)

Cross-linked polyethylene (XLPE) is the most common elastomer used as solid insulation for cables in a medium voltage range. These cables are suitable for high service temperatures and can carry a higher current density than most other types of cables. Conventional polyethylene cables are more sensitive to cold flow and abrasion than the XLPE. The breakdown strength is high and has a low relative permittivity. One disadvantage of using XLPE cables is that the ageing process happens quickly when exposed to light and oxygen, causing loss of strength, elongation and tear resistance [8]. In the PowerFactory model used for this thesis, data for XLPE submarine cable systems has been used.

To avoid problems with water treeing in the insulation material, the subsea cables have a lead sheath layer around the XLPE. Figure 2 illustrates an XLPE cable.

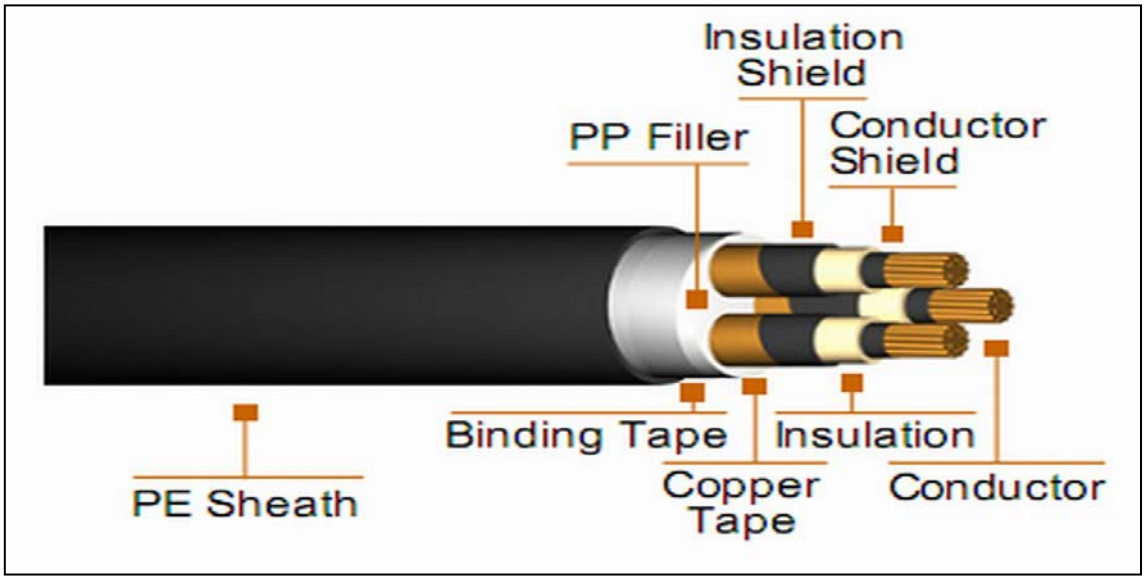

Figure 2: Illustration of a three-phase HVAC subsea cable [9].

2.1.3 Surge impedance loading

Surge Impedance Load (SIL) or natural load is defined as the power delivered at rated voltage to load impedance equal to Z_C. Z_C is the characteristic impedance and it is purely resistive. Neglecting g while $r \ll x$ gives [6]:

$$Z_C = \sqrt{\frac{z}{y}} = \sqrt{\frac{r + j\omega L}{j\omega C}} \tag{2.9}$$

If the line is considered to be lossless, the characteristic impedance will become:

$$Z_C = \sqrt{\frac{L}{C}} \tag{2.10}$$

Knowing the characteristic impedance, the surge impedance load can be expressed as:

$$P_{SIL} = SIL = \frac{V_n^2}{Z_C} \tag{2.11}$$

Where V_n is the rated voltage of the line or cable. If the power in the receiving end P_R is equal to P_{SIL}, the reactive losses are zero and the natural impedance loading is in an optimal condition with respect to voltage and reactive power control. When $P_R > P_{SIL}$, the line or cable is acting inductive and absorbs reactive power. When $P_R < P_{SIL}$, the line or cable is acting capacitive and produces reactive power [10].

A cable acts in a different way than a transmission line with respect to the Surge Impedance Load. Since the cable produces reactive power and the transmission line usually absorbs reactive power (Table 1), the SIL will be much higher for a cable than a transmission line at the same rated voltage. Dependent on the distance and the length of the line, an electrical cable will usually not be able to transfer power equal to P_{SIL} because of thermal and stability limits in the cable [11].

2.2 Reactive Power

Electrical energy is usually generated, transmitted and used as alternating current. One of the disadvantages when using AC is the reactive power flowing in the line together with the active power. Apparent power in the AC system consists of two parts, one active and one reactive part. Most of the components in the power system are either producing or consuming reactive power. To minimise the losses, it is preferable not to transfer the reactive power, so reactive compensating devices are important. The power factor limits for lagging and leading current for wind farms are presented under regulations for reactive power in FIKS given in the grid code requirements in Section 4.1.

Reactive power for an alternating power circuit with a sinusoidal current is equal to the product of the magnitude of the current, voltage and sinus of the phase difference between current and voltage. Reactive power cannot do any work. It is being measured in the unit VAr, which is short for Volt-Ampere-reactive, with the same dimension as Watt [12]. The definition of reactive power is a flow of stored energy into a circuit which is deduced from the stored energy cycle [13]. The apparent power is given in Equation 2.12.

$$|S| = |U| * |I| = \sqrt{P^2 + Q^2} \text{ [VA]} \qquad 2.12$$

Apparent power is the magnitude of the complex power [14]. The complex power is defined as [15]:

$$\underline{S} = \underline{U} * \underline{I}^* = \underline{P} + j\underline{Q} \text{ [VA]} \qquad 2.13$$

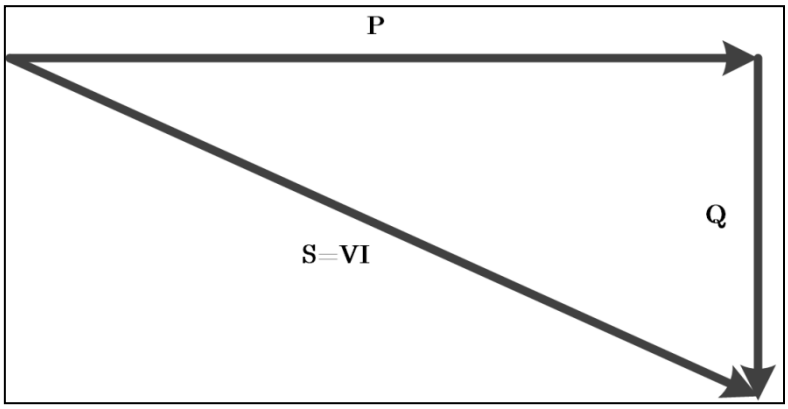

Figure 3: Vector diagram of active, reactive and apparent power.

Reactive power (Q) for a single base circuit is given by Equation 2.14.

$$Q = U * I * \sin\phi \text{ [VAr]} \qquad 2.14$$

The reactive power is dependent on the angle between the sinus curve of the voltage and the sinus curve of the current. For capacitive loads, reactive power is produced and the current leads the voltage. If the current lags the voltage, reactive power is consumed and the load is inductive [16]. Table 1 presents an overview of the reactive power impacts on the system for different components.

Table 1: Production and absorption in different electrical components [16].

Component	Production	Absorption
Synchronous generator	X (Over excited)	X (Under excited)
Overhead lines	X (Low load)	X (High load)
Cables	X	
Transformers		X
Loads		X (Usually)
Harmonic filters	X	
Variable speed drives	(X)	X (Line commutation)
Compensating devices	X	X

If the component produces reactive power, inductive compensation could improve the system abilities, while capacitive compensation might be needed if the component absorbs reactive power. To achieve this, Flexible AC Transmission Systems can be applied [17].

In offshore grids, subsea cables are used for electricity transportation. These cables produce reactive power, so voltage control is necessary. Production of reactive power increases the voltage, and inductive compensation is therefore needed to reduce the voltage to acceptable levels.

2.3 Voltage Control

2.3.1 FACTS devices

FACTS is an acronym for Flexible AC Transmission Systems. FACTS devices are power electronic devices which aim to enhance the performance of the AC transmission and are excellent in improving the stability and voltage quality of the system. The aim of using FACTS is to be able to supply reactive power to the network as quickly as possible utilising inductive or capacitive reactive power compensation specially adapted to particular requirements [18]. FACTS should have the ability to impact the system performance of the load flow, stability and voltage quality. There are several different devices under the collective term FACTS, as can be seen in Figure 4:

Principle	Devices	Scheme	Impact on System Performance		
			Load Flow	Stability	Voltage Quality
Variation of the Line Impedance: Series Compensation	FSC (Fixed Series Compensation)	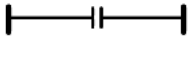	●	● ● ●	●
	TPSC (Thryristor Protected Series Compensation)	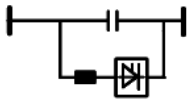	●	● ● ●	●
	TCSC (Thyristor Controlled Series Compensation)		● ●	● ● ●	●
Voltage Control: Shunt Compensation	SVC (Static Var Compensator)	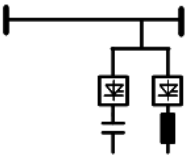	○	● ●	● ● ●
	STATCOM (Static Synchronous Compensator)		○	● ●	● ● ●
Load-Flow Control	HVDC (B2B, LDT)	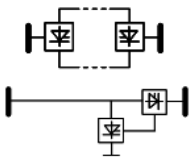	● ● ●	● ● ●	● ●
	UPFC (Unified Power Flow Controller)		● ● ●	● ● ●	● ● ●

Influence: *

○ low or no
● small
● ● medium
● ● ● strong

Figure 4: Overview of different FACTS devices [19].

FACTS can be divided into series compensation and shunt compensation. Series compensation is series connected capacitors that are inserted to compensate the line inductive reactance. The advantages of series capacitors are reductions in the transfer reactance and the effective reactive losses. It also increases the maximum transferred power for a given receiving end voltage. The simplest, most cost effective and common device used as a series compensator is the FSC – Fixed Series Compensation. The FSC provides an increase in transmission capacity and a reduction in the transmission angle for overhead lines. The Thyristor Protected Series Compensation (TPSC) and the Thyristor Controlled Series Compensation (TCSC) are both protected with a thyristor in parallel which closes if the voltage over the capacitor gets too large.

When it comes to shunt compensation, Static Var Compensators (SVCs) and Static Synchronous Compensators (STATCOMs) are the most used devices. Shunt compensators have both a reactor and a capacitor in parallel, which gives very good control abilities.

2.3.2 Wind turbine with voltage source converter

By using a wind turbine that is grid connected through a Voltage Source Converter (VSC), full control of both active and reactive power can be obtained. The basis of a VSC is a three-phase inverter with certain control mechanisms. Because the wind power production varies a lot, active and reactive power control is very important. An offshore wind turbine is usually connected to the grid through a full frequency converter. When the power capacity of the wind turbine increases, it is important to regulate the frequency and the voltage. Power electronics has been introduced as an intelligent interface between the offshore wind turbine and the grid [20]. By using pulse-width-modulation (PWM), the switching frequency can be controlled. The frequency converter is able to control the variable speed of the turbine rotor and has possibilities of controlling both the magnitude and the frequency of the sinusoidal AC curve [20].

The PWM converter (which is modelled in the simulations) shapes and controls sinusoidal three-phase output voltages in magnitude and frequency from a constant input DC voltage V_d. In this thesis, the wind farm is modelled as a DC source with a VSC transforming the DC system into a controlled AC system. In a real system, there will be a two-level voltage source converter in a back-to-back configuration which is the most frequently used three-phase converter for the range 1,5-3 MW installed capacity [21]. Through the VSC the current is transformed by PWM. A full bridge converter uses PWM to obtain the output AC voltage by switching the transistors. Figure 5 shows a one-leg switch-mode inverter, where i_0 is the AC-current, V_d is the input DC-voltage, T_{A+} and T_{A-} are the transistors and D_{A+} and D_{A-} are the diodes.

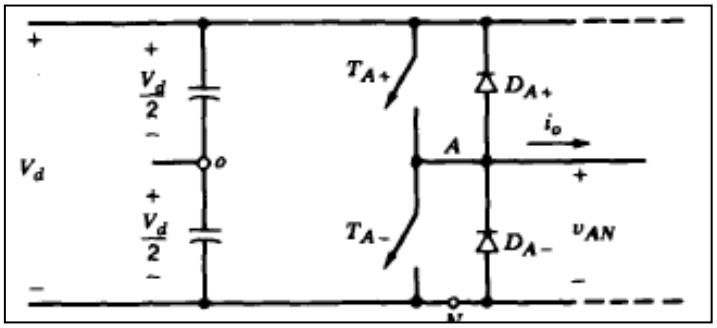

Figure 5: One-leg switch-mode inverter [20].

Switching angles are decided by a control signal given to the transistors. The control signal, $v_{control}$, is given by the PMW switching scheme and is compared to a triangular

control signal, v_{tri}, which decides the conducting transistors, either T_{A+} or T_{A-}. Equation 2.15 and 2.16 show the switching criteria for a given $v_{control}$.

$$v_{control} > v_{tri},\ T_{A+} \text{ is on},\ v_{AO} = \frac{1}{2}Vd \quad 2.15$$

$$v_{control} < v_{tri},\ T_{A-} \text{ is on},\ v_{AO} = -\frac{1}{2}Vd \quad 2.16$$

The control signal is given by Equation 2.17 and is a sinusoidal signal.

$$v_{control} = \tilde{V}_{control} \sin \omega_1 t \quad 2.17$$

Where

$$\tilde{V}_{control} \leq \tilde{V}_{tri} \quad 2.18$$

$\tilde{V}_{control}$ and $\tilde{V}_{tri}$ are the peak amplitudes of the control signal and triangular signal, respectively. $\tilde{V}_{tri}$ is generally utilised with a constant amplitude and frequency f_s [20]. The frequency f of the control signal is same as the desired value of the output signal of the converter.

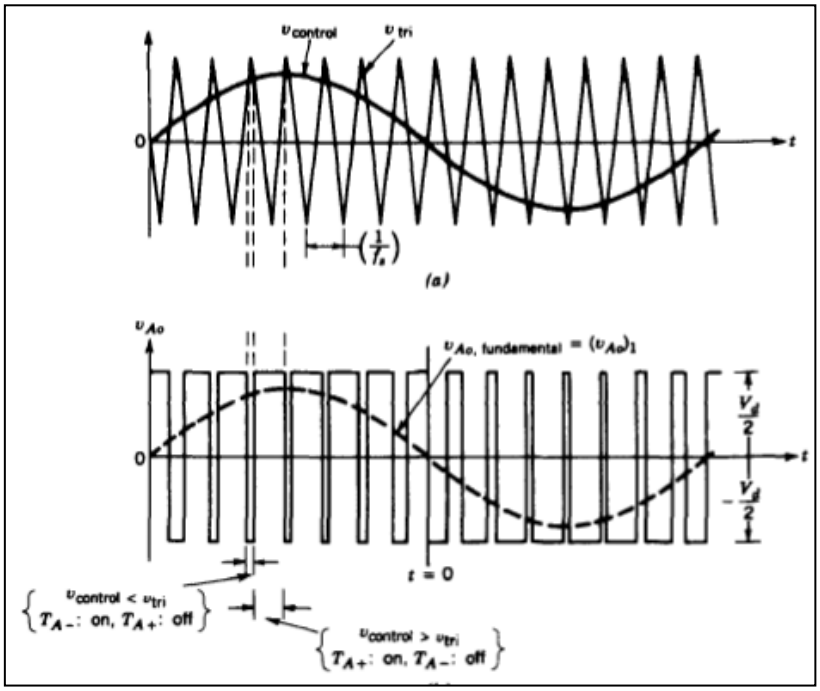

Figure 6: PWM with bipolar voltage switching [20].

Figure 6 shows the comparison between a control signal $v_{control}$ with the desired output frequency and a repetitive switching frequency triangular waveform, whose goal is to generate the switching signals [20]. V_{AO} is not a sinusoidal wave, so the fundamental component $v_{AO,1}$ needs to be filtered out [5]. Linear modulation is when $\tilde{V}_{control}$ is

smaller than $\tilde{V}_{tri}$. $\tilde{V}_{AO,1}$ will then be proportional to $\tilde{V}_{control}$. This is shown in equation 2.19, where m_a is the modulation ratio.

$$v_{AO,1} = \frac{\tilde{V}_{control}}{\tilde{V}_{tri}} \frac{V_d}{2} = m_a \frac{V_d}{2} \quad 2.19$$

The phase voltages will in the time domain be given by Equation 2.20.

$$V_{ph} = \frac{V_{DC} m_a \sin(\omega t)}{2} \quad 2.20$$

The voltage source converter consists of three phases where three of the half bridge single phase converters connected in parallel with sinusoidal modulation signals are 120° apart. The polarity of the DC voltage in the VSC is fixed for both rectifier and inverter mode, which gives the origin for the term "Voltage Source" [5]. A typical graphical presentation of a voltage source converter is illustrated in Figure 7.

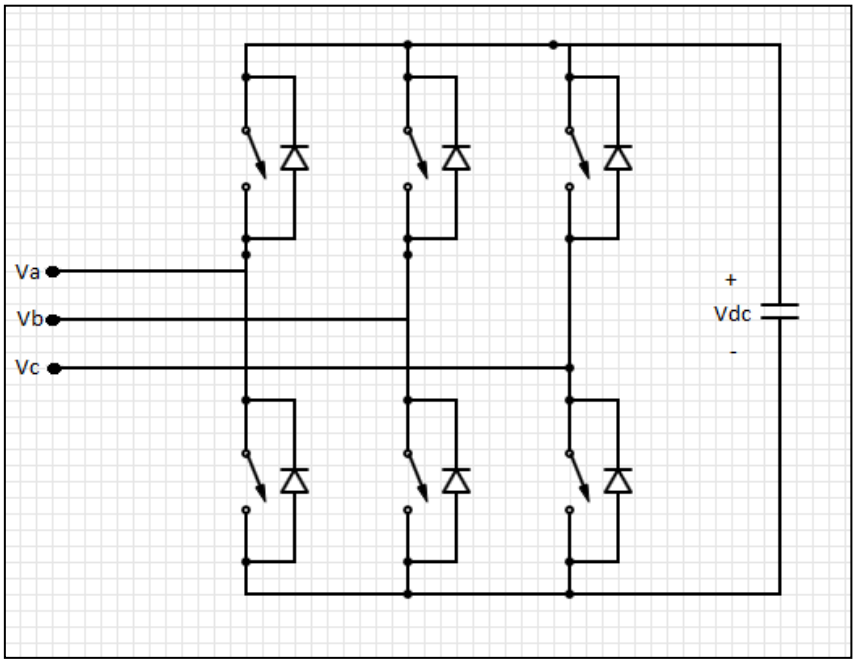

Figure 7: Voltage source converter.

The converter is designed for a maximum current. With a constant voltage, the i_{max} limit can be represented by the apparent power S_n. For a given production P and a given S_n, the reactive capability Q_{cap} can be expressed as:

$$Q_{cap} = \pm\sqrt{{S_n}^2 - P^2} \quad 2.21$$

By controlling the phase angle between the fundamental frequency generated by the converter and the line voltage of the transmission line, the active power flow between

the converter and the AC system can be controlled. Assuming a lossless reactor, the power transfer from the converter to the AC system is calculated by:

$$P = \frac{EV}{X} sin\delta \quad 2.22$$

The reactive power flow is the relative difference in magnitude between the converter and line voltages:

$$Q = \frac{V(Ecos\delta - V)}{X} \quad 2.23$$

Where E is the generated voltage of the VSC and V is the line voltage of the transmission line [22].

The model applied in the dynamic simulations supports several control conditions. The control conditions possible are given in Table 2 [23].

Table 2: Control conditions VSC.

Control conditions	Description of control abilities
V_{AC}-phi	Specifies magnitude and phase of AC terminal. Motor-side converters in variable speed applications are typical control modes.
V_{DC}-phi	Specifies DC-voltage and AC-voltage phase.
PWM-phi	PWM is directly set in magnitude and phase.
V_{DC}-Q	DC-voltage and reactive power is specified. Typical for STATCOM, UPFC and VSC-HVDC applications
V_{AC}-P	Specifies AC-voltage magnitude and active power. Equivalent to P-V characteristics of synchronous machines.
P-Q	Active and reactive power is specifies at the AC-side. Equivalent to P-Q characteristics of synchronous machines.

For the dynamic simulations performed in this thesis, the converter is set as V_{AC}-P and P-Q control conditions.

2.3.3 Static var compensator

The main components of the Static Var Compensator (SVC), also called Static Var Controller, are thyristors, capacitors and inductors. An SVC is a shunt connected FACTS device, which adjusts the voltage of a chosen bus by injecting inductive or capacitive current [24]. The SVC is constructed to automatically switch on or off the components to achieve optimal voltage in the system. The SVC consists of a Thyristor Switched Capacitor (TSC) in parallel with a Thyristor Controlled Reactor (TCR). The SVC eliminates problems like harmonics, voltage fluctuations, unbalanced loads and rapid change in reactive power in the system [17].

The thyristor switched capacitor consists of back-to-back thyristors and capacitors. This device consists of several units in parallel as shown in Figure 8. The currents can often be quite high, so the thyristors are usually connected in series with each capacitor. The current produced by the capacitor is given by Equation 2.24.

$$i = C\frac{dV}{dt} \qquad 2.24$$

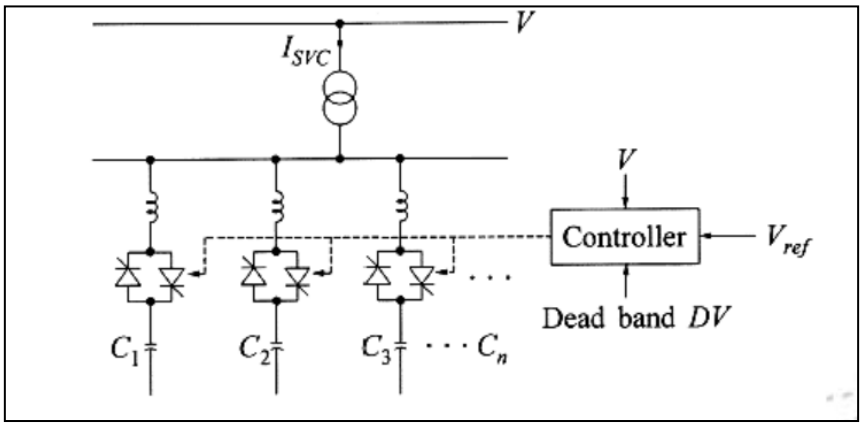

Figure 8: Thyristor switched capacitor [17].

The TSC damp inrush currents and transients and it prevents resonance [17]. If the voltage in the system drops, the thyristors connects more elements in parallel until the voltage is within its dead band. This is shown in Figure 9.

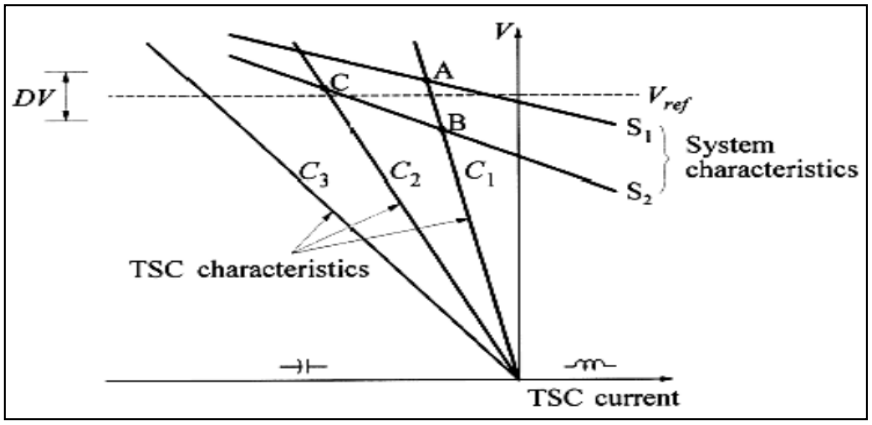

Figure 9: Thyristor switched capacitor scheme [17].

The thyristor controlled reactor (or thyristor controlled inductor) consists of inductors in series with back-to-back thyristors. The TCR consumes reactive power. By the partial conduction of a thyristor valve (triac), the TCR can control the amount of reactive power consumed by the reactor [24]. Figure 10 illustrates a thyristor controlled reactor.

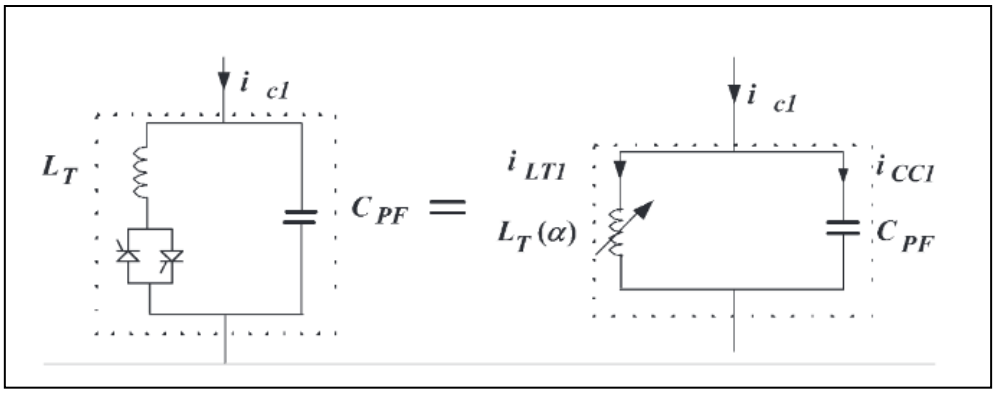

Figure 10: Thyristor controlled reactor [25].

A disadvantage of the SVC is that the reactive power produced is proportional to voltage squared which makes it less effective at low voltages. The characteristic corresponds to the parabola given in Equation 2.25.

$$Q = B_{max}U^2 \qquad 2.25$$

When all capacitors are switched on and the reactors are switched off, the maximum value of the capacitive reactance is given by Equation 2.25. If the voltage drops to for instance 0,8 pu, the maximum reactive power possible supplied by the SVC will be $Q=0{,}8^2=0{,}64$ pu [17][5]. Figure 11 shows the typical steady-state characteristics of a Static Var System (SVS).

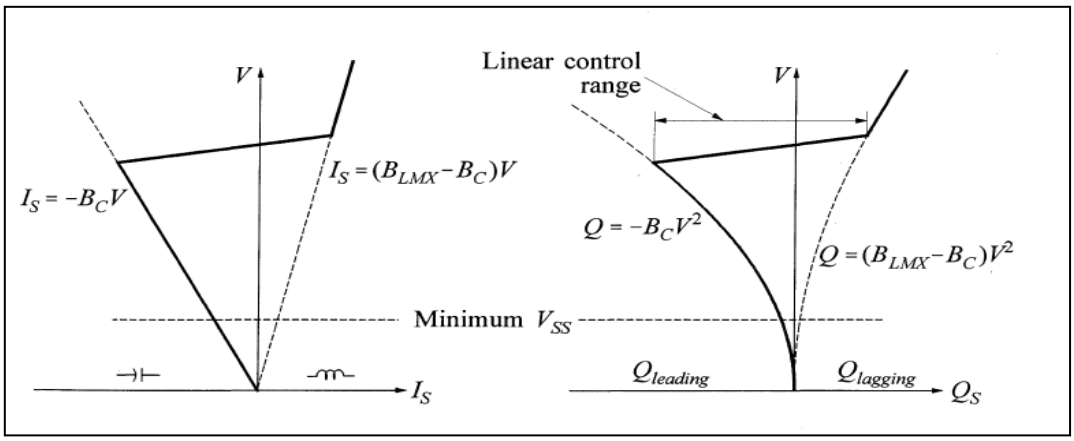

Figure 11: Voltage-current characteristics and voltage-reactive power characteristics of a Static Var System [17].

STATCOM is another reactive compensator device which has better abilities than the SVC for reactive power control, but is more expensive. For theory concerning STATCOM, Appendix 12.1 presents a brief introduction.

2.4 Transformer

In the simulations presented later in this thesis, two-winding transformers are utilised with dynamic tap changing. Transformers are necessary components in the power system and their main purpose is to link parts with different voltage levels together. There are several different types of transformers with various functions and connections.

The basic principle of a transformer originates from the laws of electromagnetic induction. A transformer consists of a laminated ferromagnetic core with a primary and a secondary coil. The coil on the primary side generates a magnetic field which is transmitted to the secondary side through the core. Current changes at the primary side, induces current on the secondary side. The ratio between the number of turns in the coils on the primary and secondary side of the transformer determines the voltage output of the transformer.

Assuming an ideal transformer, Faraday's law of induction presents the induced output voltage on the secondary side, e_S [26][27]:

$$e_S = -N_S \frac{d\varphi}{dt} = -E_{S_{max}} \cos(\omega t + 90^\circ) \tag{2.26}$$

Where

$$E_{S_{max}} = 2\pi f N_S \varphi_{max} \tag{2.27}$$

On the primary side of the transformer, the induced voltage is also dependent on the changing flux:

$$e_P = -N_P \frac{d\varphi}{dt} = -E_{P_{max}} \cos(\omega t + 90^\circ) \tag{2.28}$$

Where

$$E_{P_{max}} = 2\pi f N_P \varphi_{max} \tag{2.29}$$

Combining Equation 2.26 and 2.28 gives the relationship between the primary and secondary voltage level with respect to the number of turns in the coils:

$$\frac{e_S}{e_P} = \frac{N_S}{N_P} \tag{2.30}$$

If the resistance in the transformer is assumed to be negligible, the electrical power input is equal to the electrical power output. The output current is given by Equation 2.32.

$$P_P = I_P e_P = I_S e_S = P_S \tag{2.31}$$

$$\rightarrow \quad \frac{I_S}{I_P} = \frac{N_P}{N_S} \tag{2.32}$$

For a step-up transformer, the voltage increases from the primary to the secondary side and the current will decrease.

Three general categories classify the power system transformers [6].These are:

- **Generator step-up transformers** – connecting the generator to the transmission network
- **Transmission transformers** – connect different parts of the transmission network, usually at different voltage levels
- **Distribution transformers** – reduce the voltage at load centres to the necessary voltage levels required by the consumers

2.4.1 Transformer tap changer

The components in the electrical system are designed to operate at a particular voltage level. If the voltage deviates from the rated value, the performance of the component might be reduced and the ageing process increased [3]. The material written concerning the tap changer is mainly taken from [26] and [6].

There are different causes creating the need for tap changing:

- Load changes in the distribution grid makes the voltage differ from its preferred value
- Voltage changes in the main grid causing voltage deviations for the consumer

Tap changing transformers are used to control the voltage transformation ratio without phase shift control [28]. Tap changing is applied in the majority of the transformers in the power system because the turns ratio is controllable and voltages at all levels can be governed. Since alteration of the voltage magnitude affects the reactive power flow, the tap changing transformer can be applied as a reactive power controller. The tap changer is normally on the high voltage side of the transformer because the current is low, but it can be applied on the low voltage side as well. Two main types of tap changing transformers will be described in this section:

1) Off-load tap changing transformers
2) On-load tap changing transformers (OLTC or LTC)

The off-load tap changer taps while the transformer is de-energized and disconnected from the rest of the grid. Typically, the tap changer has four taps in addition to its nominal voltage and can tap ±5%. This type of transformer is normally used for transformers with a low rating in distribution networks. The transformer ratio is usually modified manually according to the load growth or seasonal changes, typically twice a year [26].

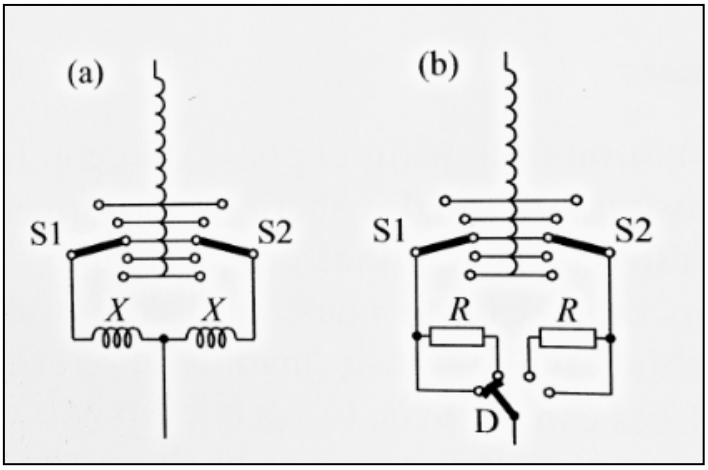

Figure 12: Two different on-load tap changers; a) with reactors; b) with resistors [6].

Figure 12 shows two principles of operation of on-load tap changing transformers. The taps selected for operation is decided by the tap selectors S1 and S2. During normal operation both tap selectors are set on the same tap in Figure 12a. The load current of the transformers flows through both chokes (inductors), which is a disadvantage because the resistance is increased by X/2. When the tap changes position, the tap selector S1 is moved, while S2 still is in the first position. During the time of the change for the first selector, the part of the windings between the taps is short-circuited by reactance 2X, which is advantageous for the solution. Tap selector S2 then taps and both S1 and S2 are in the same position. The tap changer applied in the PowerFactory model is similar to this set up.

In Figure 12b the principle is different from Figure 12a. Two resistors and a diverter switch are used to perform the tap changing. During normal operation, the switch is at the position shown in the illustration. Before the tap sequence starts, the diverter switch is moved to the middle position. The current will flow through the parallel resistors which will have an increased resistance by R/2. Selector tap S1 moves to the new position and the winding between the taps is short-circuited by resistance 2R. To finish the tap changing process, S2 is moved to the same tap position as S1 and the diverter switch D returns to its initial position [6].

However, there are issues connected to the implementation of transformer tap changers. If a large transmission line is disconnected, the voltage in the system will drop and the transformer tap changer will try to restore the voltage levels. Each tap

done by the transformer will result in an increment in the load on the transmission lines causing increasing active and reactive power loss. This leads to higher voltage drop and the reactive power output of the generators in the system increases until their maximum field current limits are reached. The generator's share of reactive loading will be transferred to other generators, leading to an overload in more generators. If the system is unable to restore its normal operation before this happens, a voltage collapse can occur [3][17].

Application of Theory in Model

As explained in the cable systems introduction, reactive power flowing in the cables is increasing with the length of the cable. This will be confirmed in the simulations. The cable type utilised in the simulation model is presented. To understand what reactive power is and how it can be dealt with, an introduction of the reactive power is presented together with different components which can improve the system's abilities by controlling the reactive power. Even though the model is simplified, it is important to present the operational manner of the components used for explanation of their behaviour. Voltage source converter, load tap changers and static var compensators are all applied and play an important part in the simulations. Since the VSC and an infinite voltage source represents the wind farm in the system model, both VSC and wind farm will be used as terminology for the control abilities.

Chapter 3

3 Wind Power

The fundamental behaviour and concepts of wind power integration are important to understand when analysing a power system with wind power production. Wind power is a variable power source which for large scale integration is dependent on control mechanisms to neutralise the variation by shaping the frequency, active power, reactive power and voltage into the desired characteristics. In this section, the basic concepts of wind power production, different turbine structures, general probability distributions and wind power statistics will be introduced.

3.1 Basic Concepts of Wind Power Production

Wind power turbines utilise the kinetic energy of the wind by converting it to mechanical power. When the air flow interacts with an airfoil, the wind velocity is increased over the convex surface resulting in a lower average pressure than the concave surface. The pressure difference between the two sides of the airfoil causes an induced net force working towards the convex side of the airfoil. This principle is presented in the following illustration:

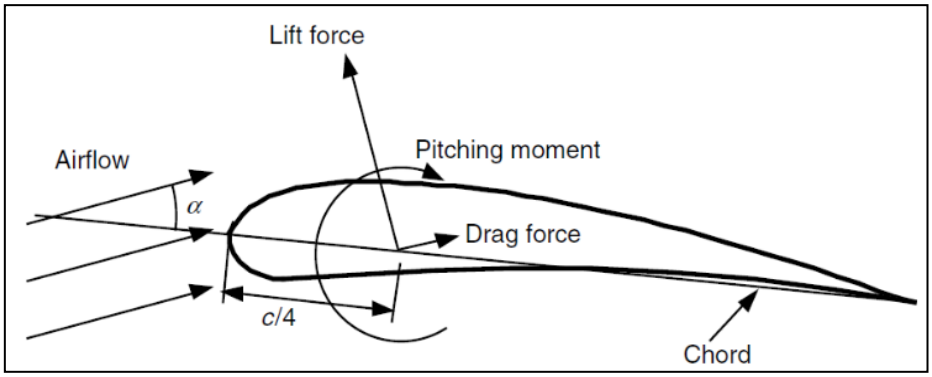

Figure 13: An oncoming air flow towards an airfoil causing positive forces and moments as shown [29].

The lift force is defined to be perpendicular to the direction of the oncoming air flow and is a direct consequence of the unequal pressure on the upper and lower airfoil surface. The drag force is defined to be parallel to the direction of the oncoming air and it is a product of both the viscous friction forces and the unequal pressure on the airfoils. The pitching moment is defined to be axis perpendicular to the airflow cross-section [29].

The definition of kinetic energy:

$$E_K = \frac{1}{2}mv^2 \qquad 3.1$$

Power is the derivative of kinetic energy with respect to time:

$$P = \frac{1}{2}\dot{m}v^2 \tag{3.2}$$

The mass flow rate is:

$$\frac{dm}{dt} = \rho A v \tag{3.3}$$

These equations lead to the power available in the wind:

$$P = \frac{1}{2}\rho A v^3 \tag{3.4}$$

To calculate the turbine power output, the power coefficient, which is the ratio of power extracted by the turbine to the total contained in the wind, $C_p = P_T/P_W$, needs to be taken into consideration. The maximum possible value for C_p, Betz limit, is 59,3%, but a three-bladed turbine will typically have a C_p approximately equal to 50% as illustrated in Figure 14. The final equation for the turbine power output is then [30]:

$$P_T = \frac{1}{2}C_p\rho A v^3 \tag{3.5}$$

The power coefficient is closely related to the tip-speed ratio. The tip-speed ratio (λ) is the relationship between the angular speed (ω) multiplied with the turbine radius (r) and the wind speed (v). A C_p-λ plot is useful because it tells how the rotational speed should change in order to maximise C_p [31].

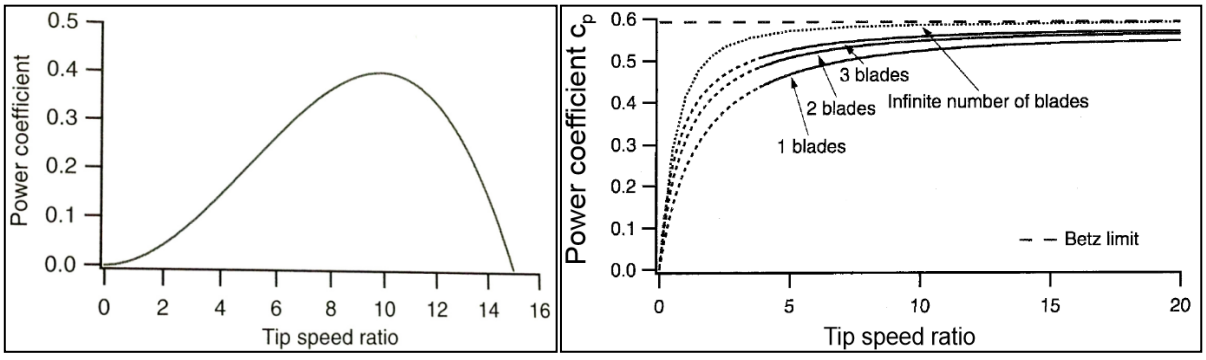

Figure 14: The illustration to the left shows a typical C_p-λ curve, while the right illustration shows the maximum achievable power coefficient as a function of number of blades [29].

3.1.1 Wind turbines

There are several wind turbine configurations to choose from when planning wind power production. A brief introduction to some of the wind turbines is presented in this section. The wind turbines can be classified into two groups: fixed and variable speed wind turbines.

3.1.1.1 Fixed speed wind turbines

Historically, most power producing wind turbines have operated at fixed speed. At the start-up sequence, the rotor is accelerated from a steady state position by the wind until required fixed speed is reached, and the breaks are released. When it operates at its fixed speed a connection to the electricity grid is made and the grid holds the speed constant and the frequency at 50 Hertz. If the wind speed exceeds the level for the rated power production, the power is regulated by either stall or pitching of the blades [32], which is explained in Appendix 12.2. Since variable speed wind turbines have been installed significantly more often during the recent years and because the wind power generators in PowerFactory is represented by a power electronic converter, this thesis will not dive deep into the different types of fixed speed wind turbines.

3.1.1.2 Variable speed wind turbines

When variable speed operation was introduced, the rotor and wind speed could be matched, making the efficiency higher. However, power electronic converters are necessary to be able to operate at variable speeds. There are two reasons why variable speed operation of wind turbines is desirable. First, below the rated speed, the wind turbine rotor can extract most energy if the tip speed ratio can be kept constant, requiring that the rotor speed vary with the wind speed. Second, operating the turbine's rotor at variable speed can reduce fluctuating stress and thereby reduce fatigue in the components of the drive train [29][33]. Variable speed operation of the wind turbine is possible for synchronous generators, induction generators (squirrel cage), wound rotor induction generators and switched reluctance generators. The first three methods of generation are the most common for variable speed wind turbines, and the two most relevant methods for the operation in this thesis will therefore briefly be introduced.

Variable speed operation of synchronous generators

There are two types of synchronous generators: 1) the ones whose fields are separately excited and 2) those whose fields are provided by permanent magnets. For both cases the output frequency is a direct function of the speed of the generator and the generators number of poles, which is essential for the synchronous speed, n, as given in the following equation.

$$n = \frac{60f}{P/2} \tag{3.6}$$

When a synchronous generator is used in a variable speed wind turbine, the output of the generator first needs to be rectified to DC and then inverted back to AC as Figure 15 illustrates.

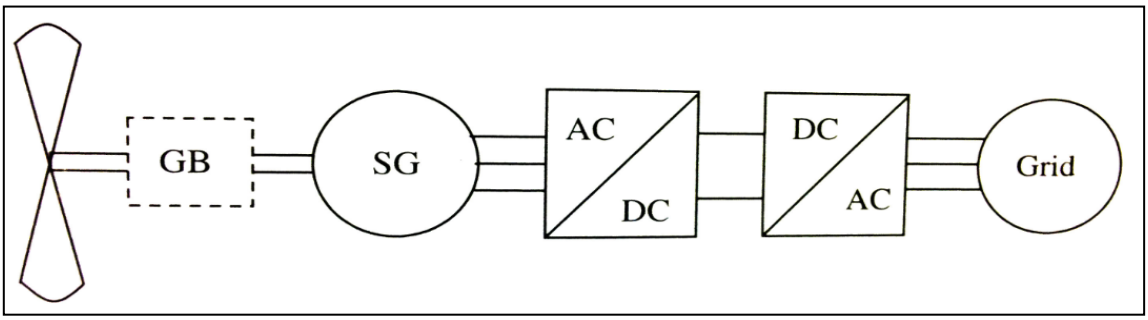

Figure 15: Variable speed wind turbine with synchronous generator [29].

In this figure, the rotor is on the left, followed by main shaft, gearbox, generator, rectifier, DC link, inverter and grid. Depending on the situation, the inverter can either be a diode rectifier or a controlled rectifier. If it is a separately excited synchronous generator, there might be voltage control on the generator itself. In the case of a permanent magnet synchronous generator, voltage control is someplace in the converter circuit [29].

Variable speed operation of squirrel cage induction generators

The method using squirrel cage induction generators (SQIG) as variable speed wind turbines is not as straightforward as for synchronous generators. Induction generators require a source of reactive power, which must be supplied by a power electronic converter. These converters are expensive and contribute to increased losses in the system. This might cause a relatively small net gain in energy production because the losses often are of the same order of magnitude as the gains in aerodynamic efficiency. However, the variable speed operation could cause reduction of fatigue damages to the rest of the turbine.

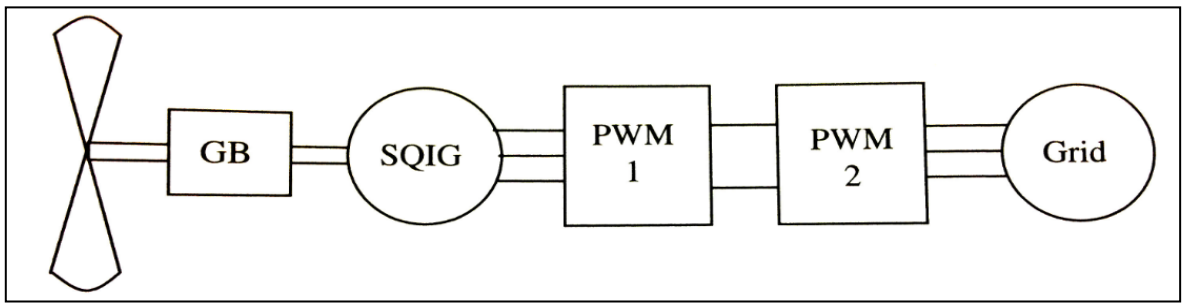

Figure 16: Variable speed wind turbine with squirrel cage induction generator [29].

The previous figure illustrates how the wind turbine rotor, gearbox, induction generator, and two PWM power converters with a DC link between them are connected together into the grid. The frequency and speed to the generator rotor are

controlled on the generator side of the converter. In addition the rotor power is converted to DC power here. On the grid side of the converter, the DC power is converted to AC at desired voltage and frequency [29].

Material concerning wind turbine control and regulation is attached in Appendix 12.2.

The wind power turbine utilised in the model in this Master's thesis is simplified, consisting of an infinite DC voltage source representing the generator and a voltage source converter with PWM controlling the power input of the turbine. The following figure illustrates the simple structure of the wind power turbine utilised.

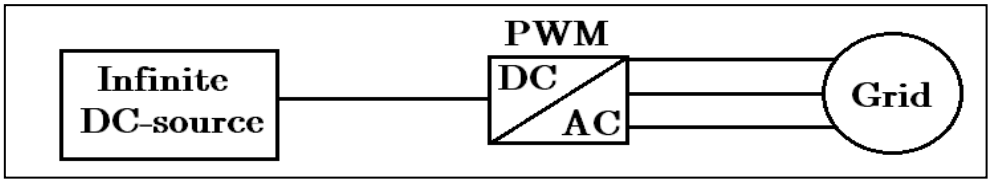

Figure 17: Simplified wind power turbine used in the model.

More about the structure of the turbine used for simulations in this thesis can be found in Section 6.2.1.

3.2 Probability Distributions and Wind Power Statistics

When planning offshore wind farms, short-term wind speeds are important to measure, to be able to estimate parameters such as power output, extreme wind load and fatigue load. To estimate design parameters of the wind farm, probability distributions are used if wind speed measurements over a long period of time do not exist. As mentioned in the introduction, the wind speed potential offshore is often larger than onshore. The reason for this is that the topology is suitable without any obstacles which can make wakes and prevent the wind from flowing smoothly through the area. To determine the wind power potential at a site, a statistical analysis is necessary. Short-term wind speed U refers to mean wind speed over a period of 10 minutes. The average wind turbine power $\overline{P}_{\mathrm{W}}$ can be calculated as follows:

$$\overline{P}_W = \int_0^\infty P_W(U) \cdot p(U) dU \tag{3.7}$$

The turbines power curve $P_W(U)$ in this expression describes the power output compared to wind speed, and p(U) is the probability density function of U. This approximation has the largest uncertainty in the estimation of the wind speed probability density function (pdf). To improve the results of the estimation, a more accurate distribution should be utilised [34].

3.2.1 Wind speed distributions

To perform statistical analysis of wind speeds and probability distributions for a site interesting for offshore wind power production, comprehensive wind speed measurement data is essential. The data should be collected at the site or at a site nearby with similar properties and topology.

3.2.1.1 Mean value, standard deviation, skewness and probability density functions

The long-term average wind speed, $\overline{U}$, using the entire amount of data collected is given by:

$$\overline{U} = \frac{1}{n} \sum_{i=1}^{n} U_i \tag{3.8}$$

The standard deviation of the individual speed average can be found by using the following equation:

$$\sigma_U = \sqrt{\frac{1}{1-n} \sum_{n-1}^{n} (U_i - \overline{U})^2} \tag{3.9}$$

The skewness, showing how unsymmetrical the distribution is, can be calculated as follows:

$$G = \frac{1}{n}\frac{\sum_{i=1}^{n}(U_i - \overline{U})^3}{\sigma^3} \quad 3.10$$

Where n is the number of observations in U, which is a random variable for the wind speed. To present the wind conditions in a more comprehensive and explanatory manner, the probability distribution needs to be taken into consideration.

The probability density function describes the relative likelihood for the occurrence of different wind speeds. The probability that the wind speed is between the limits U_a and U_b for a given interval with a given probability density function can be calculated by [29]:

$$p(U_a \leq U \leq U_b) = \int_{U_a}^{U_b} p(U)dU \quad 3.11$$

The mean, standard deviation and skewness for a continuous probability density function are calculated by:

$$\overline{U} = \int_0^{\infty} U \cdot p(U)dU \quad 3.12$$

$$\sigma_U = \sqrt{\int_0^{\infty} \left(U - \overline{U}\right)^2 \cdot p(U)dU} \quad 3.13$$

$$G = \frac{\int_0^{\infty}(U - \overline{U})^3}{\sigma^3} \quad 3.14$$

3.2.1.2 Cumulative distribution function

The cumulative distribution function (cdf) gives an expression for the probability or time fraction that the wind speed is equal to, or below, a certain chosen wind speed, U. The cumulative distribution function F(U) for a continuous wind speed U' defined for a chosen value U is given by [29][35]:

$$F(U) = P(U' \leq U) = \int_0^{U} p(U')dU' \quad 3.15$$

3.2.1.3 Weibull and Rayleigh distribution

For wind data analysis, the Rayleigh and Weibull distributions are often applied. The Rayleigh distribution has only one parameter while the Weibull distribution uses two. Both the Rayleigh and Weibull are skewed distributions and only valid for values larger than zero.

The only parameter in the Rayleigh distribution is the mean wind speed, and the probability density function and cumulative density function are given by:

$$p(U) = \frac{\pi}{2}\left(\frac{U}{\overline{U}^2}\right) \cdot \exp\left[-\frac{\pi}{4}\left(\frac{U}{\overline{U}}\right)^2\right] \quad 3.16$$

$$F(U) = 1 - \exp\left[-\frac{\pi}{4}\left(\frac{U}{\overline{U}}\right)^2\right] \quad 3.17$$

The two parameters in the Weibull distribution are the shape parameter, k, and the scale parameter, c. Both the scale parameter and shape parameter are functions of $\overline{U}$ and σ_U, and decide the outline of the distribution. The probability density function and cumulative distribution function for the Weibull distribution are given by:

$$p(U) = \left(\frac{k}{c}\right) \cdot \left(\frac{U}{c}\right)^{k-1} \cdot \exp\left[-\left(\frac{U}{c}\right)^k\right] \quad 3.18$$

$$F(U) = 1 - \exp\left[-\left(\frac{U}{c}\right)^k\right] \quad 3.19$$

When determining the shape and scale factors for a Weibull wind speed distribution at a potential site for wind power production, many factors must be taken into consideration, for example the season, location, hub height and topology. Typically, the scale parameter is in the range of 8<c<14 and the shape parameter in the range 1,8<k<3 [36]. The Rayleigh distribution is a special case of the Weibull distribution where the shape parameter has a given value equal to 2 [37]. In Appendix 12.3, two methods for calculation of c and k are shown [29].

By using MATLAB, some plots have been made for the Weibull and Rayleigh distributions with different values for k and c. Plots for the Weibull distributions are shown in the following figures.

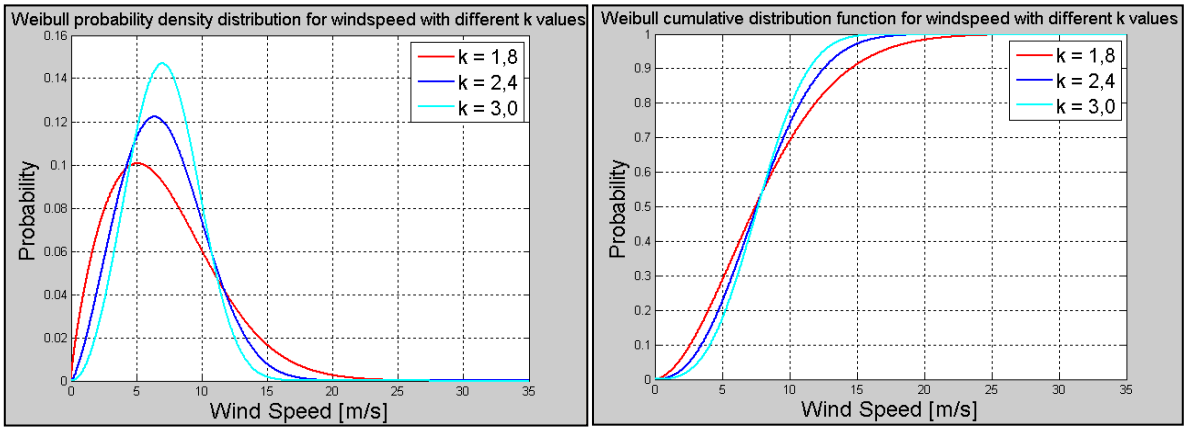

Figure 18: Weibull probability density function and cumulative distribution function plot using c=8 and different k values.

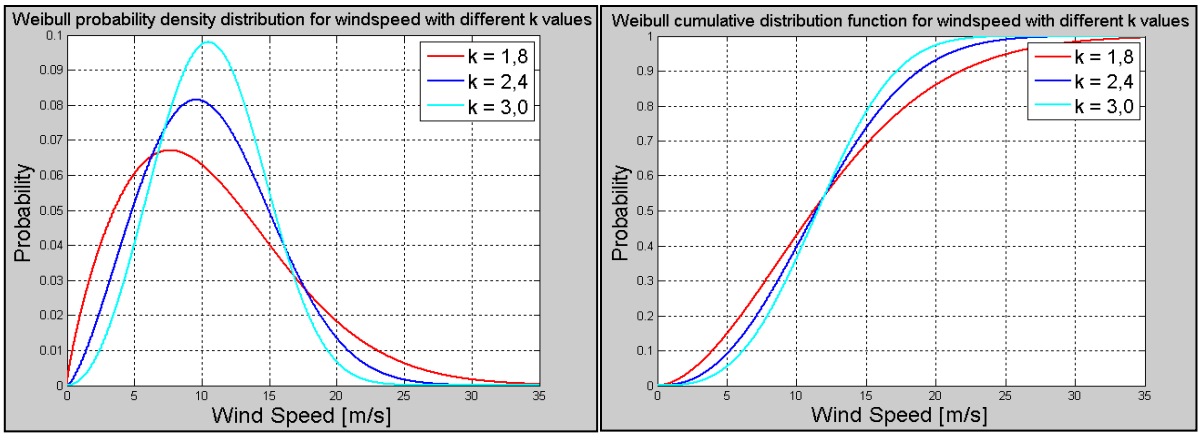

Figure 19: Weibull probability density function and cumulative distribution function plot using c=12 and different k values.

If the shape parameter increases, the curve will have a sharper peak and less variation, as seen in Figure 18 and Figure 19. When the scale parameter increases, the curves will stretch out and move towards higher wind speeds.

Plots showing the Rayleigh distribution function with different mean wind speeds are displayed in Figure 20. Mean wind speeds chosen in this graph, 6.5, 8 and 10.1 m/s, represent typical wind speeds for onshore, offshore and remote offshore locations, respectively [38].

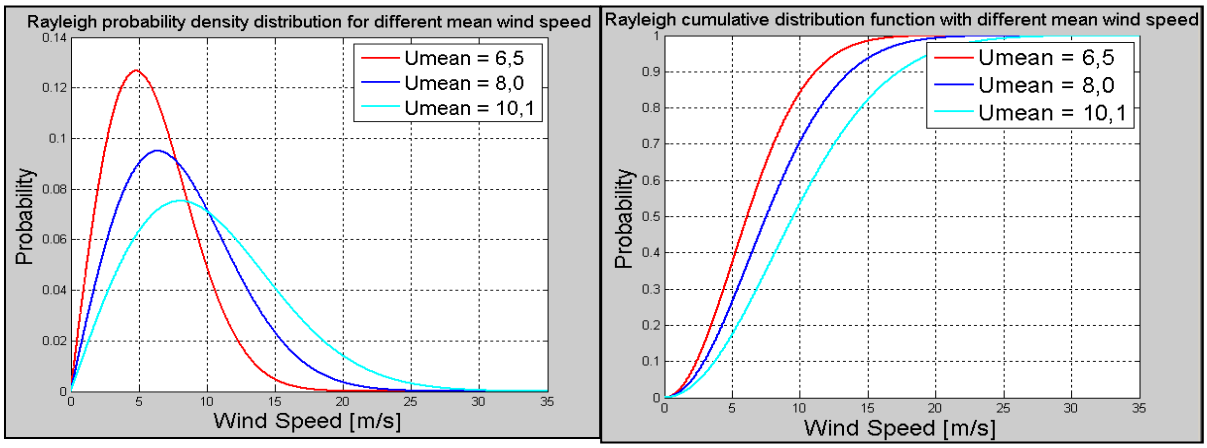

Figure 20: Rayleigh probability density function and cumulative distribution function plot using different mean wind speeds.

As Figure 20 shows, an increased mean wind speed gives a lower peak in the probability plot and moves the distribution towards higher wind speeds. The MATLAB scripts made for to plot the graphs are attached in Appendix 12.4.

Application of Theory in Model

In this thesis, the power production in the simulation model consists of one wind power production unit equivalent to 100 turbines. Some background concerning wind power has been added to provide a basic understanding of the concepts of wind power production and to present similar wind turbine models as the one used in this thesis to show the simplifications made. The Rayleigh density probability and cumulative function will in the simulations be used to calculate the annual production for comparison of cable losses with and without an SVC.

Chapter 4

4 Grid Code Requirements

Typical requirements related to reactive capability and voltage control for wind power, both specifically in Norway and generally in the European Union, will be described and compared in this section. Grid code requirements exist to ensure security of supply in the electric system. The infrastructure and economy of a country are essential when shaping the grid codes, so each country, or a combined group of countries, has an independent grid code, each with its own unique structure and restriction base. A grid code is a regulation that describes all the technical requirements of the components in the grid.

4.1 FIKS – Funksjonskrav i Kraftsystemet

In Norway, Statnett has the responsibility to define and publish the grid codes for the Norwegian main and transmission grid. The regulations defined by Statnett are described in the document FIKS (Funksjonskrav I KraftSystemet) which is published annually.

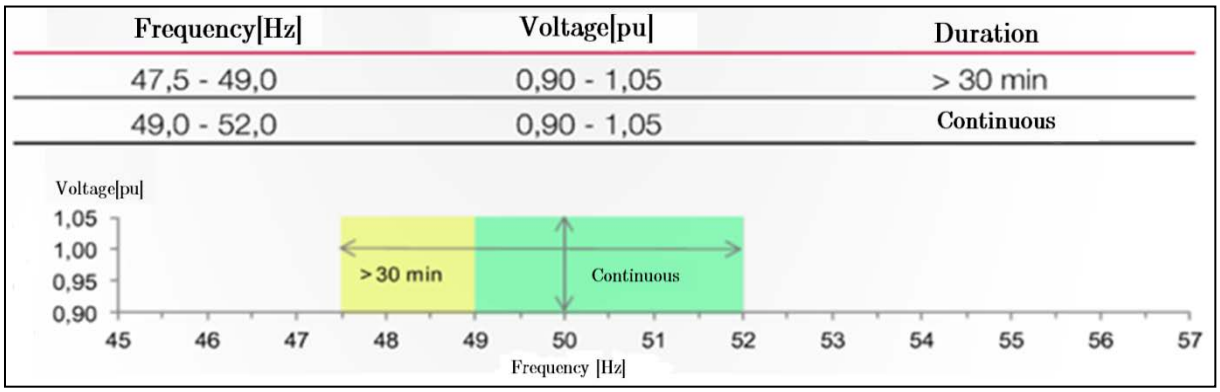

Figure 21: The voltage and frequency limits a wind power plant shall operate within [39].

To understand the requirements given by the grid codes and how they are applied in the simulations, some of the most important regulations and restrictions related to wind power production and connection are shown in this section. The regulations for wind power in FIKS are applicable for wind parks with rating larger than 1 MVA. One of the regulations written in FIKS for reactive power is [39]:

- *"Wind parks ≥ 1 MVA at full load shall have a power factor cosϕ≤0,95 capacitive and cosϕ≤0,95 inductive referred to the grid side of the transformer."*

In FIKS, some of the regulations with respect to voltage control in wind power systems are:

- *"Generally:*
- *Wind turbines with power converters shall be equipped with dynamic voltage control within the current rules. The voltage controller shall not be set with dead band.*
- *Functions:*
- *The voltage controller shall work freely without unnecessary limitations within its performance boundaries for the wind park and the related compensation systems.*
- *Wind parks shall be able to control the voltage at its own connection point within the limits given by FoL §3. In addition, it can be relevant to exploit the reactive capacity to support the voltage in the main grid.*
- *Settings:*
- *Voltage controllers shall be PID-type and have the possibility for active and reactive settings for statics."*

In FIKS, the regulations for the converters with installed capacity above 25 MW are divided into two separate parts; Voltage Source Converters and Line Commutated Converters. The converter regulations with respect to the reactive power for VSC are described as follows in FIKS:

- *"Converters connected to other countries shall be able to deliver/receive reactive power in addition to compensation of own consumption. This shall be defined in each area where this is relevant (increased transmission in the grid also gives increased reactive losses).*
- *VSC is not a net consumer of reactive power (can both consume and produce) and cannot be directly used for voltage control. Reactive power capacity seen from the grid side of the converter shall be cos$\phi \leq$0,95 capacitive and cos$\phi \leq$0,95 inductive measured compared to nominal rating.*
- *Reactive power shall have the possibility to be activated as regulated size or as a function, for example emergency power."*

In addition to voltage control and reactive compensation, the requirements in FIKS set restrictions for active power, frequency, the abilities in the grid, dimensions of the wind power generators, relays and the start and stop time of the wind turbine generators [39].

4.2 ENTSO-E

The grid code requirements for the European Union are published by ENTSO-E. The ENTSO-E network code defines a common framework of grid connection requirements and obligations for network operators in a non-discriminatory manner throughout the European Union. These grid codes are of great importance for system operation, system development, cross-border network issues and market integration issues. Since Norway has a common synchronous area with the Nordic countries, the regulations in ENTSO-E are applicable. The grid codes given by ENTSO-E are less detail based than the grid codes defined by countries for their own use [40].

The requirements for offshore power park modules in ENTSO-E are divided into general provisions, frequency stability requirements, voltage stability requirements, the robustness of power generating modules requirements, system restoration requirements and general system management requirements. The general provisions state that an offshore power park module that does not have an offshore connection point should be considered an onshore power park module subject to the requirements for onshore power park modules. Offshore connection points shall be defined by the Relevant Network Operator.

The voltage stability requirements state that offshore power park modules shall be operating within the ranges of the network voltage at the connection point and that the wind farm shall be able to stay connected to the network. The minimum periods an offshore power park module shall be capable of operating for different voltage ranges in each synchronous area are given in Table 3 .

Table 3: The minimum time periods an offshore power park module shall be able to operate in for different voltage ranges in different synchronous areas [40].

Synchronous area	Voltage range	Minimum time period for operation
Continental Europe	0,85 pu -0,90 pu	60 minutes
	0,90 pu – 1,118 pu*	Unlimited
	1,118 pu – 1,15 pu*	To be decided by each TSO, but not less than 20 minutes
	0,90 pu – 1,05 pu**	Unlimited
	1,05 pu – 1,0875 pu**	To be decided by each TSO,but not less than 20 minutes
	1,0875 pu – 1,10 pu**	60 minutes
Nordic countries	0,90 pu – 1,05 pu	Unlimited
	1,05 pu – 1,10 pu	60 minutes
Great Britain	0,90 pu – 1,10 pu*	Unlimited
	0,90 pu – 1,05 pu**	Unlimited
	1,05 pu – 1,10 pu**	15 minutes
Ireland	0,90 pu – 1,10 pu	Unlimited
Baltic countries	0,85 pu – 0,90 pu*	30 minutes
	0,90 pu – 1,12 pu*	Unlimited
	1,12 pu – 1,15 pu*	20 minutes

	0,88 pu – 0,90 pu**	20 minutes
	0,90 pu – 1,10 pu**	Unlimited
	1,10 pu – 1,15 pu**	20 minutes

* The voltage base for pu values is below 300 kV.
**The voltage base for pu values is from 300 kV to 400 kV.

Concerning the reactive power capability below the maximum capacity, the P-Q/P_{max}-profile shall take any shape within the boundaries presented in Figure 22. The profile is defined by each Relevant Network Operator in coordination with the relevant TSO. The P-Q/P_{max}-profile is expressed by the ratio of the actual value and the maximum active capacity in pu, versus the ratio of the reactive power and the maximum active capacity.

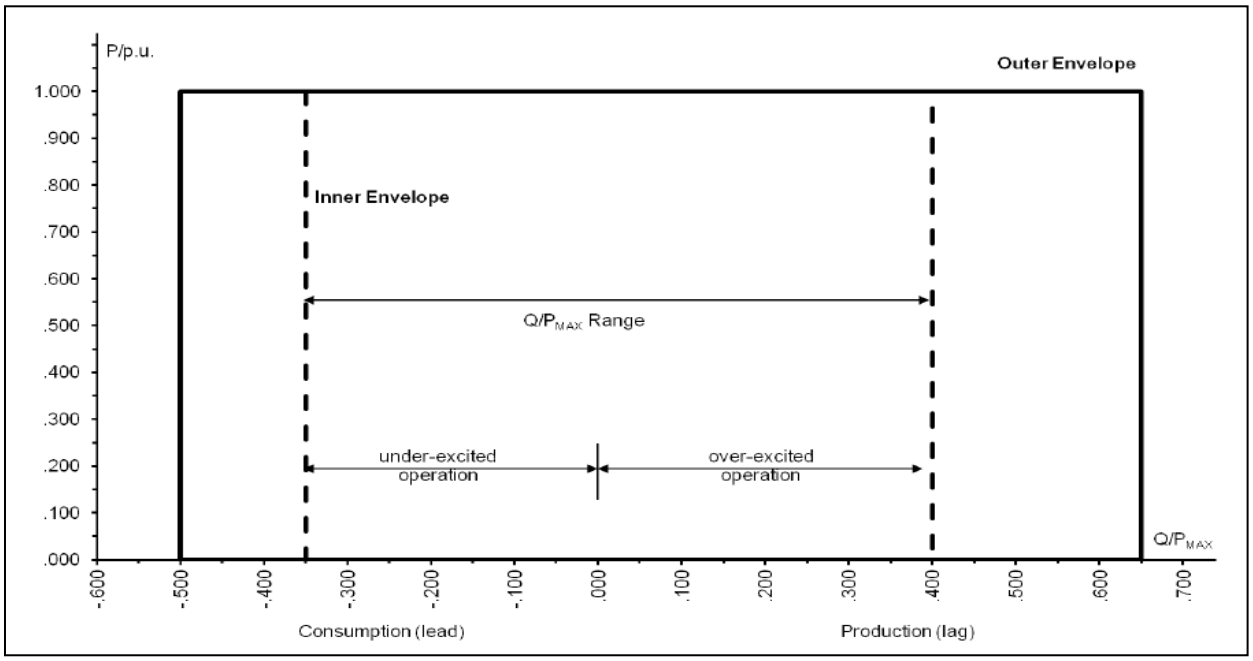

Figure 22: The P-Q/Pmax-profile of a power plant module at connection point [40].

The ENTSO-E requirements in the grid codes concerning the reactive power capability state that the power park module shall be capable of providing reactive power automatically by voltage control mode, reactive power control mode or power factor control mode. The set point voltage at the connection point by provision of reactive power exchange with the network shall cover at least 0,95 to 1,05 pu. If the grid voltage value at the connection point is equal to the voltage set point, the reactive power output shall be zero [40].

Application of Theory in Model

The main reason for including parts of the grid codes into this thesis is to present the operational and fundamental restrictions for the components and parameters in an offshore system. The limits concerning the voltages in the system are followed in the simulations, but it is assumed that Figure 21 is restrictive for all simulations. Regulations regarding wind parks above 1 MVA are applicable and followed to a certain degree. Some deviations from the grid codes are accepted in order to simplify the model which is described in Section 5.1.2. The reactive capability in the model is simplified to be +/- 50% of the active power production. To illustrate the inaccuracies and differences between the restrictions in the simulation model and the restrictions for a real system (Figure 22), the acceptable limits for reactive capability is presented. In FIKS, the regulations of the VSC are explained. It is stated that the VSC should be able to both consume and produce reactive power, which is the case in the simulations.

Chapter 5

5 Simulation Software

5.1 The Simulation Software DIgSILENT© PowerFactory

During the work on this thesis, a deep dive into the workings of PowerFactory was necessary in order to be able to utilise the simulation tool in such a manner that the model would have the desired design along with the ability to make the various components in the system work in coordination with a dynamic operational base. PowerFactory was a suitable simulation program to solve the tasks in a realistic manner because of its complexity and access to countless components with various control mechanisms. The method applied for modelling and the system software PowerFactory will be presented in this section.

5.1.1 Purpose of the simulations

The main goal in this Master's thesis is to utilise and develop a dynamic model for simulations. The specific purpose of this model is to enable an analysis of the coordination of three dynamic components, and to find which accompanying transmission strategies will lead to the longest possible cable lengths. In order to find the most beneficial transmission strategies, it is important to investigate the coordination of reactive power compensation between the three components. The components in question are:

- A Voltage Source Converter (VSC)
- Two two-winding on-Load Tap Changing transformers (LTCs)
- A Static Var Compensator (SVC)

To implement various wind power production in PowerFactory, the simulation event attribution is applied. By utilising simulation events, step responses in the active power production can be implemented in an easy and orderly manner. To obtain a consistent operation scenario throughout the cases, the power production is increased with the same step responses for many scenarios.

To achieve the goals for the simulation, the following strategy is chosen:

- Learn the basics of DIgSILENT© programming language and get a better understanding of the general structure of PowerFactory
- Define and implement a model used for simulations with dynamic components
- Tune the SVC and VSC to achieve realistic and decent transient curves
- Combine Excel and the PowerFactory graphs to analyse the plots and graph values further

- Make several "dummy" models to test the properties of the dynamic components isolated from the other components
- Systematically examine the behaviour of each component in the model to obtain a complete overview and understanding of the overall behaviour
- Evaluate different cases and scenarios to solve the pre-determined tasks and challenges within the restrictions described in the grid codes

5.1.2 General assumptions and simplifications

When utilising a simulation tool like PowerFactory, a lot of assumptions are necessary. Some of the main assumptions made are explained below.

Wind Power production is an unpredictable power source which varies a lot. In many of the simulations performed in this thesis the wind power variations are simplified to a step function of active power. Since the goal is to make the dynamic components cooperate and to find the best coordination scenario between these, a simple production plan is desirable, in order to make the key results more visual and easier to analyse.

The wind farm is represented by an infinite voltage source and a VSC. These components represent 100 wind turbines.

The economical perspective of operation of the components is not emphasized and the power markets are not considered, thus making the analysis purely technical. As explained further in the section describing the system model, the main grid is represented by an external grid.

Concerning the grid codes, some simplifications have been made. FIKS states that the controller shall be a PID type, while the controller implemented in the model is a PI type. The voltage limitations given in the grid codes are as a simplification considered acceptable between $0{,}90<U<1{,}05$ pu.

5.1.3 Advantages and disadvantages of DIgSILENT© PowerFactory

For the purpose of this thesis, one of the main advantages of using PowerFactory is the short simulation time. This makes it possible to run multiple simulations and handle the results in a tidy way without spending too much time waiting for the simulations. It is also easy to obtain the results graphically. Other notable advantages of using the PowerFactory simulation software are its applicability to the modelling of generation-, transmission-, distribution- and industrial grids, the analysis of these grids' interaction and its overall functional integration [41]. Many of the components, used to build the model, for instance cables and busbars are easy to implement just by adding blocks and giving them the preferred values.

One disadvantage with PowerFactory might be its complicated user interface, which makes the process of learning the software time demanding. Although there are many possibilities to manipulate the simulations in various different ways until the wanted

results are obtained. The program is very complex, and it is a challenge to get a clear overview of the possibilities and functionalities of the software. Another disadvantage is that some of the built in components, like the VSC, does not have a graphical representation for over instance block diagrams. It should be noted, however, that this can be made. The built in models often are too simple and dependent on the implementation of external models in order to be able to operate in the desired fashion.

5.1.4 PowerFactory overview

PowerFactory is written by DIgSILENT©, and is a computer aided engineering tool made to analyse transmission, distribution and industrial electrical power systems. The name DIgSILENT© stands for DIgital SImuLation and Electrical NeTwork calculation program. It is a vertically integrated model concept which allows models to be shared for all analytic functions.

When implementing external control mechanisms and models it is possible and sometimes necessary to change the command lines and equation sets by writing codes into the equations of the components. This is done using the DIgSILENT© Simulation Language (DSL) [42].

5.1.4.1 Static model and simulations

When analysing a static model, the system is in a steady-state condition, and only the static conditions such as load flow, are important. Static analysis is based on admittance/impedance descriptions. The loads in the model used to perform static analysis are voltage dependent, i.e. they have constant power and constant current or impedance. To perform the load flow iterations, the Newton-Raphson method is applied. Material concerning the Newton-Raphson method is attached in Appendix 12.5.2.1. Static analysis considers the conditions without any disturbances in the system and without planned changes. It is used to see whether the system can operate for a specific scenario. It is normal to run simulations for optimal power flow with static methods. Power system analysis and power flow calculations are explained further in Appendix 12.5. Load flow simulations are performed in order to interpret the system, but the load flow simulations are not included in the results.

5.1.4.2 Dynamic model and simulations

Components described by differential equations can be categorized as dynamic components. Dynamic simulations apply dynamic models of the components, and dynamic simulations use simulation tools to model the time varying behaviour of the system. This might be a time consuming process, depending on the complexity and time scale of the simulations. Transient analysis contains information about how the system, in a short time-frame, changes from a state (often equilibrium) when a disturbance affects the system. Transient analysis is an important part when working with dynamic simulations. All the results presented in this thesis are dynamic simulations.

Chapter 6

6 The Model Design

The model built and utilised in PowerFactory for simulations in this Master's thesis is a simplified system with the purpose of analysing the production of offshore wind power and its transmission to the main grid. The structure of the offshore system is simple, consisting of a wind power park with its internal grid, a transformer station, and subsea transmission cables connecting the offshore system to the main grid. The system model applied for simulations in this thesis will be explained in this section.

The figure below shows a simple illustration of the model. In Appendix 12.11 the actual model used in DIgSILENT© PowerFactory is presented.

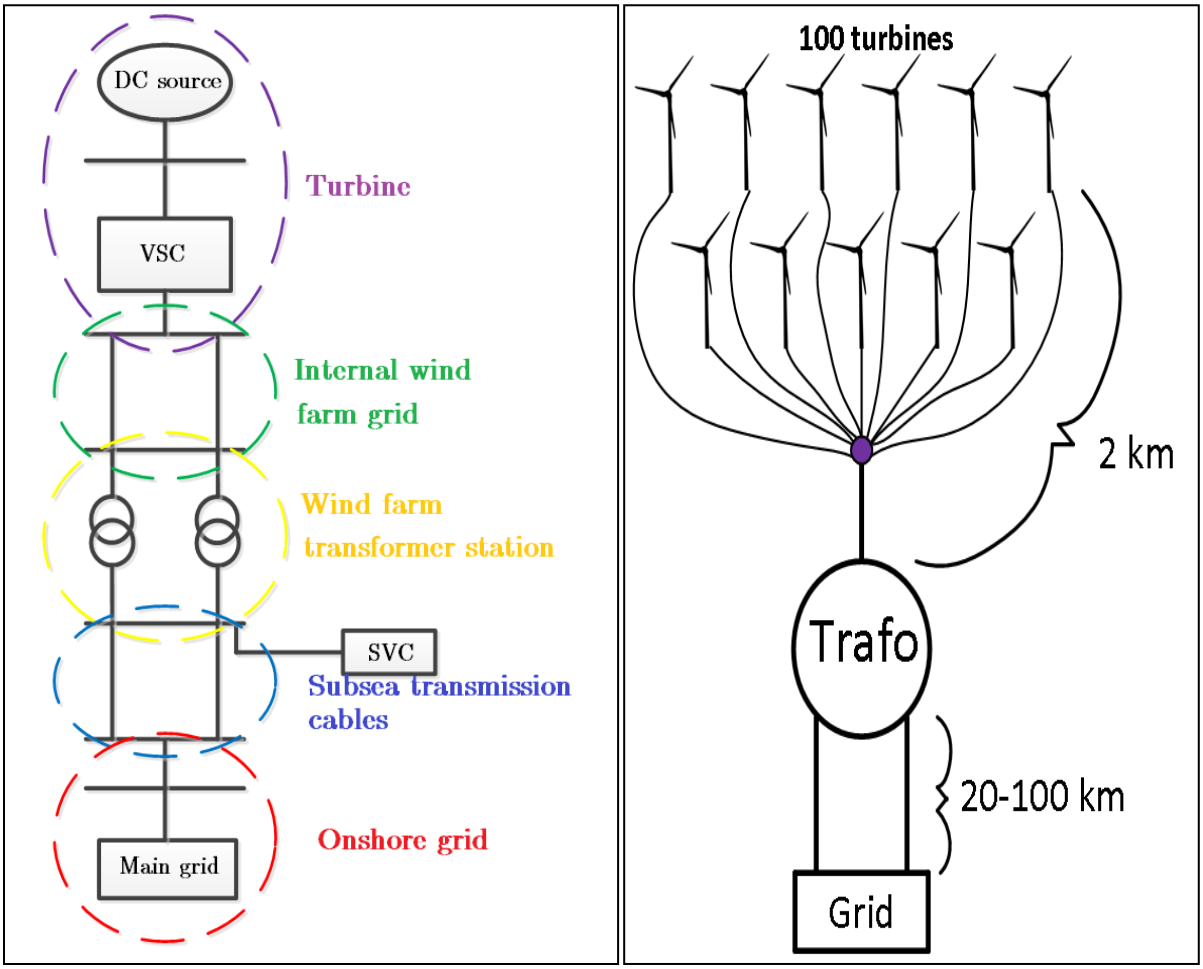

Figure 23: Simplified illustration of the model built and used in this Master's thesis.

The offshore wind park is represented by an infinite DC source connected to a controllable pulse-width-modulated converter, namely a VSC. These two elements represent all the turbines in the wind power park in one component. The internal grid

exiting from the turbines has impedance modelled to represent one hundred cables in parallel, each with a length of two kilometres.

The offshore wind park has a rated voltage of 33 kV, while the transmission and main grid are given a rated voltage level of 300 kV. Two transformers are connecting the 33 kV level to the system using a rated power of 300 kV. The two subsea cables transferring the power from the wind farm are linking the offshore system to the shore. Between the subsea transmission cables and the main grid, represented by a stiff external grid, a one kilometre long overhead line with a short-circuit impedance is applied to represent the stiffness of the system. A Static Var System (SVS) is connected on the offshore or onshore side of the subsea cables dependent on the case simulated.

6.1 The Cables and Overhead Line

The two subsea cables in the internal offshore grid are, as mentioned earlier, representing one hundred subsea cables in parallel. Reasoning behind choice is that they all need to transmit the power to a common connection point.

Equations 6.1, 6.4 and 6.5 show the calculations done to convert each of these two cables into 50 cables.

$$r_{50\ cables} = \frac{r_{one\ cable}}{50} \tag{6.1}$$

Where

$$r = \frac{\rho L}{A} k \tag{6.2}$$

And

$$k = [1 + k_t \Delta t] \tag{6.3}$$

$$L_{50\ cables} = \frac{L_{one\ cable}}{50} \tag{6.4}$$

$$C_{50\ cables} = C_{one\ cable} \cdot 50 \tag{6.5}$$

Data given for the subsea cables are found in Appendix 12.6. The chosen subsea cable is a three-core cable with optic fibres, lead sheath and wire armour. The cables from the wind farms have a cross-section area of 95 mm^2, which is given by the current rating.

Table 4: Rated values for different parameters. The current rating is calculated in Appendix 12.7.

Parameter	33 kV side of the transformer	300 kV side of the transformer
Voltage	33 kV	300 kV
Apparent power	1000 MVA	1000 MVA
Current (per cable)	174,955 A	825 A

Equation 6.6 shows how the current rating was calculated for the internal grid of the wind farm. In the data sheet for this cross-section, the thermal limit for continuous operation is 90°C, while the values in the sheet are given for 20°C.

$$I_{rated} = \frac{S_{rated}}{V_{rated} * \sqrt{3} * 100} \tag{6.6}$$

The apparent power rating S_{rated} is divided by 100 to find the rating for each cable. When inserting the values into the model, I_{rated} is multiplied by 50 because the two cables in the model represent 50 cables each. Since this is taken into consideration with the impedance as well, the cable values should be correctly adjusted.

The parameter values used in the implementation of the long subsea cables transmitting the produced power to shore are given in Appendix 12.6. The chosen cross-section of the cables is 1000 mm^2 to make the cables as robust as possible and to be able to carry a large current. The current rating used in these cables is also given in the cable data sheet.

Between the long cables connecting the offshore system to shore and the grid, an overhead line is connected because of the need to determine the short-circuit impedance in order to ensure a stable and strong system. The short-circuit capacity plays an important part in the power quality of the grid. A low short-circuit capacity and a high x/r ratio will give a weak grid, while a high short-circuit capacity in combination with a low x/r ratio gives a stiff grid [43]. The short-circuit current at can be calculated from Equation 6.7, while the short-circuit ratio is given by Equation 6.8.

$$S_{SC} = \frac{3}{2} V_r I_{SC} \tag{6.7}$$

$$r_{SC} = \frac{S_{SC}}{S_r} \tag{6.8}$$

The impedance implemented for the overhead line is presented in Appendix 12.7.3.

The whole offshore system in the model is directed through the overhead line into a node connecting it to "the main grid". The external grid was set in the simulations to control as a slack bus.

6.2 Implementation of the Dynamic Components for Dynamic Simulation

6.2.1 Voltage source converter

The voltage source converter (wind farm) is set either as a P-V controller, deciding the active power (P) and the voltage (V), or as a P-Q controller with fixed active (P) and reactive power (Q) output. With P-Q control, the reactive power output is set to zero.

6.2.1.1 P-V Control

The P-V controller consists of an active power control loop and a voltage control loop. In Appendix 12.8 the control system as it appears in PowerFactory is presented.

In the model, the parameters given can be varied to tune the converter so it presents the desired transient response. The active power control loop and the voltage control loop will be described further.

Table 5: Brief description of the parameters in the VSC controller.

Parameter	Description
T_{rp}	Filter time constant, active path [s]. Removes slow oscillations in the active path.
T_{rq}	Filter time constant, reactive path [s]. Removes slow oscillations in the reactive path.
K_p	Proportional gain – id-PI-controller [pu]. Produces an output value proportional to the current error value in the active power control loop. Affects the peak value of the transient response.
T_{ip}	Integrated time constant – id-PI-controller [s]. Removes slow oscillations in the active control loop.
$AC_{dead\ band}$	Dead band for proportional gain [pu]. Decides the acceptable voltage level. Set to zero in this thesis.
K_{iq}	Proportional gain for AC-voltage support [pu]. Produces an output value proportional to the current error value in the voltage control loop. Affects the peak value of the transient response.
T_{iq}	Integrator time constant – iq-PI-controller [s]. Removes slow oscillations in the reactive control loop.
i_{d_min}	Maximum discharging current [pu]. Sets restrictions for the maximum discharging current.
i_{q_min}	Minimum reactive current [pu]. Sets restrictions for the minimum reactive current.
i_{d_max}	Maximum charging current [pu]. Sets restrictions for the maximum charging current.
i_{q_max}	Maximum reactive current [pu]. Sets restrictions for the maximum reactive current.

Active power control loop

The active power control loop is based on a PI controller and decides the active power output of the converter. The active power loop is illustrated in Figure 24.

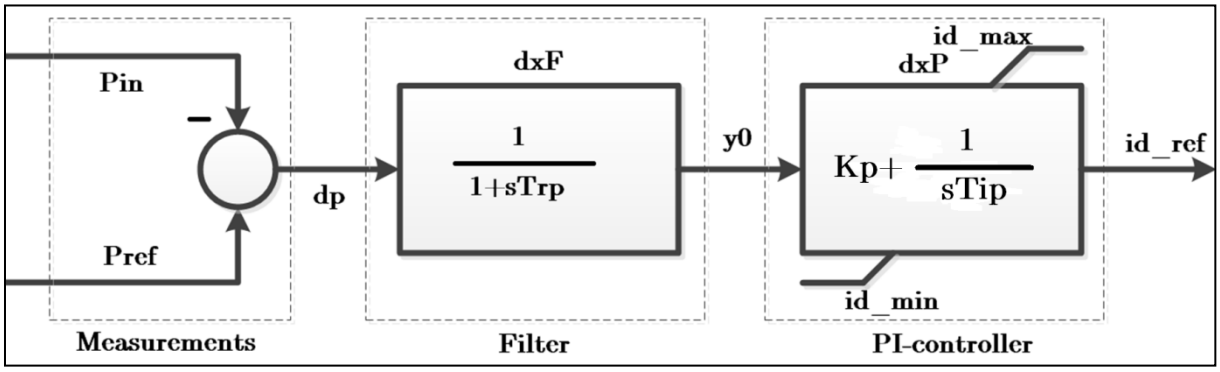

Figure 24: Active power control loop.

The first block in the illustration above measures the active power in (P_{in}) and computes the error ($dP=P_{ref}-P_{in}$). P_{ref} is the active power reference which can be controlled in per unit.

The second block represents a low pass filter with the cut-off frequency as the parameter. T_{rp} is the filter time constant for the active path, and it is a function of the cut-off frequency:

$$T_{rp} = \frac{1}{\omega_C} \qquad 6.9$$

In the third block, a PI controller with its maximum and minimum limits is presented. The PI controller itself consists of a proportional gain, K_p, and an integrator time constant, T_{ip}. The current in the d-axis, id_{ref}, is the parameter limiting the active power. In the simulation events, the active power can be fixed at a desired value by controlling id_{ref}. id_{ref} is applied to an internal controller which produces the pulse-width-modulations (P_{md}) in the d-axis.

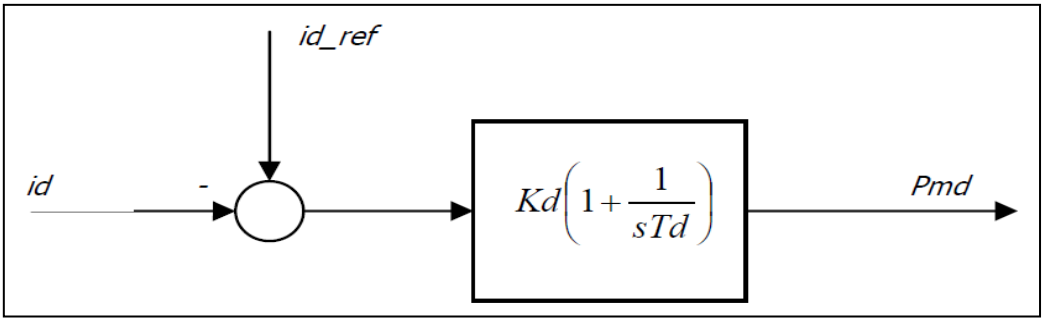

Figure 25: Block diagram of the built in current controller in the d-axis [42].

The input currents to the controller are the AC-currents expressed in a reference frame defined by an input signal, cosref. The output signal is defined in the same

reference frame and transformed back to a global reference using the same cosref. If the built-in current controllers are all set to zero (K_p=0, T_{ip}=0, K_{iq}=0, T_{iq}=0), the controller is disabled and the converter output current, i_d, is equal to the input variable id_{ref}. Hence the PWM converter is operating as a current source [42]. The Park Transformation, which describes the conversion from a three phase sinusoidal signal into quantities in a two-axis reference, is presented in Appendix 12.10.

In steady state analysis, dp=dxF=dxP=id_{ref}=0. When the simulation is run with dynamic conditions, these parameters differ from zero, and PI control is performed until dp is compensated. In reality it could be desirable to utilise droop characteristics making the voltage stability more flexible.

Voltage control loop

The voltage control loop decides the voltage output of the converter.

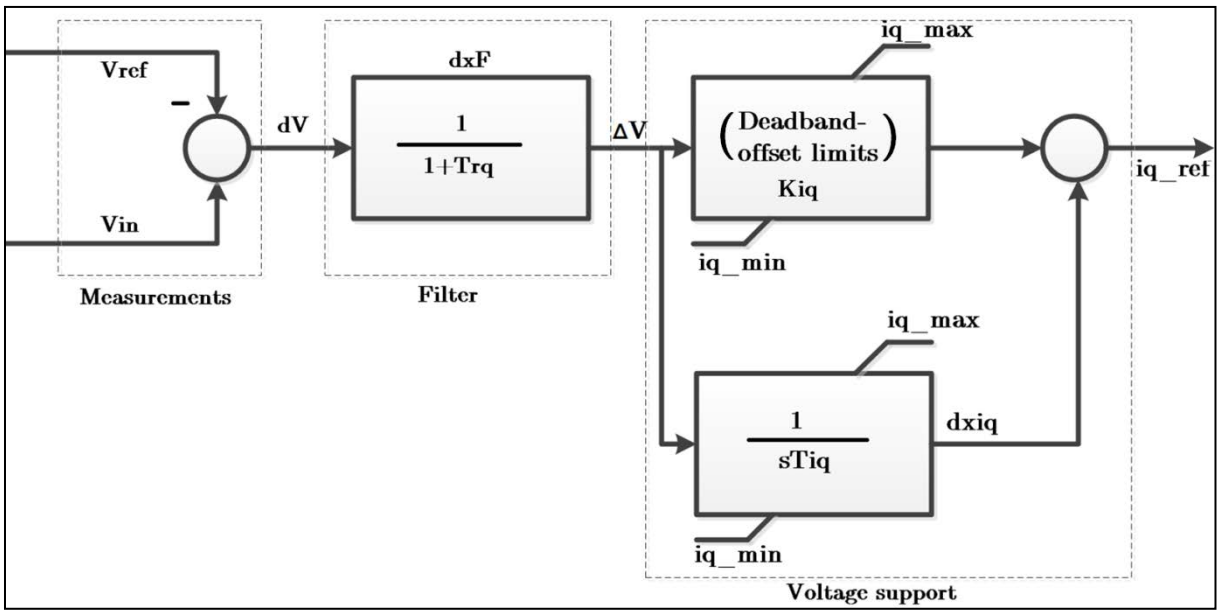

Figure 26: Voltage control loop.

From the measurements blocks, V_{in} is measured using a special device called a StaVmea measuring device. V_{ref} is the controllable reference voltage, while dV is the voltage error.

The second block in Figure 26 is the measurement filter, which is a low pass filter dependent on the cut-off frequency. The reactive path of the filter time constant, T_{rq}, can be calculated in the same way as the active path given in Equation 6.9.

The dead band with offset and limits contains the reactive current support characteristics. The dead band is set to zero in the simulations performed in this thesis.

The last block, in the lower right corner of Figure 26, is a limited non-windup integrator which compensates for the error. This block also smoothes out the response of the reactive current for large transients in the input voltage.

iq_{ref} is, just like id_{ref}, applied to an internal PI controller which produces the q-axis pulse-width-modulations (P_{mq}).

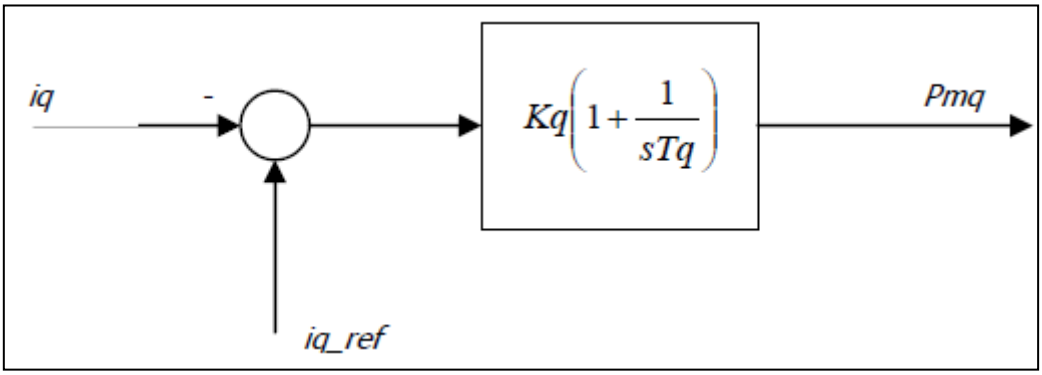

Figure 27: Block diagram of the built in current controller in the q-axis [42].

The reference frame defined by the input signal for the q-axis is given by sinref. Setting the built-in controllers to zero will in this case lead to a converter output current, i_q, equal to the input variable iq_{ref} [42].

6.2.2 On-load tap changing transformer

The on-load tap changing transformer used in the PowerFactory model is a built-in model where the parameters of the transformer are easily modified. A general set-up for the control mechanisms of a tap changer transformer is described below.

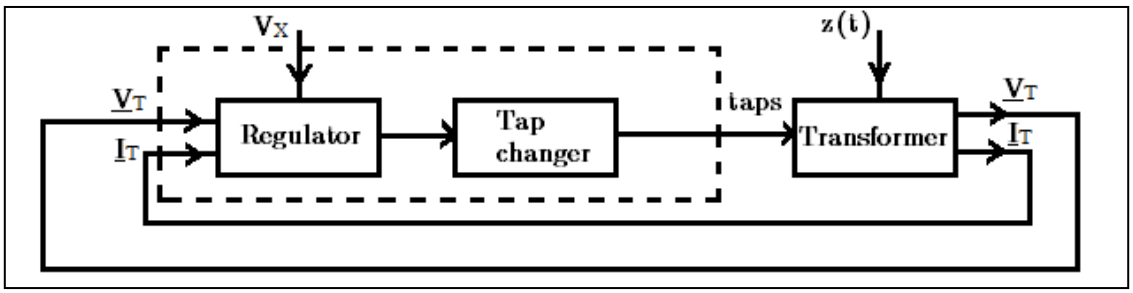

Figure 28: Block diagram of a transformation ratio control [6].

On-load tap changing allows the transformer to be connected to the system during taps. Typical regulation range is ± 20%. Reactive power or voltage at a certain point in the network may be the controlled using the tap changer, depending on the point of installation of the transformer and its planned function in the system.

To prevent abrasion and ageing of the tap changer, the regulator tries to minimise the number of taps per day. Figure 28 shows a simplified block diagram of a typical regulating transformer. Disturbances into the transformer, for example configuration changes and network loading, is represented in the block diagram by z(t). The

regulator receives current measurements, $\underline{I}_T$, and voltage measurements, $\underline{V}_T$, from a chosen side of the transformer and affects the transformer through a tap changer. The tap changer taps according to the signal given by the regulator. By comparing the voltage and current measurements to a reference signal, a control signal is made and the required control task is executed. V_X is an external control signal which can additionally be added to the regulator in the form of, for instance, a supervisory controller.

A more general overview of the control system is shown in Figure 29 [17].

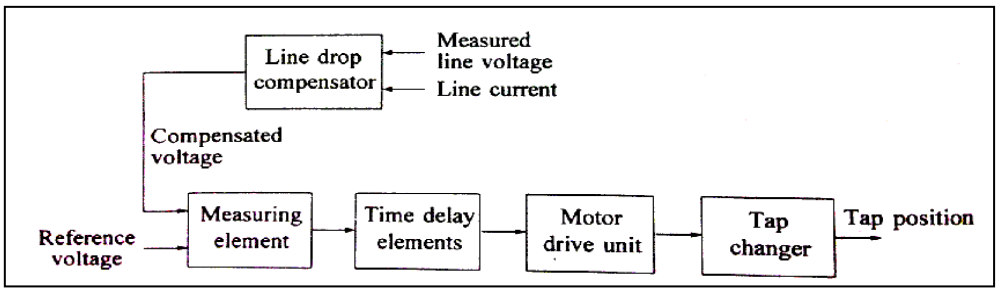

Figure 29: Functional block diagram of a control system for automatic changing of transformer taps [17].

The function of the line drop compensator is to regulate the voltage at a remote point along the line or the feeder. Voltage at a remote point is simulated by computing the voltage across the compensator impedance (R_C+jX_C). The magnitude of the compensated voltage will then become [17]:

$$V_C = \left|\widetilde{V_T} + (R_C + jX_C)\widetilde{I_T}\right| \qquad 6.10$$

By adjusting parameters in the voltage regulator, coordinated control of the transformers with on-load tap changing can be achieved. At least three parameters can be tuned in the voltage regulators connected to the LTC-transformers [3]:

- Desired voltage level, U_B
- Allowed voltage difference, ΔU
- Time delay, T

ΔU is the maximum allowed voltage difference in one direction between the reference voltage and the measured voltage before regulation is performed. The dead band of the regulator contains the voltage difference between the minimum and maximum allowed voltage. The time delay is the time between the registration of an unacceptable value and the regulation. By adjusting the allowed voltage difference in the voltage regulator, it decides how much the voltage can deviate from the reference value [3].

6.2.3 Static var compensator

The SVC implemented in the PowerFactory model has the ability to be set in two different reactive control modes.

- Reactive power control mode contributes with a constant reactive power production or consumption to the system.

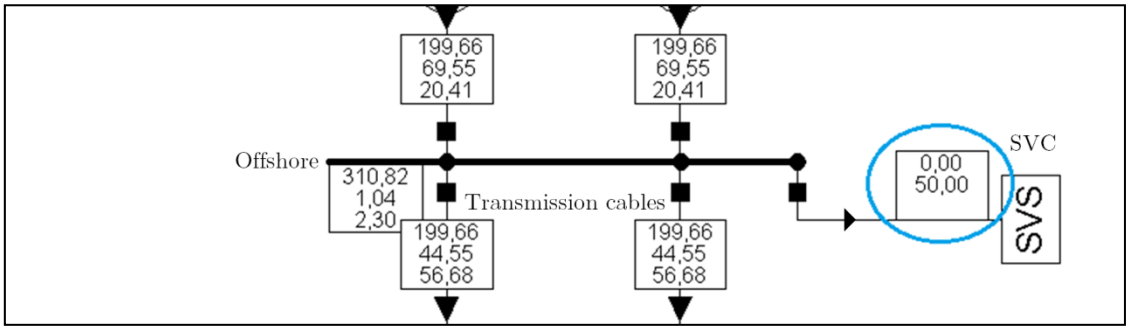

Figure 30: Reactive power control mode of the SVC.

In the illustration above, the reactive power set point is set to consume 50 MVAr. Thus, 50 MVAr is directed into the SVC.

- Controlling the bus in voltage control mode aims to keep the voltage at a selected voltage set point by contribution of sufficient reactive power to achieve the desired voltage level, as long as the reactive power from the SVC does not exceed its reactive power rating. The following figure points out the controlled voltage at a chosen bus by the SVC with a voltage set point of 1,00 pu.

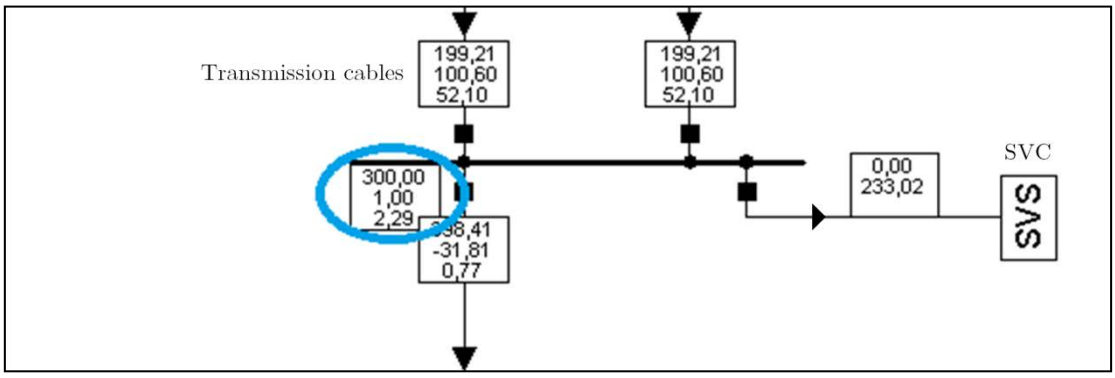

Figure 31: Voltage control mode of the SVC.

The control system for the SVC utilised in the model is a standard model inserted from the database library in PowerFactory. The standard model is chosen because it has all the characteristic properties desired to operate the SVC as intended. An overview of the control system for the SVC is presented in the following figure. The "real system" as it looks in the PowerFactory model is presented in Appendix 12.9.

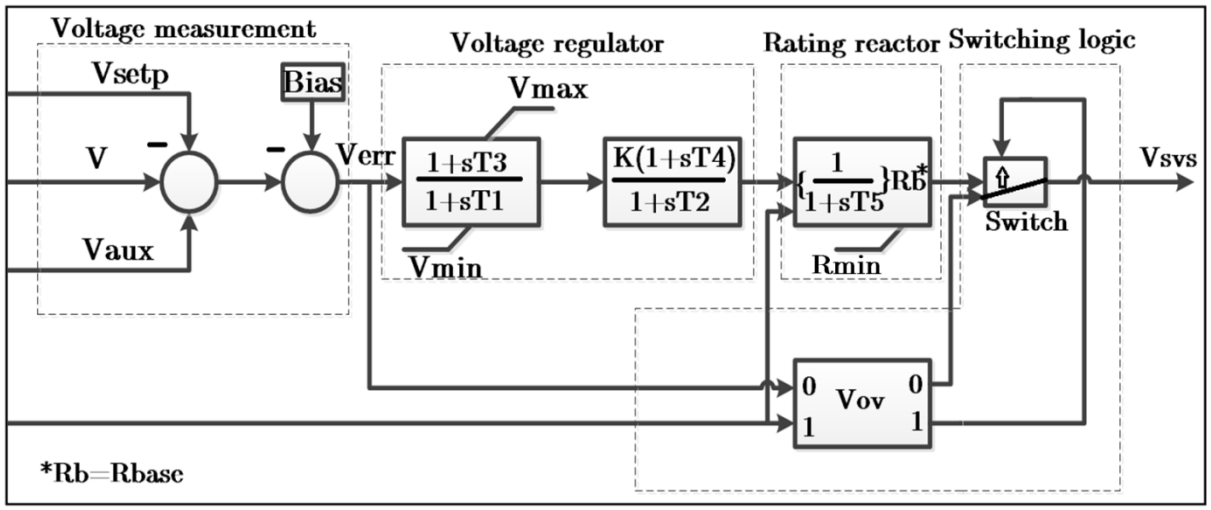

Figure 32: Presentation of the control system in the SVC.

The main components presented in the control system of the SVC are a voltage measurement circuit, a voltage regulator, a reactor block and a logical switch.

The voltage measurement circuit measures the voltage and the voltage error (V_{err}). A voltage set point can be inserted by the user. If necessary, a bias can support by adding a constant value.

The voltage regulator consists of a filter and a proportional regulator. The gain of the proportional regulator is reciprocal of the droop characteristics. V_{min} and V_{max} sets the minimum and maximum voltage limits for the voltage regulator.

The reactor block is restricted by a reactor minimum, R_{min}, and it decides the rating of the SVC in MVAr. R_{base} is equal to the rated reactive power of the SVC. This block is in many areas of applications seen as a TCR block representing the variation of reactor susceptance as a function of the firing angle, thyristor firing circuits and linearising circuit used for compensating the non-linear relationship between the susceptance and the conducting angle [17].

V_{ov} represents the override voltage which controls the switching logic. The following equations give the outcome of the switching logic:

$$1, if\ V_{err} > V_{ov} \quad 6.11$$

$$\frac{R_{min}}{R_{base}}, if\ V_{err} < V_{ov} \quad 6.12$$

The controller as it appears in PowerFactory is given in Appendix 12.9.

6.3 Description of the Case Scenarios Analysed

In the simulations, different scenarios were tested in PowerFactory to determine the effect of applying an SVC in transmission of active power for large distances with wind power production. The dynamic components inserted to control both active power, voltages, currents and reactive power will first be analysed to establish their behaviour and make sure that they react as they are meant to.

All the results presented are obtained with dynamic simulations. After the demonstration of different components in the system, simulations will be performed to find the most beneficial location of the SVC and to check if the SVC is necessary. These simulations will be performed with the wind farm controlling both active and reactive power (P-Q) and active power and voltage (P-V). For the scenario with the wind farm specifying P-Q parameters, the cable lengths will be increased progressively to compare the consequences of the reactive power increase. Only the maximum lengths possible for valid operation are examined in the scenario with P-V control. Additionally, LTCs will be activated if the voltages are too high to determine their contribution. It will also be confirmed that the reactive current in the cables increases with increasing cable length.

Coordination between the load tap changer and the static var compensator will be examined with the SVC connected on the offshore side of the transformer and to the same node as the one where the LTC is specifying the voltage.

In the last case, the Rayleigh distribution for a specific mean wind speed will be compared to a wind speed sensitivity curve to calculate annual production and the annual loss reduction of applying an SVC in the system for transmission purposes.

Current loading is an expression describing the cable current as a percentage of the maximum current possible in the cables:

$$Current\ loading = \frac{Current\ flowing\ in\ the\ cables}{Maximum\ current\ limit\ in\ the\ cables} \qquad 6.13$$

The results are defined to be acceptable if the voltages and currents are within their limits and if a valid initialisation of the operation is achievable.

Hypothesis

It is expected that an offshore location of the SVC will be the most beneficial solution for all the simulations and scenarios. The background for this hypothesis is that the reactive power produced in the cables will lead to large currents which will be controlled more efficiently when the SVC is located closer to the production. The cable currents are assumed to be high when the SVC is onshore, since all the reactive power is "pulled" towards the onshore side of the cables. Additionally, the active power losses in the cables are expected to be higher without any compensating device compared to when the SVC is located offshore.

Chapter 7

7 Power Flow Simulation and Results

Before the simulations relevant to the main objective are analysed, testing different components is necessary for confirmation of the system behaviour. The parameters for the VSC, SVC and LTC need to be tuned so the transient does not oscillate too much and the desired behaviour can be obtained.

7.1 Testing the VSC

The wind farm is as described in 6.2.1 specifying active power and voltage or active and reactive power at a chosen bus. To see if the controller is working properly, these abilities are tested. Additionally, it is desirable to make a step function for the active power output so the output of the turbine can be changed during the simulations.

Active power step function

According to the description of the voltage source converter controller, it should be able to control active power by modifying the reference value. Adding a simulation event and changing the pu value of the power reference will change the produced active power during the simulations. To test the controller, an active power step of 2 pu after 12 seconds is implemented. The active power production will step from 400 MW to 800 MW.

This modification in the active power production in the turbine gives the following response of the reference value (green) and the actual value (blue) in pu of the active power:

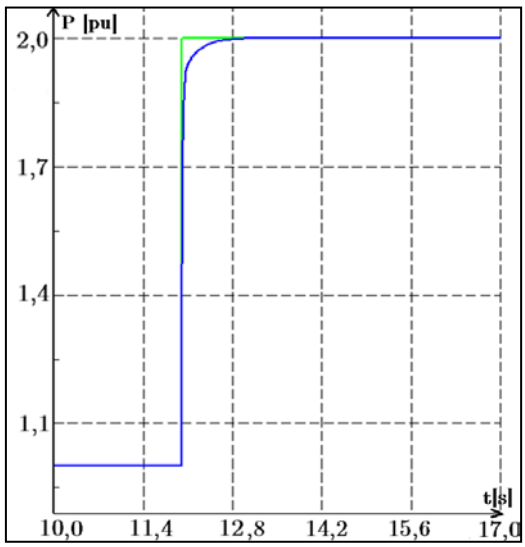

Figure 33: Active power set point modified by changing the reference value.

Active power and voltage control (P-V control)

By changing the settings of the control mode on the converter to Vac-P, active power and voltage set point can be determined.

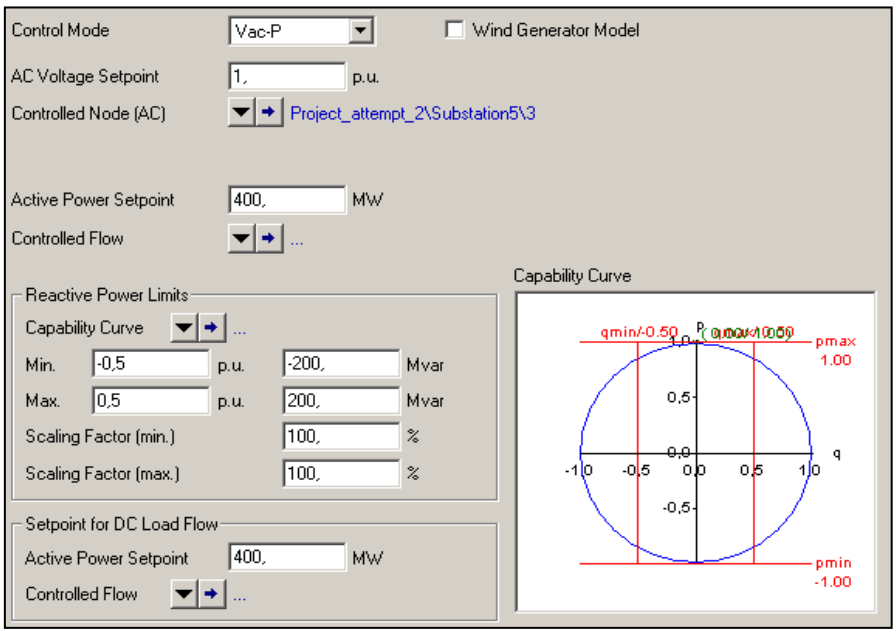

Figure 34: P-V control of the voltage source converter.

In the previous figure, active and reactive capability curve is displayed in the lower right corner. Figure 22 presents the capability curve regulations for a power plant module. In the simulations, the maximum reactive power contributions from the VSC are simplified to be +/- 50% of the active power production.

The active power produced by the turbines is set to be 400 MW. By applying a large step in the active power production (from 400 MW to 800 MW after 12 seconds) the voltage at the controlling bus will remain constant:

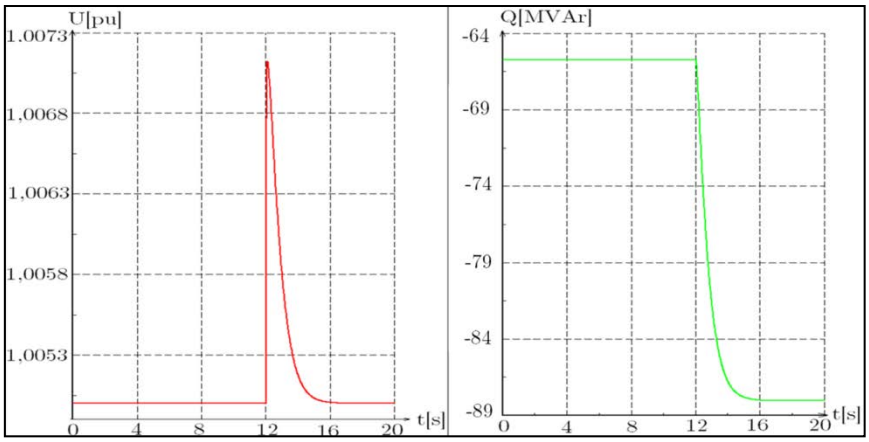

Figure 35: PV control. Left graph: Voltage kept constant. Right graph: Reactive power necessary to keep the voltage constant at 1,005 pu.

As illustrated in the previous graph, some oscillations arise in the transient time domain after the active power step before the voltage returns to its reference value. In order to keep the voltage constant at 1,005 pu, the reactive power changes. In this case, reactive power production is positive, so the wind farm consumes reactive power. The oscillations can be controlled by tuning the controller, which will be explained further later in this section.

Active and reactive power control (P-Q)

When altering the control mode from P-V to P-Q mode, the active and reactive power output of the converter is specified. The reactive power is being kept at a constant level while the voltage will compensate for the constant reactive power and stabilise at a different level. The same active power step as in the previous case is applied to the power production.

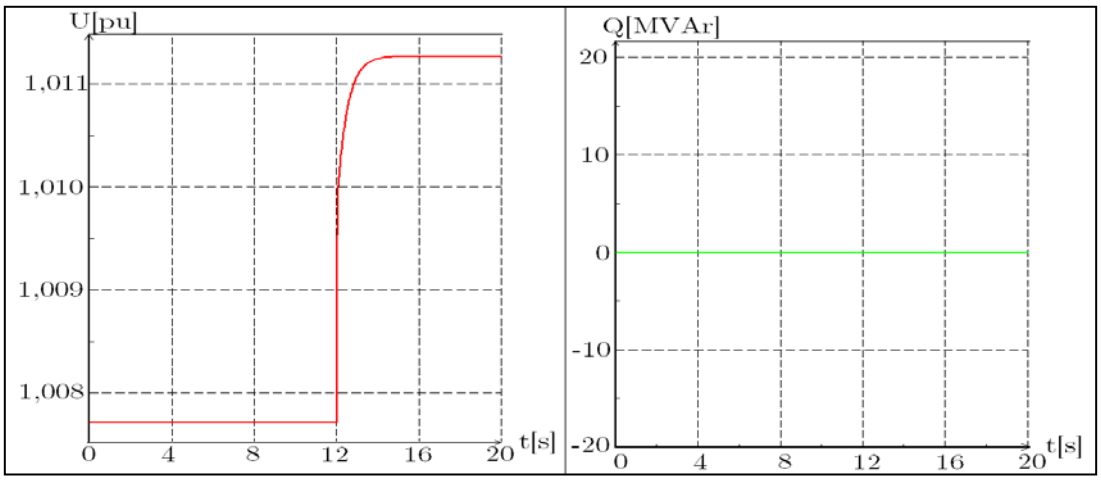

Figure 36: PV control. Left graph: Voltage changes to keep the reactive power at zero. Right graph: Reactive power kept constant.

Tuning the controller

It is important to tune the controller for transient conditions control in order to obtain the desired output signal from the converter. Oscillations due to changes in the wind can cause instabilities if they are too large. By tuning the controller, oscillations can be constrained both in amplitude and duration.

Table 5 describes the parameters in the controller. By decreasing the integrator time constant, T_{ip}, the number of oscillations increases, while decreasing the proportional gain for AC voltage support, K_q, the magnitude of the oscillations increases. The following figures show the mode of operation when modifying these parameters.

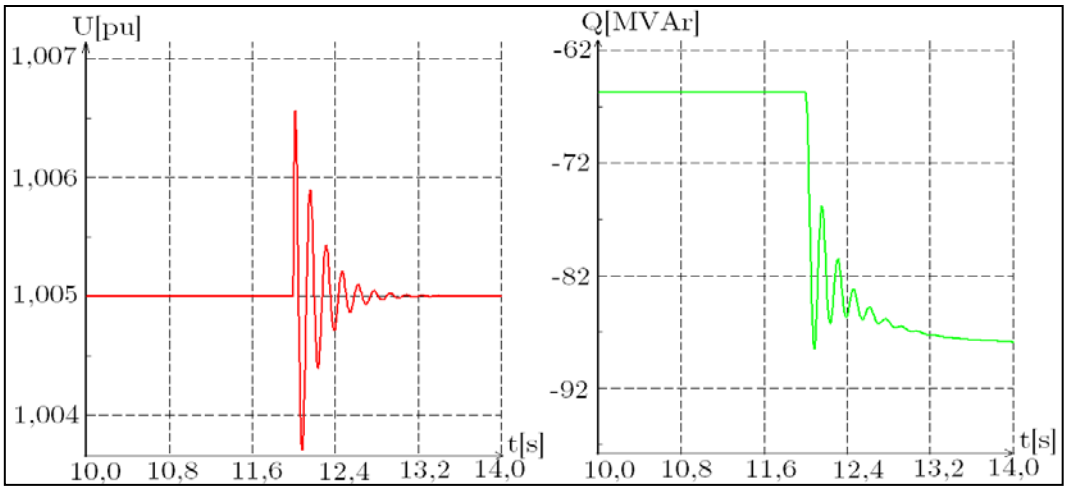

Figure 37: A small proportional gain (K_q) and a small integrator time constant (T_{iq}). The left graph shows the voltage and the graph on the right side shows the reactive power.

However, if the integrator time constant has a large value and the proportional gain is increased, the transient response will appear differently:

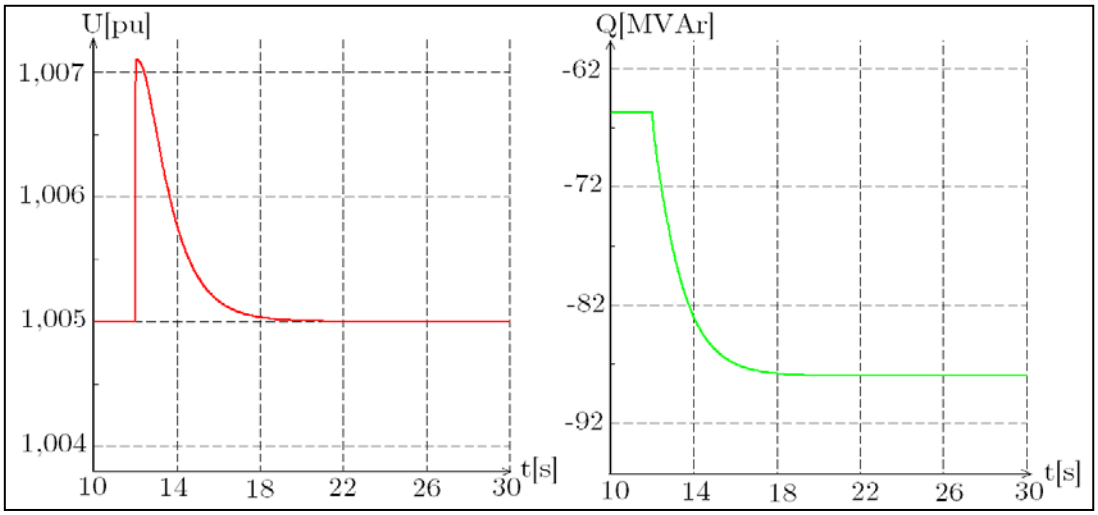

Figure 38: High proportional gain (K_q) and a high integrator constant (T_{iq}).On the left is the voltage and the reactive power is on the right graph.

After several simulations testing different values for the parameters in the controller, some parameter values resulting in good transient responses was chosen. The following table shows the parameter values chosen for the VSC in the simulations:

Table 6: Parameter values for the VSC used in the simulations.

Parameter name	Value
T_{rp} – Filter time constant, active path [s]	0,1
T_{rq} – Filter time constant, reactive path [s]	0,1
K_p – Proportional gain [pu]	2
T_{ip} – Integrated time constant [s]	0,2
$AC_{dead\ band}$ – Dead band for proportional gain [pu]	0
K_q – Proportional gain for AC-voltage support [pu]	0,5
T_{iq} – Integrator time constant [s]	0,1
i_{d_min} – Minimum discharging current [pu]	0
i_{q_min} – Minimum reactive current [pu]*	-0,5
i_{d_max} – Maximum charging current [pu]	1
i_{q_max} – Maximum reactive current [pu]*	0,5

*Differs dependent on the control mode of the VSC

7.2 Testing the Transformer Tap Changer

The purpose of utilising a tap changer on the transformer in this model is to decrease the voltages on the 33 kV-side of the transformer where the wind power production is present. The approvable voltage level is given by the grid codes to prevent instability in the system, and by utilising a tap changer transformer, the voltage at a chosen side can be decreased if it is outside the grid code limitations. More information about how the tap changing transformer operates is presented in Section 2.4.1.

To prevent the voltages exceeding its approved limits, i.e. outside the range $0{,}90 \leq U \leq 1{,}05$, a lower and upper bound for the tap changer is set. 15 taps are set as a maximum limit for the tap changer with initial tap position 0 and an additional 0,25% voltage increase or decrease per tap. The details concerning the tap changer as it is implemented in the PowerFactory model are given in the following figure. As the figure shows, using the line drop compensator is optional.

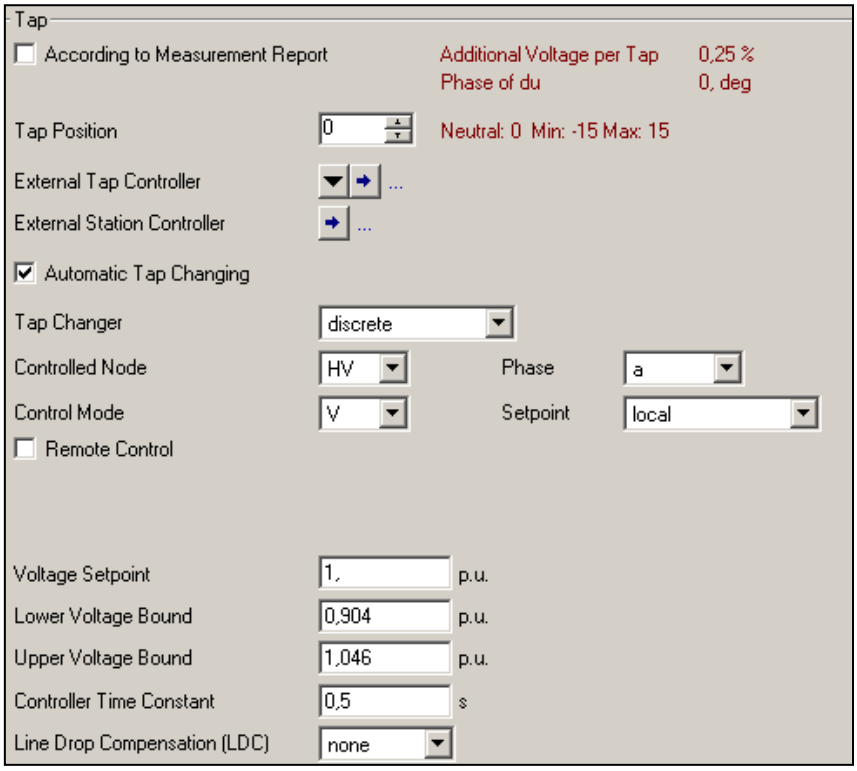

Figure 39: Tap changer applied in the PowerFactory model.

To test the tap changer transformer, a scenario is made making the voltages higher than the acceptable limits on the 33 kV side of the transformer. The wind farm is controlled in PQ mode with the reactive power output fixed at 0. To prove that the transformer taps as it is supposed to, an example is presented:

Example

The voltage at the controlling bus on the low voltage side of the transformer has in this scenario an initialised magnitude V_1. After one tap, the voltage is V_2.

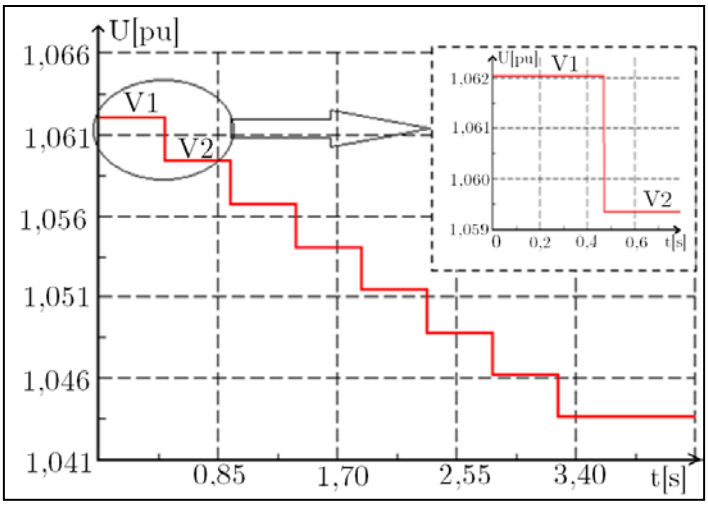

Figure 40: Voltage at the controlled node on the low voltage side of the transformer during taps.

In the figure above, the following voltage values are measured:

V_1=1,062023 pu and V_2=1,05937 pu

One tap should result in a voltage magnitude 0,25% lower than the previous voltage level, so to check if the voltage level after one tap is corresponding to the value measured, it can easily be calculated:

$V_2 = V_1(1\text{-}0{,}0025) = 1{,}062023(1\text{-}0{,}0025) =$ 1,059368 pu

The insignificant difference between the measured and calculated value is most likely caused by rounding off the measurement values. It can therefore be concluded that the tap changer taps as it should. As the figure also indicates, the tap changer taps until the voltage is below the chosen upper limit of 1,046 pu. The taps performed by the tap changer are as follows:

Figure 41: Taps performed by the tap changer.

7.3 Analysing the Behaviour of the SVC

The SVC is one of the crucial components in the simulations, so it is important to make sure the SVC behaves as it should and produces or consumes the reactive power as necessary for the system. To test the SVC, the voltage on the controlling bus is compared with the reactive power contributions from the SVC and the expected reactive power contributions are calculated by hand to check if the behaviour is correct.

The model is first run without the SVC in order to get a basic overview of the voltage at the controlling bus. An active power production step from 100 MW to 200 MW is performed after 12 seconds, resulting in an increase of the voltage as shown in the following figure:

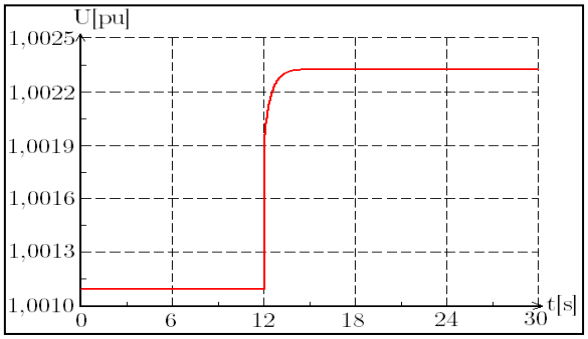

Figure 42: Voltage at the node where the SVC is to be connected.

The voltage set point of the SVC is set to 1,0007 pu in this scenario. Since the voltage in the graph is above 1,0007 pu, it is expected that the SVC will consume reactive power in order to force the voltage down for the initialisation. When the voltage increases due to the active power produced, it is expected that the SVC connected to node 1 (illustrated in Figure 46) will consume more reactive power to stabilise the voltage. Since node 1 is close to the main grid, which is represented as a slack bus, and the impedance between the main grid and node 1 is small, the voltage will remain at a low value.

With the SVC included, the voltage on the node controlled by the SVC is graphed in the following illustration:

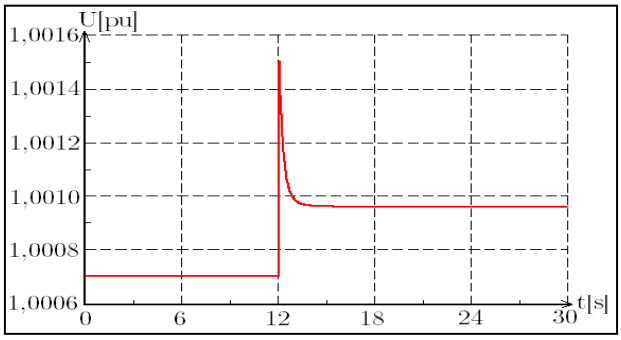

Figure 43: Voltage at the node controlled by the SVC.

Figure 43 supports the expectations concerning the voltage controlled by the SVC. Before measuring the reactive power contributed by the SVC, an expected calculated value is prepared.

The initialised voltage with the SVC controlling the voltage is 1,0007 pu. After the step in active power production, the voltage stabilises at 1,00096 pu. The formula applied in order to calculate the reactive power compensation from the SVC is:

$$Q_{produced/consumed,SVC} = \Delta V \cdot K \cdot Q_{rated,SVC} \qquad 7.1$$

$\Delta V = V_{initalized} - V_{after\ step} =$ 1,00096-1,0007= 0,00026 pu

K=100, $Q_{rated,SVC} =$ 310 MVAr

$Q_{produced/consumed,SVC} =$ 0,00026·100·310 = <u>8,06 MVAr</u>

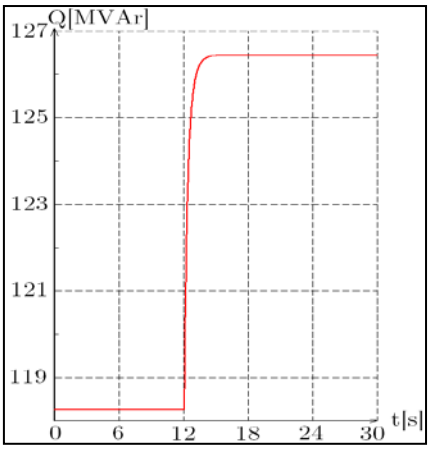

Figure 44: Reactive power contributions from the SVC with an active power production step.

As illustrated in the previous figure, the reactive power consumption initialised by the SVC has a value of 118,26 MVAr. After the step in active power production, the reactive power consumed by the SVC increases and stabilises at 126,45 MVAr. The reactive power difference between the initialisation and the stabilised value after the active power step is:

126,45 -118,26 = <u>8,19 MVAr</u>

Difference between the calculated value and the measured value:

8,06 – 8,19 = <u>0,13 MVAr</u>

Since the difference between the calculated and the measured value is relatively small compared to the amount of reactive power consumed by the SVC, it has been demonstrated that the SVC is working properly.

7.4 Simulations for P-Q Operation of the Wind Farm

The simulations performed in this section and Section 7.5 are set to increase the active power production stepwise every 12th second, with the wind farm specifying active and reactive power into node 4. As the figure below illustrates, the active power production starts at 400 MW and increase to 800 MW in 20 steps with 20 MW increase per step. To indicate the maximum length of the cables for valid operation, the simulations are run with cable lengths in the range from 20-100 km. The cable lengths are tested with intervals of 20 km.

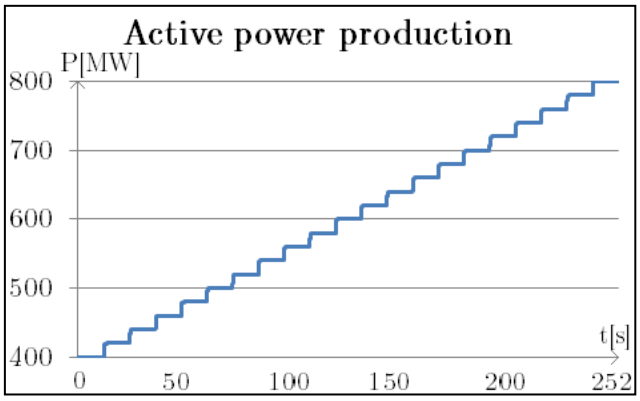

Figure 45: Active power production steps. 20 steps with 5 % power production increase per step.

A simple representation of the model is presented in Figure 46. This representation of the model shows the entire system with nodal numbering, to make it easier to understand exactly where in the system the results refer to. Only a summary of the most important results will be provided in the main document, while more graphs providing further details about the results can be found in Appendix 12.11. Table 7 gives an overview of the controlled nodes for the different dynamic voltage control devices.

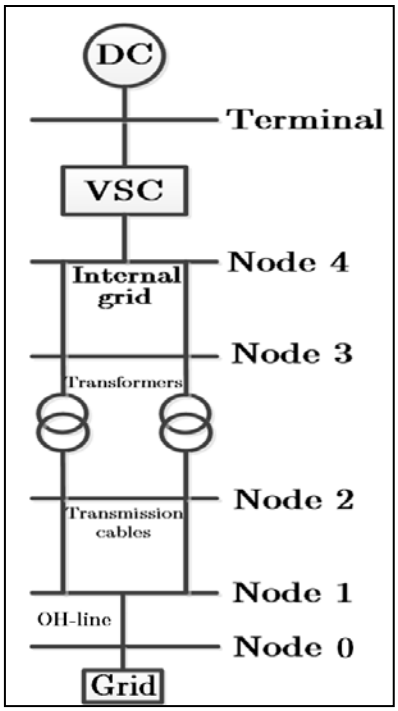

Figure 46: Simple nodal representation of the system.

Table 7: Nodes specified for the different dynamic control devices.

Dynamic voltage control devices	Controlled node
Voltage source converter	Node 4 is specified
Load tap changer	Voltage in node 3 is modified if it is outside 0,904<U<1,046
Static var compensator	Specifies node 1 for an onshore and node 2 for an offshore location

Additionally, the main grid is set as a slack bus, specifying the voltage to 1,00 pu and the voltage angle to 0°.

7.4.1 Base case scenario

To create a foundation for comparing the different control mechanisms, a base case scenario is established. The base case scenario describes the behaviour of the system with the SVC disconnected. For simulations with the purpose of analysing the behaviour of the system, it is important to investigate limiting factors in the power transmission. The low impedance implemented for the overhead line causes a low voltage drop to the system analysed and few losses in the line itself.

Cable length: 20 km

Using short transmission cables causes a moderate amount of reactive power production which keeps the current loading in the cables within its acceptable limits.

The voltages are all within the grid code limitations by far and they are displayed in Appendix 12.11.1.1, while the current in the cables is displayed in Figure 47.

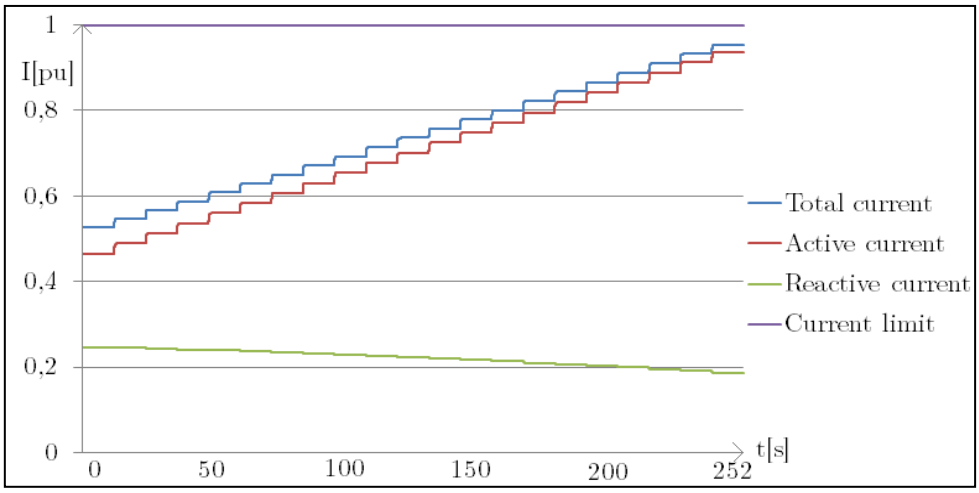

Figure 47: Current loading base case. 20 km long cables.

Cable length: 40 km

When the wind farm is located 40 km from shore without any reactive compensation, the reactive power flow in the cables is high. As shown in Figure 48, reactive power in the cables is decreasing for increasing active power production, but the total current increases since the active current is proportional to the progressive increase of power production. Thus the current loading exceeds its maximum limit when the active power production increases from 760 MW to 780 MW. Since there is a large production of reactive power in the cables and the reactive power in the wind farm is fixed at zero, the two nodes on each side of the cables will be composed of a different current loading. The highest current in the cables is onshore when no reactive power compensation possibilities are offshore.

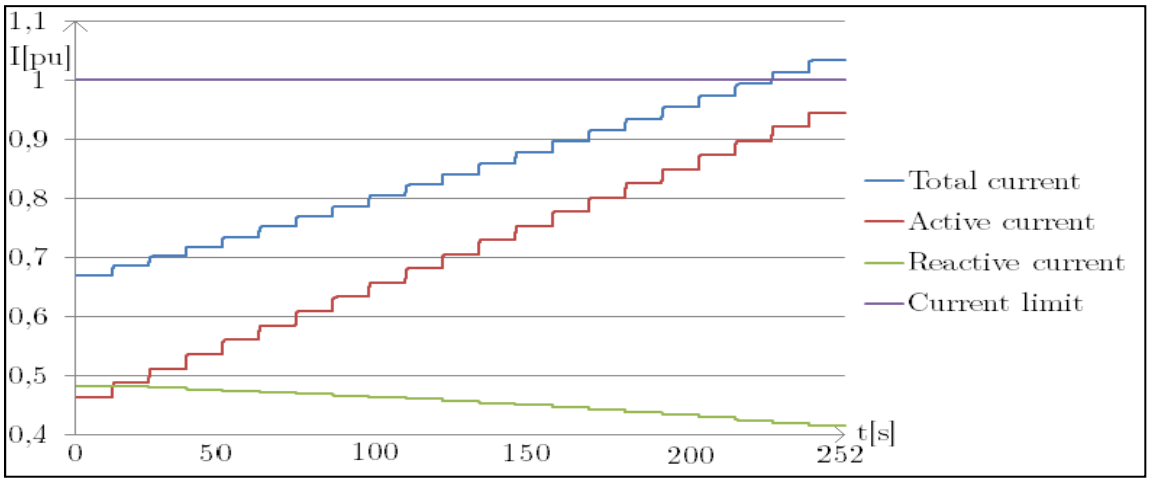

Figure 48: Current 40 km long cables. P-Q operation of the wind farm in base case scenario.

Figure 49 illustrates the active and reactive load flow in the system for 400 MW production. As the figure illustrates, the voltages are low. The reactive power flowing in the system is mainly caused by the production in the cables.

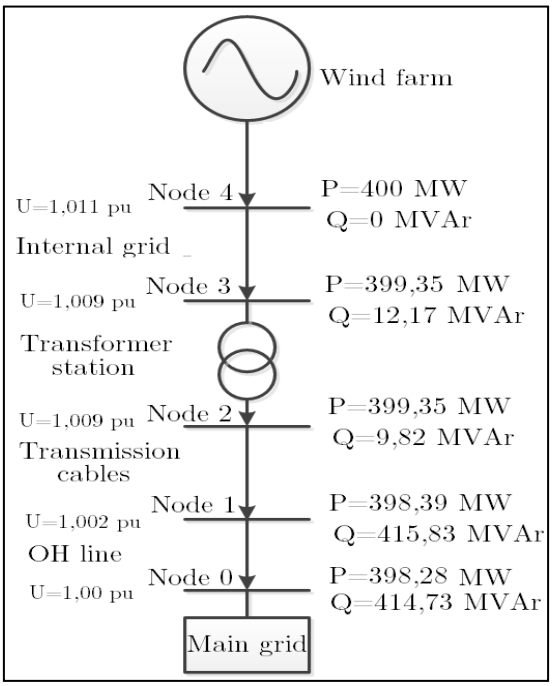

Figure 49: System characteristics for 40 km long cables in base case.

Cable length: 60 km

At 60 km, the current loading in the cables exceeds its limits if the active power production is higher than 600 MW. The voltages in all nodes are acceptable, with the highest voltage magnitude in Node 4 of 1,02 pu. Secure operation of the system is not possible due to the high current presented in Figure 50, making it unfavourable to operate the system if the wind power plant is further than 40 km from shore without applying any sort of reactive power compensation.

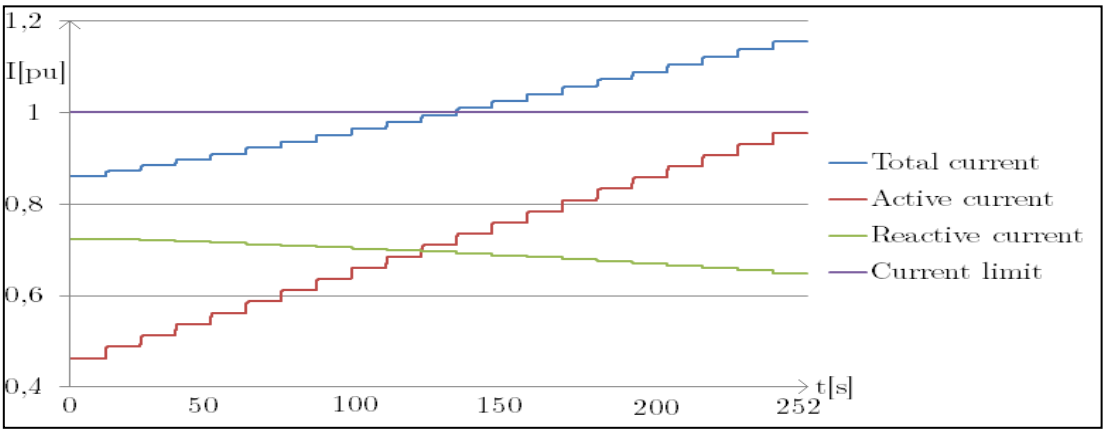

Figure 50: Current 60 km long cables. P-Q operation of the wind farm in base case scenario.

By comparing the current curves for 40 and 60 km long cables given in Figure 48 and Figure 50, the difference in reactive current is tremendous. The reactive current loading for 400 MW production at 40 km is close to 0,5 pu, while for 60 km it is almost 0,75 pu.

Cable length: 80-100 km

Placing the offshore wind power plant 80-100 km from shore with P-Q control mode of the VSC without any reactive power compensation is a hopeless case resulting in way too high current in the cables. For 80 km, the voltages are acceptable, but reaching 100 km long cables, the voltage exceeds the grid code limitations offshore when the active power production increases above 660 MW.

To keep the voltages within the grid code limitations, the load tap changer is activated. The following figure illustrates the voltages in the system with the load tap changers activated.

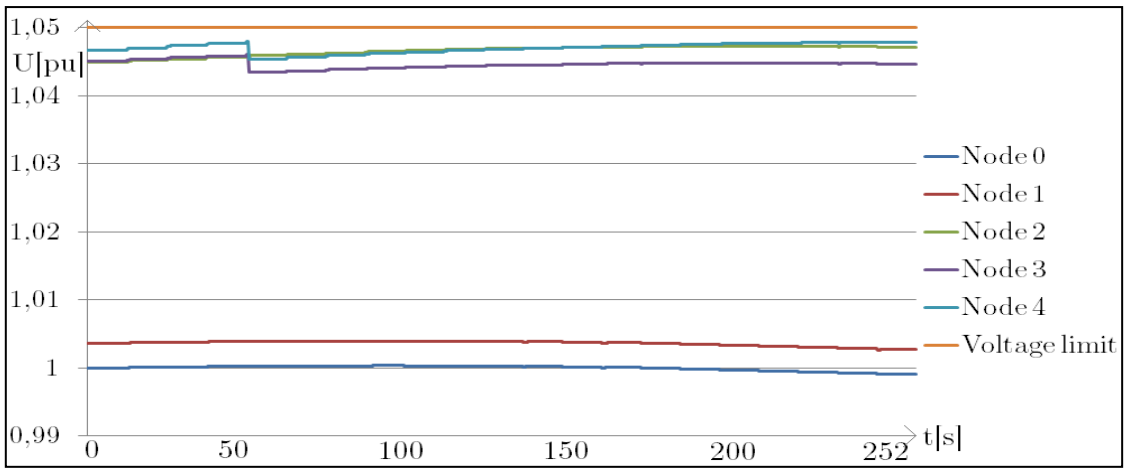

Figure 51: Voltages with LTC activated for 100 km cable length in base case.

A summary of the average reactive power production in the cables for active power increase from 400-800 MW and the current loading at 800 MW production is presented in the following table. The active power production when the cable current exceeds its limit is also presented.

Table 8: Average reactive power production and current loading in the subsea cables for 400-800 MW production in the base case.

Cable length	Reactive power production in the transmission cables	Current loading at 800 MW production	Active power production making the current exceed the subsea cables limits.
20 km	200 MVAr	0,955pu	Does not exceed limits
40 km	401 MVAr	1,033 pu	780 MW
60 km	605 MVAr	1,155 pu	620 MW
80 km	813 MVAr	1,311 pu	Immediately
100 km	1027 MVAr	1,493 pu	Immediately

As seen from the table, the reactive power production is proportional to the cable length, as it theoretically should be (ref. Equation 2.7 in the theory).

7.4.2 SVC located onshore

The SVC is activated in the model and placed onshore to determine its contribution from this location. All other system characteristics are identical to the base case.

The static var compensator can as described in Section 6.2.3 operate in reactive power or voltage control mode. In this location the simulations are performed in voltage control mode of the SVC. The challenge with this approach is to determine the voltage set point of the SVC, which is done by tentatively testing different set points and by interpretation of the resulting system behaviour. Additionally, as far as possible, both the voltages and current loading in the cables are kept within their limitations.

If the voltage set point of the SVC is above the voltage of its connected node, reactive power will be produced and a minor increase in the voltage will be experienced. Since no reactive power compensation devices are located offshore, the produced reactive power from the SVC will increase the reactive power flowing towards the external grid.

By consumption of reactive power in the SVC, reactive power flowing from the cables to the external grid will be reduced, but it will only have a minor affect on the reactive flow in the cables. The voltage will decrease slightly when the SVC consumes reactive power.

Cable length: 20 km

For cables 20 km long, both the voltages and the current flowing in the cables are within their limits, as expected.

Cable length: 40 km

Since the current is outside its acceptable range on the onshore side of the cables, an onshore location of the SVC will not contribute to system improvements without additional reactive compensation offshore.

The current exceeds its maximum limit when the production increases from 760 MW to 780 MW.

Cable length: 60-100 km

Contributions from the SVC onshore do not affect the system abilities notably, and similar results as in the base case are obtained. The LTCs tap in the same way as illustrated in Figure 51, but with a large consumption of reactive power, the transformer will tap later in the simulation. The voltage graph is displayed in Appendix 12.11.1.2.

The system characteristics will be similar to the characteristics without the SVC presented in Table 8.

The following graph illustrates how the reactive current in the cables increases with increasing cable length.

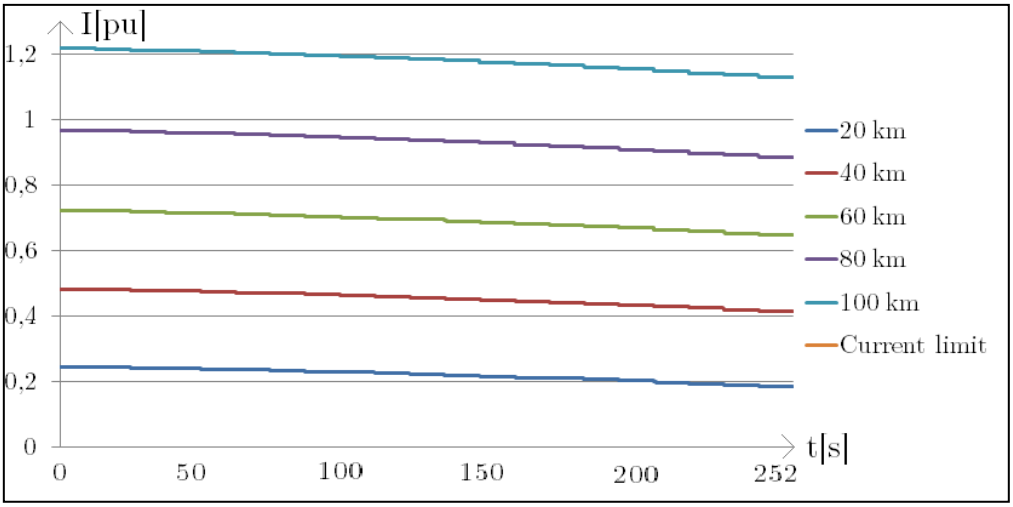

Figure 52: Reactive current flowing in the cables for cable lengths in the range 20 km<L<100 km.

There is a massive increase of reactive current in the cables when the cable length increases. The active current in the cables only experiences minor changes.

7.4.3 SVC located offshore

The SVC is positioned on the offshore side of the transmission cables between the transformers and the cables. The rest of the case is equal to the previous one.

By placing the SVC offshore, the reactive power produced by the cables can exit both on the onshore and offshore side, presenting a more convenient reactive power distribution in the cables. Since the wind farm, represented by the VSC, keeps the reactive power from the turbines at zero, the reactive power flowing in the system is principally the reactive power produced in the cables.

Cable length: 20 km

Running the simulations with 20 km cables and a stepwise increased production from 400 MW to 800 MW does not cause any problems transmitting the active power. The following figure illustrates the active power losses without any reactive compensation compared with the active losses with the SVC offshore. As indicated in the figure, the losses are constantly higher for the scenario without the SVC.

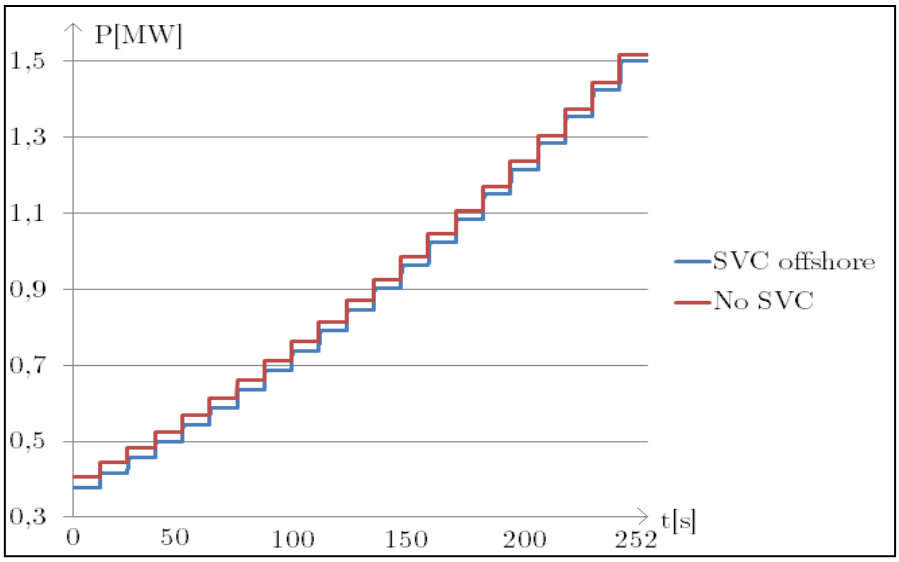

Figure 53: Active power loss with and without the SVC with 20 km long cables.

Cable length: 40 km

Introducing 40 km cable length did not give valid results for the scenarios without reactive compensation or with the SVC onshore for the production increase from 400 to 800 MW. The cable current increased above its acceptable limits when the production surpassed 780 MW. With the SVC offshore on the other hand, consumption of reactive power composes the cable current more equal on both sides, making it possible to operate with larger distances. The voltages in the system are all far from their limits as the following illustration shows. The SVC specifies the desired voltage value in node 2.

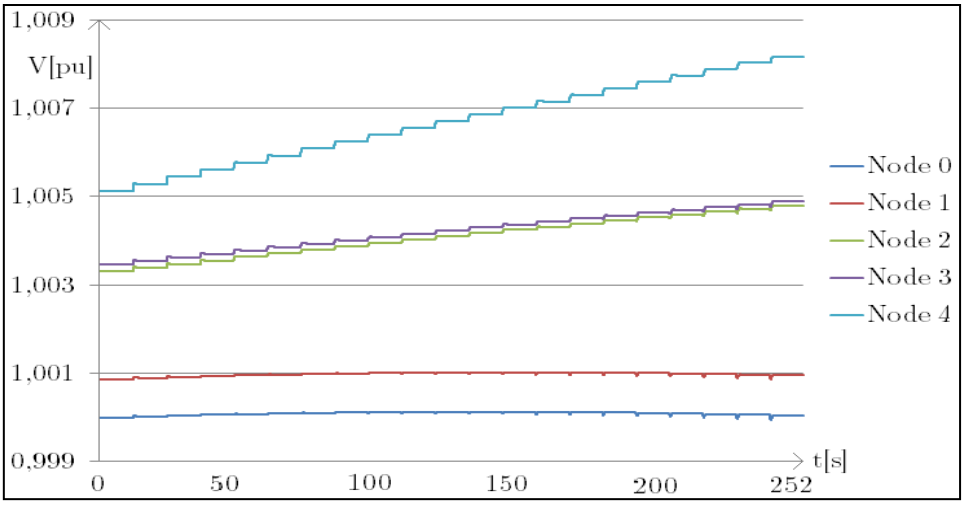

Figure 54: Voltages with the SVC located offshore. Cable length: 40 km.

The current loading in the cables is within its limit as can be seen from the following graph:

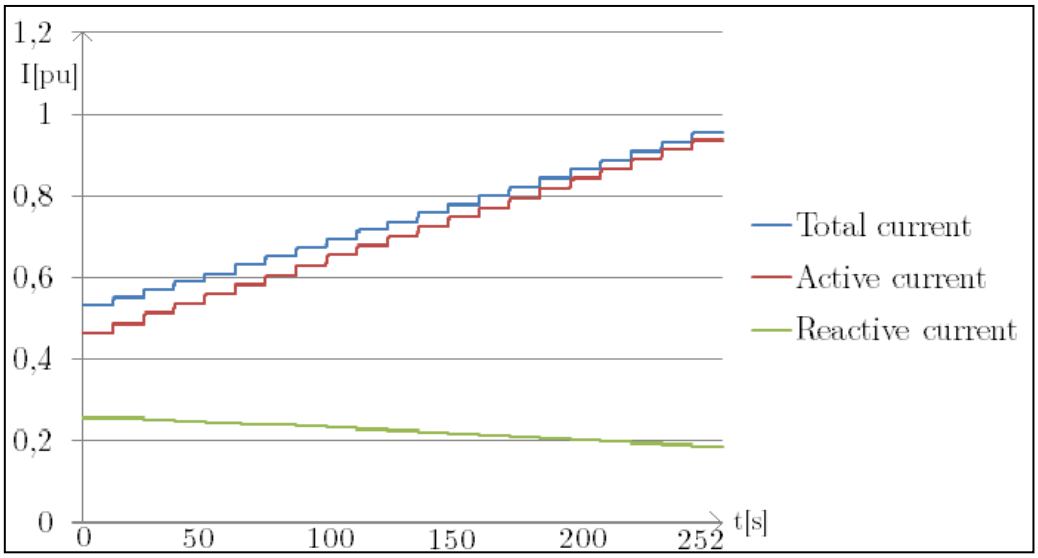

Figure 55: Current in the 40 km long transmission cables with the SVC offshore.

Reactive power flows from the internal grid, where the cables produce a small amount of reactive power, through the transformers into the SVC. The reactive power compensation necessary to keep the current as illustrated in Figure 55 is presented in Appendix 12.11.1.3.

Cable length: 60 km

The even distribution of reactive power in the transmission cables caused by consumption from the SVC leads to a valid operation of the system when the cable length is increased further to 60 km. Figure 56 illustrates how the produced reactive power with unit MVAr flows out of the cables and into the SVC leading to less current flow in the cables for 400 MW production and 60 km long cables. At this specific voltage set point, the SVC consumes slightly less than 300 MVAr.

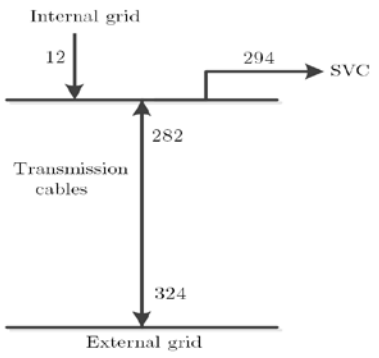

Figure 56: Reactive power flow from the transmission cables.

Neither the voltages in the system or the current loading in the 60 km long cables causes any operational issues placing the SVC offshore. The current in both ends of the cables illustrated by their per unit values is presented in the following figure. As the figure illustrates, the composition is slightly different for each side of the cable. Onshore, the reactive current decreases, while it increases offshore.

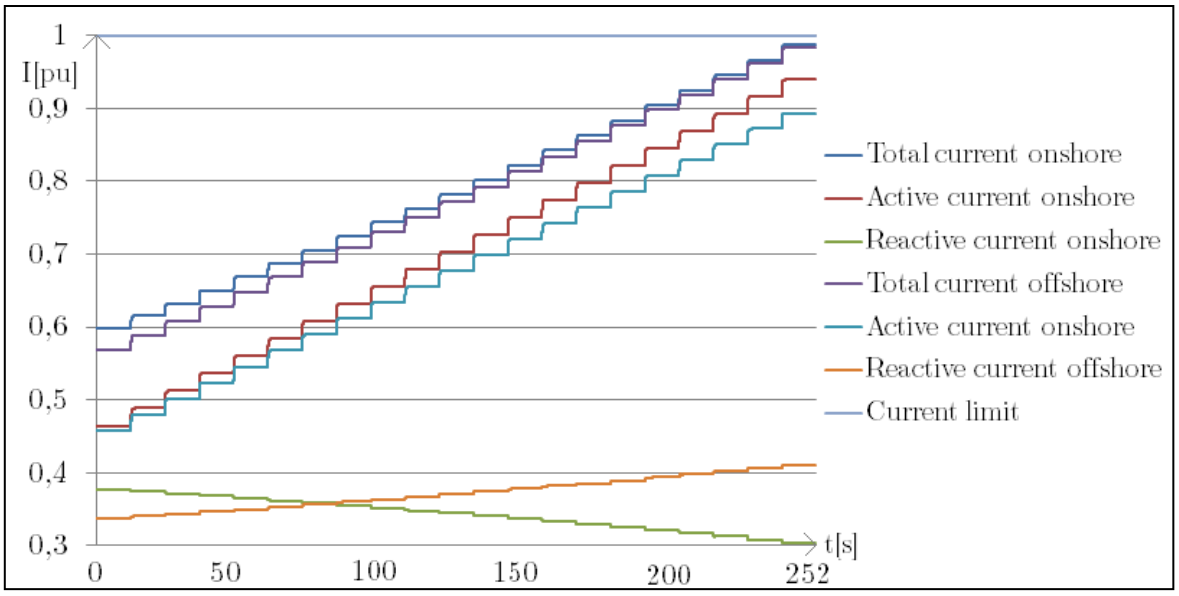

Figure 57: Current loading for both sides of the 60 km long cables.

The voltages in all nodes are in the range of 1,00<U<1,01 pu, so there are no problems with the voltages and LTCs are not necessary to utilise.

The active losses in the system are increasing with the cable length mostly because of the reactive power produced in the cables, which takes up the capacity that should be used for active power. Figure 58 illustrates the losses through the cables for 20, 40 and 60 km long cables for a stepwise production increase from 400 to 800 MW.

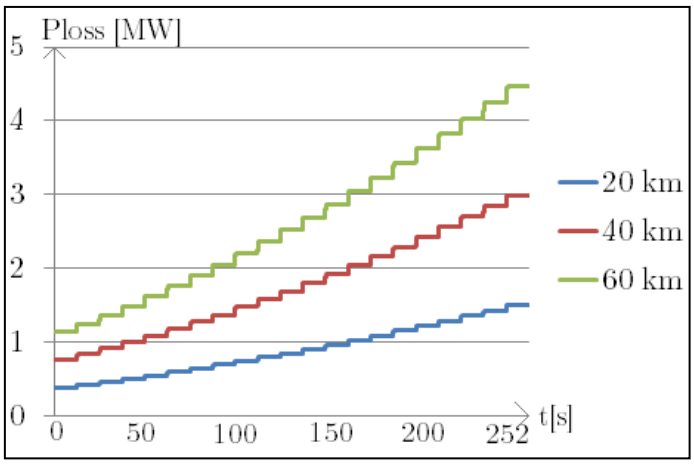

Figure 58: Active power losses with the SVC offshore for 20-60 km cable length.

In Figure 99 in Appendix 12.11.1.3, the reactive power consumption in the SVC for 60 km long cables is graphed.

Cable length: 80 km

The current is the limiting factor in the operation. When the active power increases above 700 MW, the current exceeds its limits. The current is displayed in the upcoming figure.

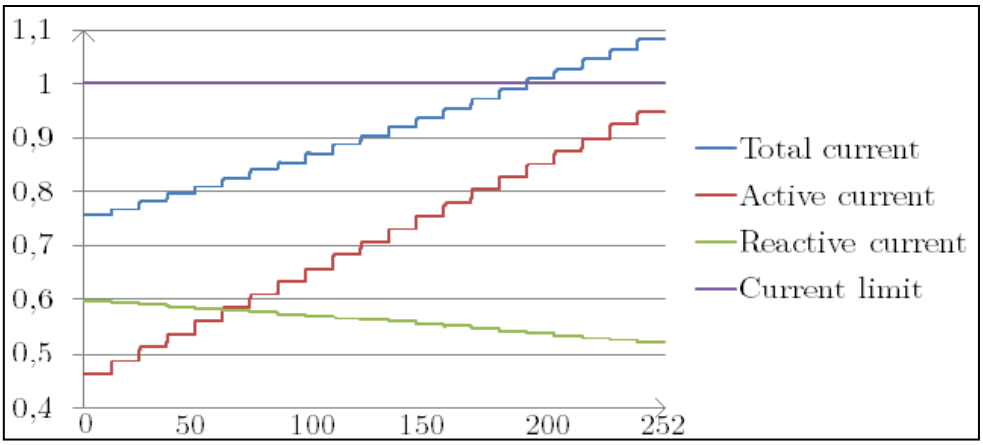

Figure 59: Current loading in the 80 km long cables with the SVC offshore.

Cable length: 100 km

When the offshore system is further away than 80 km, the characteristics of the system have a negative development. With 100 km long cables, the current in the cables are way too high, but the voltages are still fine. Table 9 presents the current loading in the cables at 800 MW production and how much the active power production is when the limits are exceeded.

Table 9: Current loading in the subsea cables for 800 MW production in the base case.

Cable length	Current loading at 800 MW production	Active power production making the current exceed the subsea cables limits.
20 km	0,935pu	Does not exceed limits
40 km	0,954 pu	Does not exceed limits
60 km	0,987 pu	Does not exceed limits
80 km	1,082 pu	720 MW
100 km	1,229 pu	480 MW

7.4.4 Summary of results with the wind farm in P-Q control mode

The results of the simulations performed in P-Q operation of the wind farm are summarised below. "ok" represents an operation with voltages and current characteristic within their limits and "no" means that the voltages or current loading in the cables are too high. If the current loading exceeds 100 % before 800 MW production, it is not acceptable in the table. As seen from this summary, SVC onshore has very limited effect, and does not cause a noteworthy improvement of the results. SVC offshore, on the other hand, results in better system operations.

Table 10: Summary of system characteristics with the wind farm operating in P-Q mode.

System characteristics		Voltages					Current loading				
	Cable length	20	40	60	80	100	20	40	60	80	100
No SVC	No LTC	ok	ok	ok	ok	no[1)]	ok	no	no	no	no
	With LTC	ok	ok	ok	ok	ok	ok	no	no	no	no
SVC onshore	No LTC	ok	ok	ok	ok	no[1)]	ok	no	no	no	no
	With LTC	ok	ok	ok	ok	ok	ok	no	no	no	no
SVC offshore	No LTC	ok	ok	ok	ok	ok	ok	ok	ok	no	no
	With LTC	ok	ok	ok	ok	ok	ok	ok	ok	no	no

[1)] The voltage in node 4 is unacceptable.

7.5 P-V Control of the Wind Farm

When applying P-V control mode to the wind farm in the model, a correct initialisation of the production can be difficult to obtain due to limitations in the reactive compensation devices. The voltage set point of the wind farm has a large influence on the system characteristics. Four different voltage set points are compared in these simulations. 1,000 pu, 1,005 pu, 1,010 pu and 1,015 pu are the voltage set points tested for the system, both without any reactive power compensation, and with the SVC onshore and offshore.

Reactive power restrictions of the VSC are set to +/- 50% of the active power initialisation. Active power production increases from 400 to 800 MW during the operation scenario.

Since both different system characteristics and different voltage set points are analysed, only a few chosen cable lengths will be presented. To compare the system abilities for the different scenarios, operation for two different cable lengths will be presented for each scenario. These two cable lengths are:

- The longest cable length within acceptable operation conditions for all of the tested voltage set points of the VSC
- The longest cable length where a least one of the voltages set point provides an acceptable operation.

The maximum cable lengths possible to apply for the different voltage set points and system characteristics are presented in Table 11.

Table 11: Summary of maximum cable lengths for different voltage set points.

	Without SVC	SVC onshore	SVC offshore
Max cable length $U_{setp, VSC}$:1,000 pu	42 km	42 km	62 km
Max cable length $U_{setp, VSC}$:1,005 pu	54 km*	54 km*	66 km*
Max cable length $U_{setp, VSC}$:1,010 pu	26 km*	26 km*	58 km
Max cable length $U_{setp, VSC}$:1,015 pu	28 km**	28 km**	35 km*

*The operation for these cable lengths is presented in this section
**The current in the cables are too high

7.5.1 Base case scenario

The first set of simulations is performed with 26 km long cables, which is the maximum cable length giving a valid initialisation for all the voltage set points. However, with a voltage set point of 1,015 pu, it is not possible to obtain a valid operation without the SVC. The other set of simulations has a cable length of 54 km, which is the maximum for initialisation with a voltage set point of 1,005 pu. These results are obtained without an SVC in the system.

Cable length: 26 km

The currents for the mentioned voltage set points tested for 26 km long cables can be seen in the following figure.

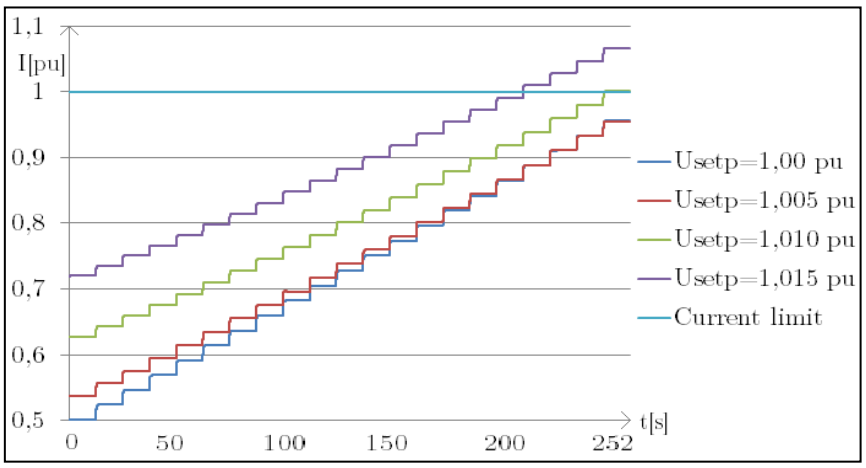

Figure 60: Currents in the 26 km long cables for different voltage set points of the wind farm.

As Figure 60 illustrates, all voltage set points of the wind farm gives acceptable currents except for 1,015 pu. All the voltages are within the acceptable range 0,90<U<1,05 given by the grid codes.

The active power loss in the cables for a sample of chosen active power productions are displayed below.

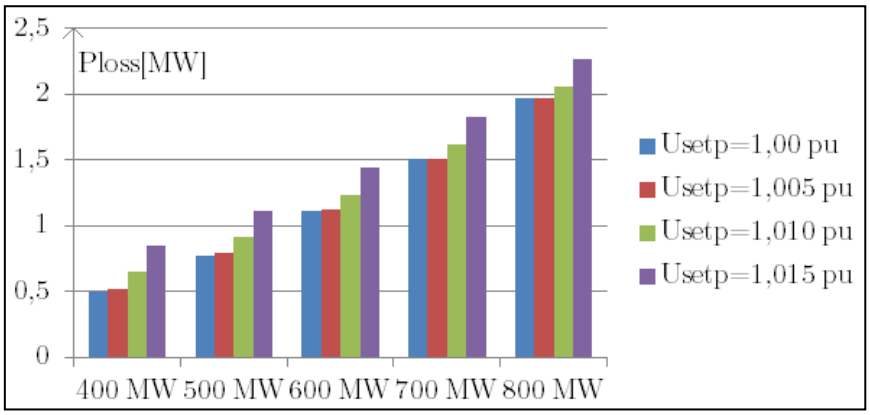

Figure 61: Active power loss with different voltage set points in the VSC and 26 km long cables.

The active power loss in the system is closely related to the current in the cables, as can be seen from the two previous figures.

The voltage set points are chosen to cover the entire range of the voltage source converter's abilities. As the following figure illustrates, when the voltage set point is low, the wind farm is at its limit for consumption. On the other hand, high voltage set points (in this case 1,015 pu) makes the wind farm produce reactive power at its

maximum limit to keep the voltage at the desired set point. Consumption is defined to be positive in Figure 62.

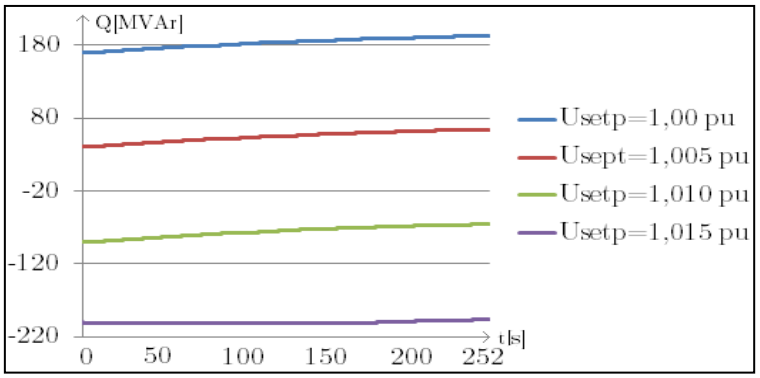

Figure 62: Reactive power consumed by the wind farm for different voltage set point with 26 km long cables.

Cable length: 54 km

The cable length is increased to 54 km to see how the system behaves with local regulation on the wind farm as the only voltage control in the system.

Initialisation of the system is not possible with the voltage set point at 1,000 pu. The reason is that the maximum limit for consumption in the wind farm is reached, and the voltage set point cannot be held. The active power produced in the start-up sequence for a voltage set point of 1,000 pu is lower than commanded. After a short period of time, the active production stabilises at the correct value, but the consumption of reactive power in the VSC increases above the maximum allowed limit.

The voltages are low in all the nodes for all voltage set points simulated. In Appendix 12.11.2.1, the graphs for the voltages with 54 km long cables are attached.

With 1,000 pu as the set point, the current is within its limit because the wind farm consumes more reactive power than allowed, as seen in Figure 63. For the voltage set points 1,010 pu and 1,015 pu, the current is too high as graphed the following figure. The reactive power consumed by the wind farm is shown in the graph to the right.

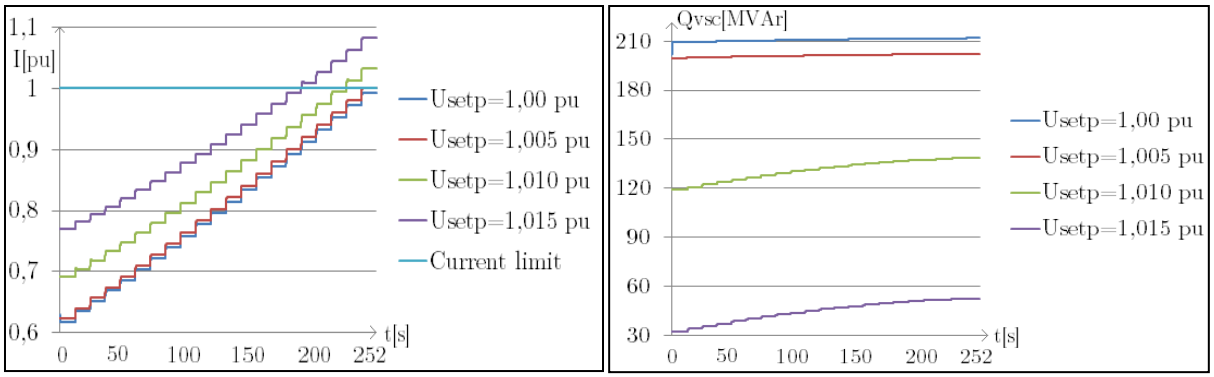

Figure 63: Current in the 54 km long cables and reactive power consumption in the wind farm for different voltage set points.

The reactive power consumption necessary is higher for all voltage set points for this cable length, than for 26 km long cables because the reactive power production in the cables is larger.

7.5.2 SVC located onshore

Contributions from the SVC affect the reactive power flowing in the overhead line towards the external grid. Only a minor part of the contribution flows through the cables and affects the wind farm if there is available capability offshore. Thus, it was not possible to operate the system with longer cables than in the previous section.

To illustrate the effects of applying the SVC onshore, the reactive power flow and cable current compared to system operation without the SVC is presented. In Figure 64, the reactive power flow to the wind farm, main grid, SVC and in the cables is illustrated with 26 km long cables and a voltage set point of 1,000 pu. In this scenario, the highest cable current was on the offshore side of the cables, which might lead to better results when the SVC is consuming reactive power. For all the other scenarios, the highest current was onshore and the SVC would have to produce reactive power to affect the cable transmission, but the reactive power flowing towards the external grid would then also increase. However, the contributions from the SVC onshore only affect the offshore system slightly even with large reactive power consumption as the figure illustrates.

Only 13 MVAr of the 153 MVAr consumed by the SVC affects the offshore system, which means that 8,5 % of the contributions from the SVC onshore is utilised for offshore adjustments. The rest is consumed from the main grid.

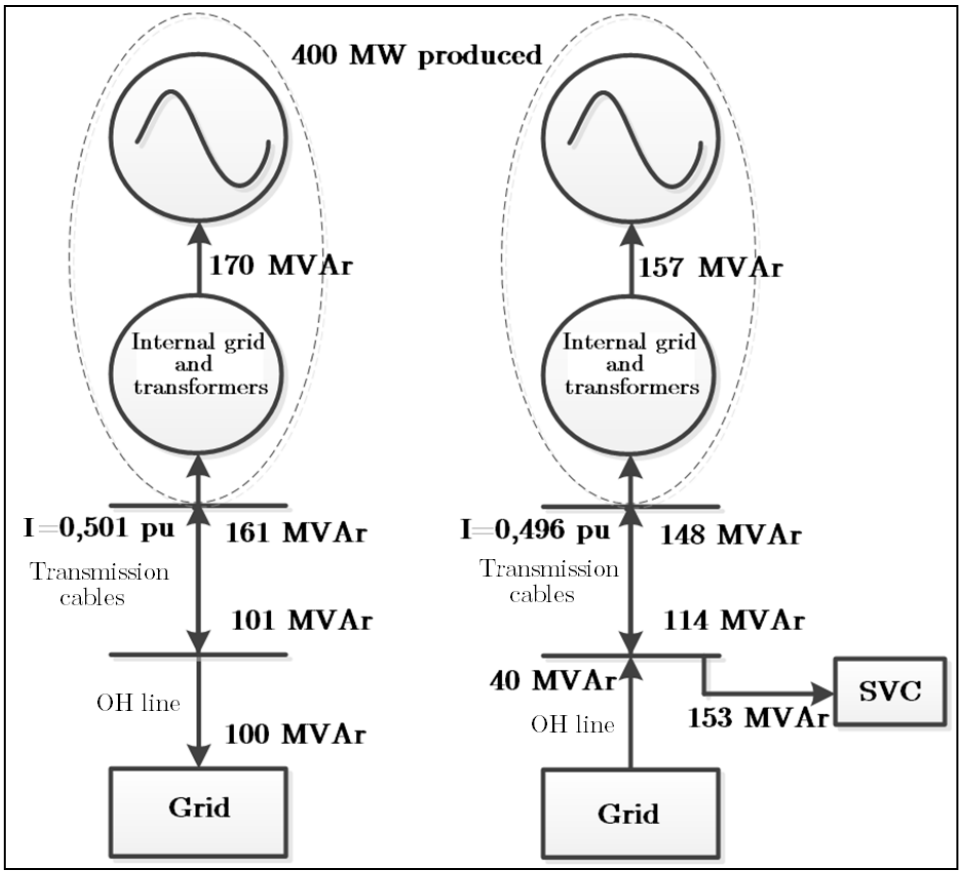

Figure 64: Reactive power flowing in the system without SVC and with the SVC consuming reactive power onshore for 400 MW production.

A scenario where the highest cable current is on the onshore side of the cable is presented. The cables are 26 km long and the voltage set point of the wind farm is 1,005 pu.

To make the SVC onshore decrease the current in the cables, reactive power needs to be produced. As Figure 65 illustrates, the SVC is producing 262 MVAr. 22 MVAr of this is entering the cables, which is 8,4% of the total reactive power contribution from the SVC. The rest of the produced reactive power flows into the main grid, which makes the reactive power flow in the overhead line large. The cable current only decreases slightly.

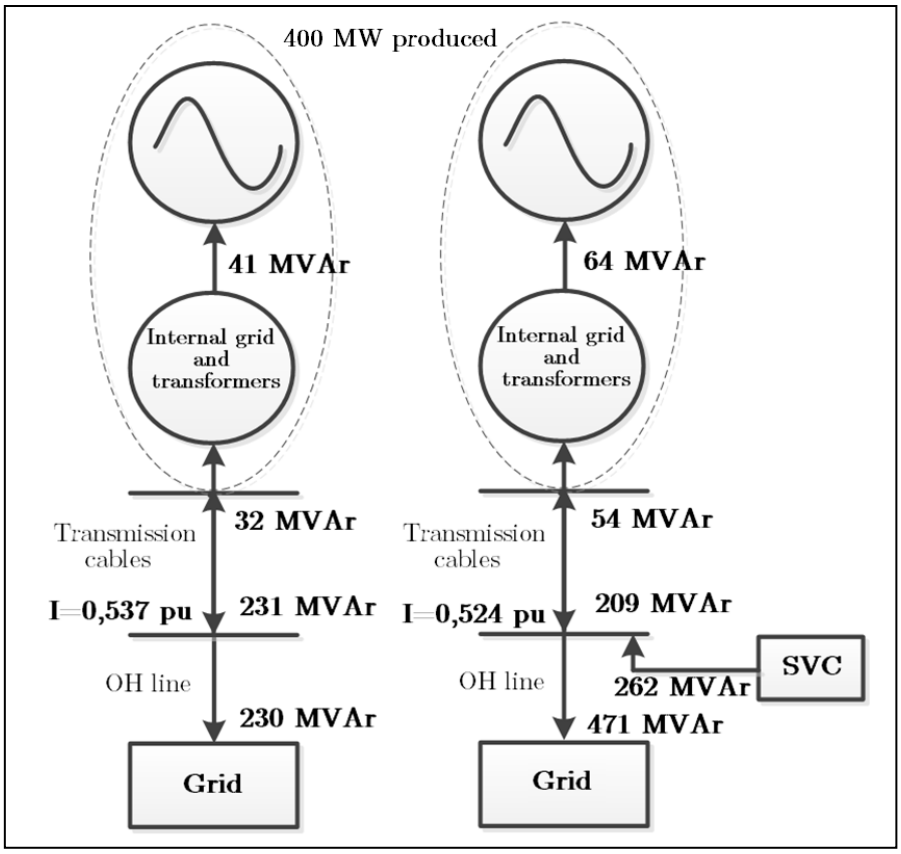

Figure 65: Reactive power flowing in the system without SVC and with the SVC producing reactive power onshore for 400 MW production.

7.5.3 SVC located offshore

Performing simulations with the wind farm in P-V control mode provides stable voltages throughout the system. However, due to the rated reactive power limits of the VSC, initialisation of the system can be hard to manage. To be able to initialise the system with the given restrictions on the reactive power consumption in the wind farm, the voltage set point of the SVC needs to be in accordance with the voltage set point of the wind farm. A valid operation for all voltage set points is achievable for cable lengths up to 35 km. The maximum possible cable length was 66 km, obtained with a voltage set point of 1,005 pu.

Cable length: 35 km

The currents when operating the system with the SVC offshore and different voltage set points of the VSC for 35 km long cables are illustrated in the following figure. As the figure shows, the current for the voltage set point of 1,015 pu reaches its maximum limit. The active power is still increasing from 400-800 MW during the simulation.

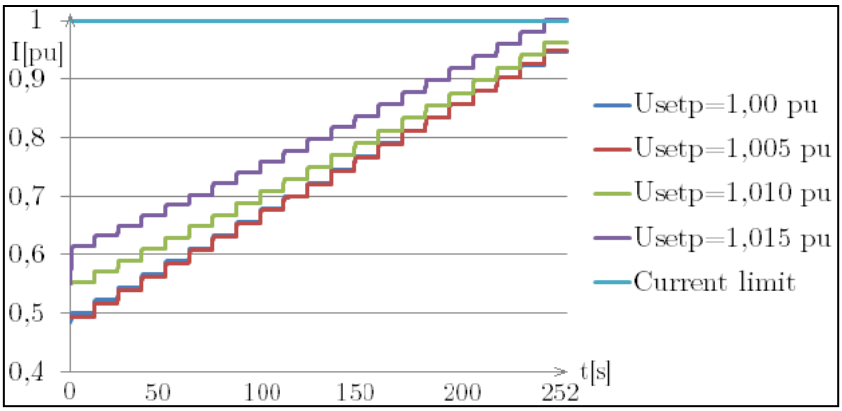

Figure 66: Currents with different voltage set points of the VSC. SVC located offshore. Cable length: 35 km.

In the simulations performed in this section, the current in the cable is kept as low as possible, given that a valid initialisation is obtained, thus making the active power losses in the cables small.

The voltages are all within the limits given in the grid codes by a large margin. The reactive power compensation necessary for the given operation for both the wind farm and SVC is illustrated in Figure 66. Negative value in the graph represents reactive power production.

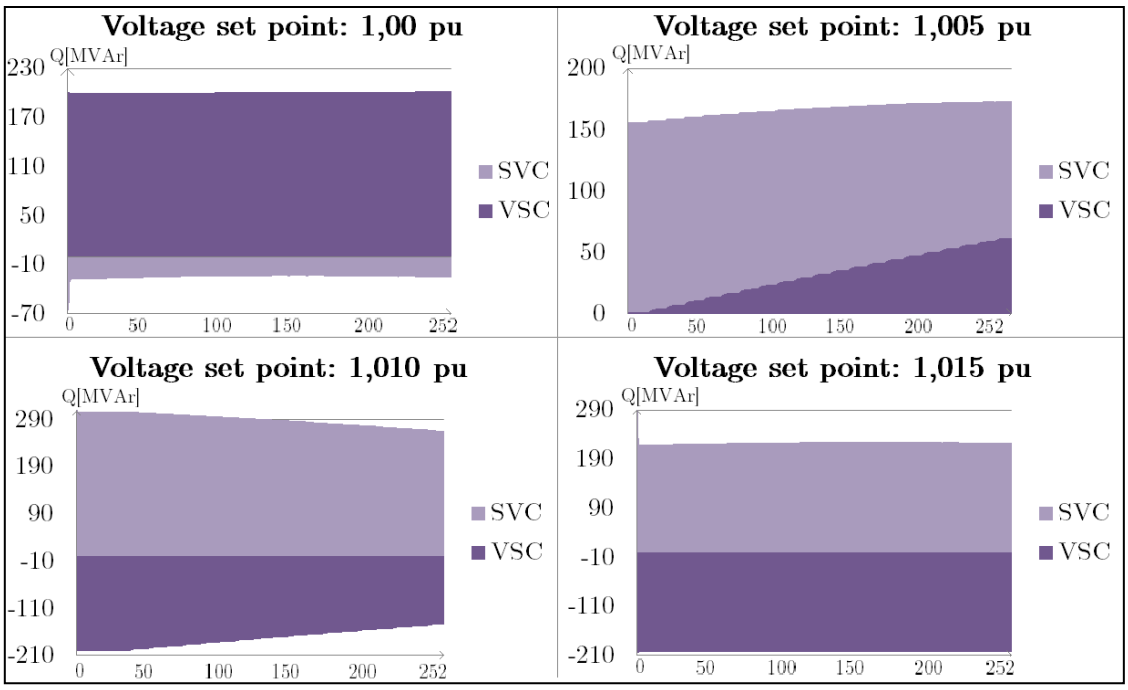

Figure 67: Reactive power consumption from the VSC and SVC at different voltage set points of the VSC. Cable length: 35 km.

Cable length: 66 km

The maximum cable length giving a feasible solution is obtained by setting the voltage set point of the VSC to 1,005 pu. The system is possible to operate with the wind park 66 km away from shore with an SVC located offshore. The following illustration presents the current in the cables for different voltage set points of the wind farm with 66 km long cables.

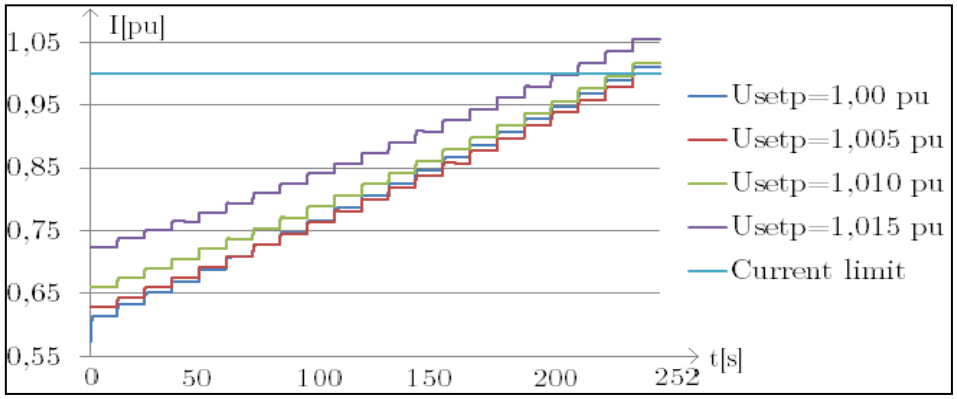

Figure 68: Currents with different voltage set points of the wind farm. SVC located offshore. Cable length: 66 km.

As the graph above illustrates, the cable current is within the rated value for a voltage set point of 1,005 pu. All the other voltage set points simulated in this thesis provides higher currents than acceptable for 66 km cable length.

The reactive power consumption of the VSC and the SVC located offshore to obtain the results given in Figure 68 can be illustrated as follows:

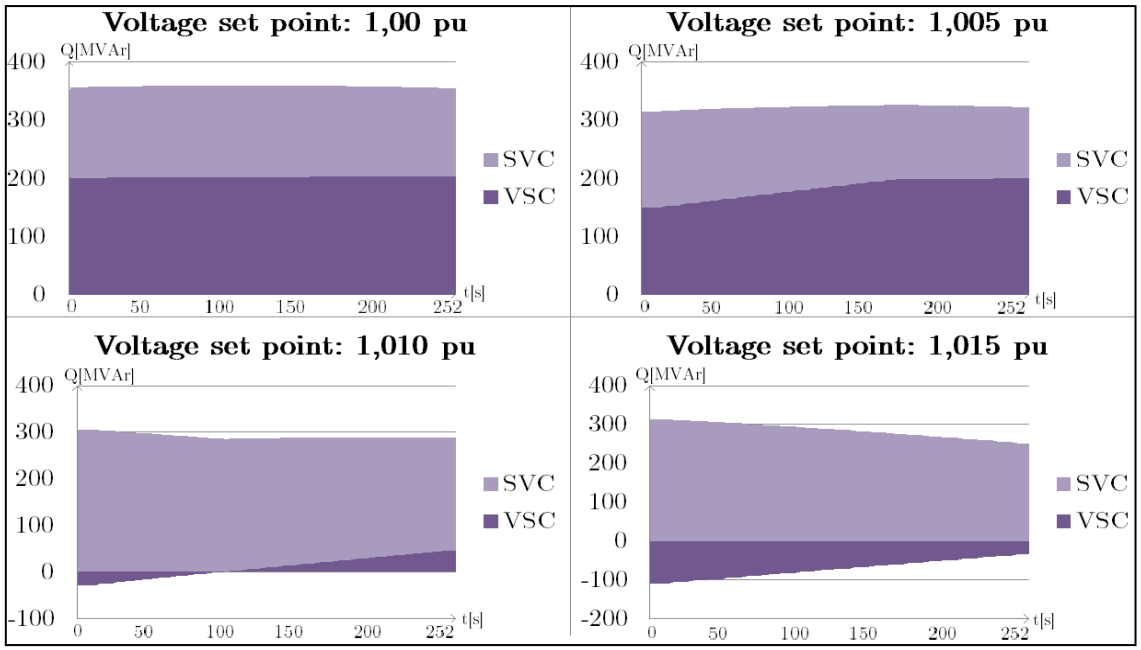

Figure 69: Reactive power consumption in the VSC and SVC at different voltage set points of the wind farm. Cable length: 66 km.

As the figure shows, the wind farm consumes a large amount of reactive power for low voltage set points to keep the voltage low. When the voltage set point is higher, reactive power is produced in order to keep the voltage high.

7.5.4 Summary of results with the wind farm in P-V control mode

Table 11 summarises the maximum possible cable lengths for different voltage set points of the wind farm. For all simulations performed in P-V control mode of the wind farm, a voltage set point equal to 1,005 pu provides the longest cable lengths possible for a feasible solution, while a voltage set point of 1,015 pu provides the shortest cable lengths.

The voltages for all simulations with the wind farm operation in P-V control mode are within the grid code limitations. The cable current and the rated value for reactive power compensation and production give the limitations of the system.

7.6 Coordination between the LTCs and the SVC

The sole purpose of this case is to interpret the coordination between the different control devices to establish whether or not counteractions can cause imbalances. To manipulate the system to operate with high voltages, the overhead line connected is implemented with high impedance, which causes a large voltage drop between the main grid and the transmission cables. The SVC will be tested both on the 300 kV side of the cables and on the 33 kV side of the transformers to examine if either of the locations will cause coordination issues, and to determine the SVC's control abilities closer to the wind farm.

7.6.1 SVC located on the 300 kV side of the transformer

First, the SVC is placed on the offshore side of the cables. The controlling nodes for the different voltage control devices are given in Table 12.

Table 12: Nodes controlled by the different voltage control devices.

	Wind farm	Load tap changer	Static var compensator
Controlled node	Node 4	Node 3	Node 2

The wind farm specifies the reactive power output to zero and the active power to step up the production in three steps every 12th second with 100 MW increase for each step starting at 400 MW. The voltages in the system without any reactive power compensation are displayed below for 52 km cable length. The voltage at the main grid (node 0) is approximately 1,00 pu for all simulations, so it will not be plotted in the voltage graphs.

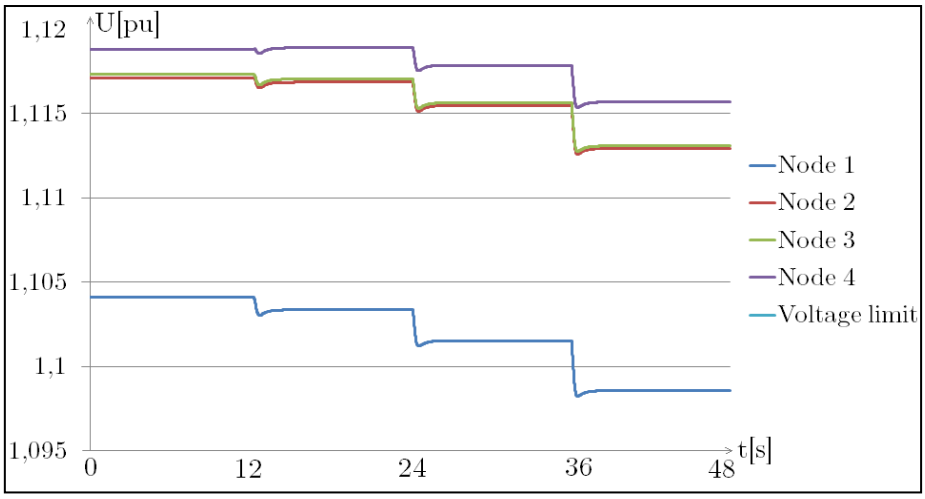

Figure 70: Voltages without reactive compensation.

The voltage regulations presented in the grid codes are simplified to be applicable with maximum and minimum voltage limits in the range 0,90<U<1,05 pu. All the voltages in the graph above are outside the grid code limitations.

The voltages when the SVC is located offshore are presented in the following graph.

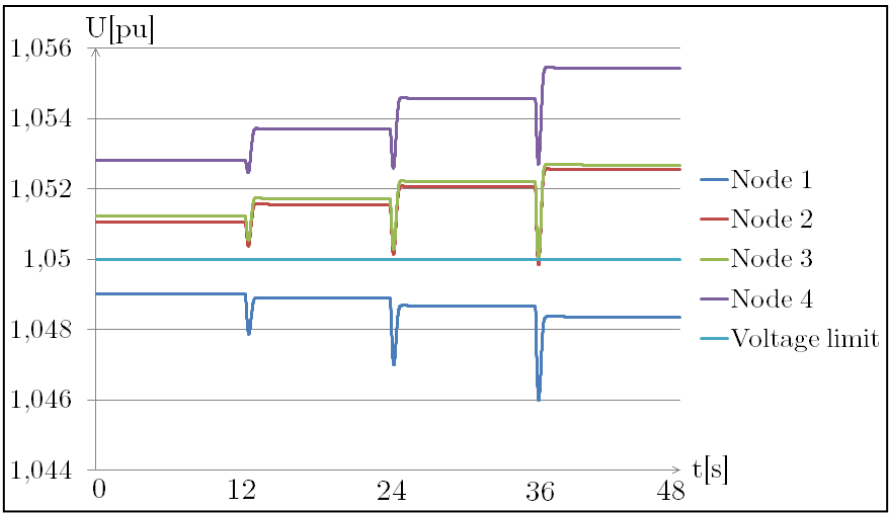

Figure 71: Voltages with the SVC located offshore.

Significantly lower voltages are possible to achieve when the SVC supplements the system. However, the voltages on the 33 kV side of the transformer and the voltage in node 2 are above acceptable limits. Reactive power consumed from the SVC is at its maximum limit. In Appendix 12.11.3, the graph of the reactive power consumed by the SVC is attached.

Only the LTCs are active in the system in the following graph.

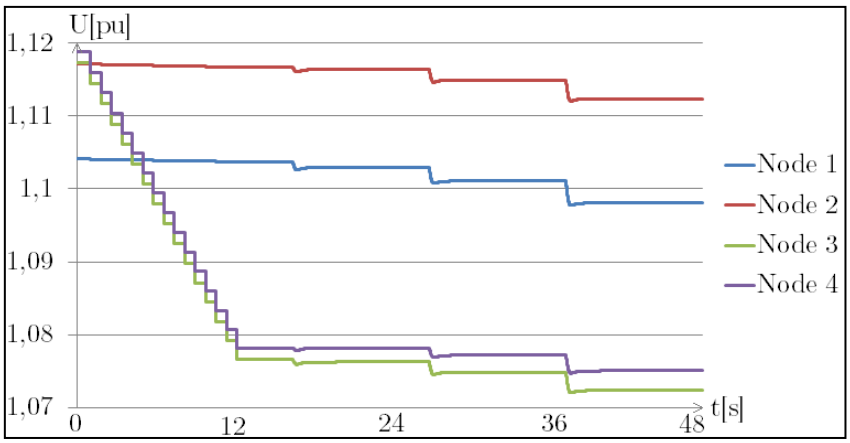

Figure 72: Voltages with the LTCs activated.

The voltages with the LTCs activated are all too high, even when the tap changer taps as much as possible. However, the voltages on the 33 kV side are decreased significantly. When applying both the LTCs and the SVC offshore, the following voltages are obtained:

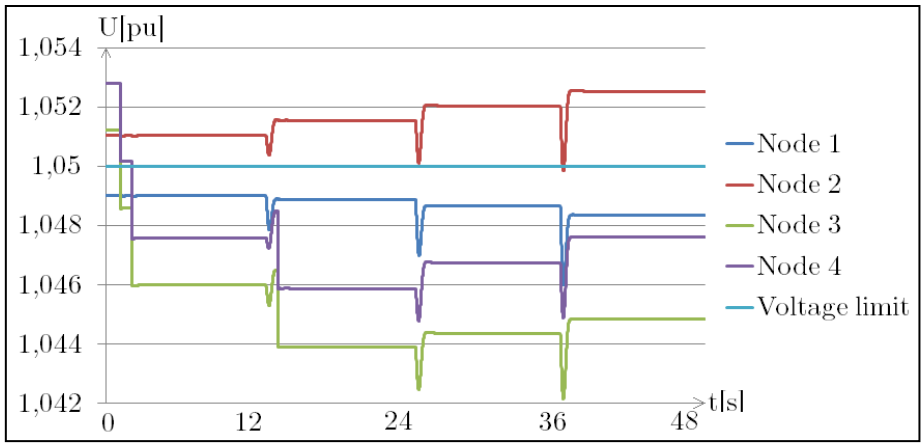

Figure 73: Voltages with both the SVC on the offshore side of the cables and the LTCs is activated.

The load tap changer taps three times to decrease the voltage level on the 33 kV side of the transformer. All the voltages are within acceptable range, except the voltage in node 2, which is the node with the SVC connected. For the operation with only the SVC contributing to the system, the voltage in node 2 had approximately the same magnitude as in this case. The reactive power consumed by the SVC is displayed in the figure below.

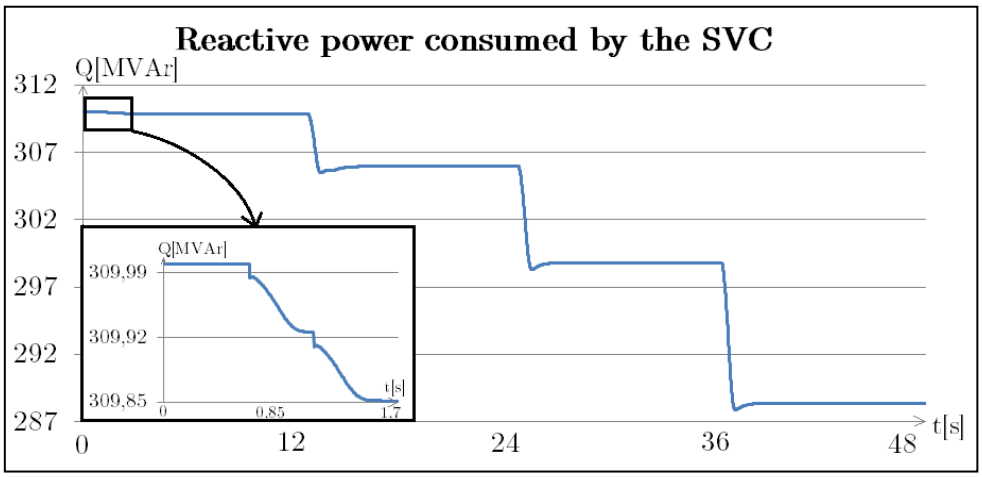

Figure 74: Reactive power consumed by the SVC in node 2 with the LTC on.

There does not seem to be any coordination issues of significance between the SVC and the LTCs when the SVC is located in node 2 and the LTCs taps at node 3. Figure 74 illustrates the insignificant influence the tap changer has on the performance of the SVC.

7.6.2 SVC located on the 33 kV side of the transformer

The SVC is moved to node 3 (33 kV side of the transformer) to investigate the system performance with the SVC in this location. In the first scenario, the simulations are performed without the LTCs activated.

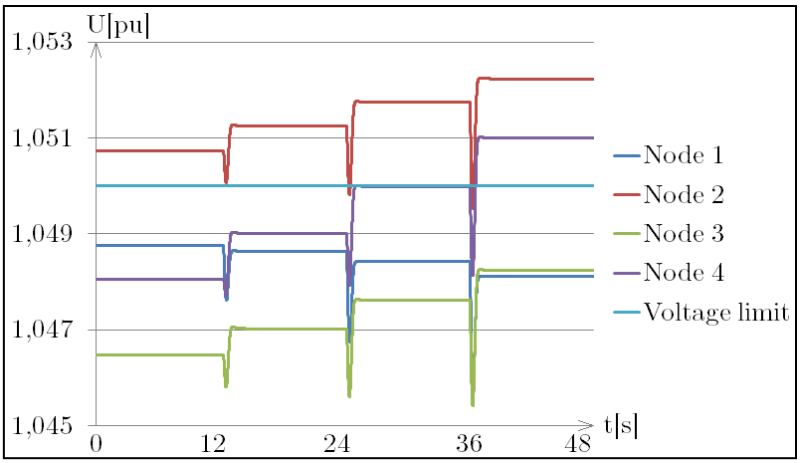

Figure 75: SVC connected to node 3 on the 33 kV side of the transformers.

Improved voltage characteristics are achieved with the SVC connected to the node on the 33 kV side of the transformer compared to the SVC located on the 300 kV side of the transformer, but the voltage in node 2 is still too high as it is for all the scenarios. However, the voltage in node 4 was consistently too high when the SVC was connected to node 2. In this case, the voltage in node 4 only exceeds the limit when the active power production steps up to 700 MW.

The LTCs are activated and the SVC is connected to the same node as the LTCs. The corresponding voltages are shown in the following figure:

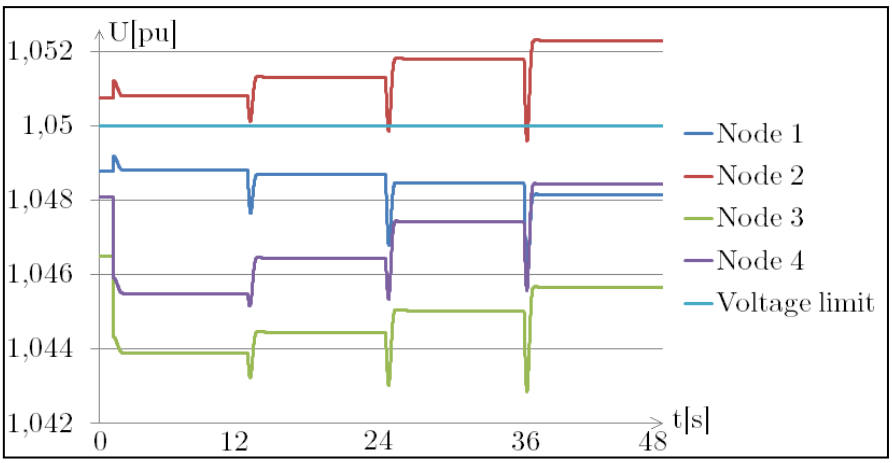

Figure 76: Voltages with the SVC connected to node 3 and the LTCs activated.

The SVC consumes reactive power as it should, and the tap changer taps when the voltages are outside the pre-determined interval, as can be seen in Figure 39, is set to be 0,904<U<1,046.

The reactive power consumed by the SVC is presented in the following figure:

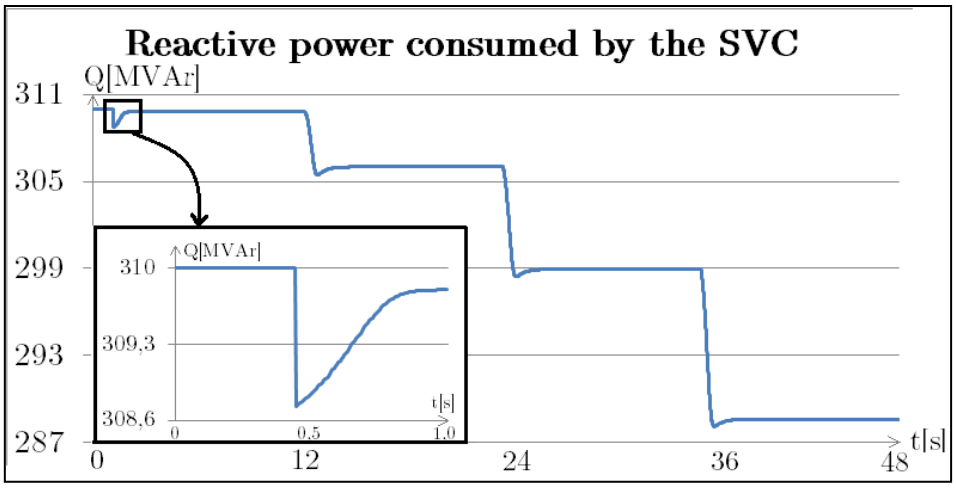

Figure 77: Reactive power consumed by the SVC with both the SVC and LTCs controlling the same node.

Figure 77 illustrates that the reactive power consumed by the SVC is slightly affected by the tap from the LTCs due to the small voltage increase in node 2. Coordination issues between these two components can be considered insignificant for the relevant scenarios.

Comparing results in Figure 71 with those in Figure 75, where the SVC is connected on the 300 kV side of the transformer, it can be seen that the best voltage control is achieved with the SVC on the 33 kV side.

The problem when the SVC is connected to node 2 is the voltages on the nodes close to the production and the voltage on the offshore side of the cables. With the SVC located at node 3, the voltages close to the production decrease, while the voltage in node 2 is approximately the same.

7.7 Annual Production and Cable Losses

In order to determine the benefits of applying a compensation device to an offshore system, annual losses in the cables have been estimated both without the SVC and with the SVC placed offshore. Additionally, the annual active power production has been calculated. In Section 3.2, wind speed statistics utilised to estimate the annual production in offshore wind power plants were introduced.

A scenario with specific characteristics is made to simulate the loss reduction of applying an SVC on a yearly basis. It is assumed that a Rayleigh distribution with a mean wind speed of 9 m/s decently represents the probability distribution of the offshore wind speeds. A wind speed sensitivity curve is compared with the Rayleigh distribution to determine the active power production probability. The wind speed sensitivity curve is valid for annual mean wind speeds in the interval 7-9 m/s and is represented as follows:

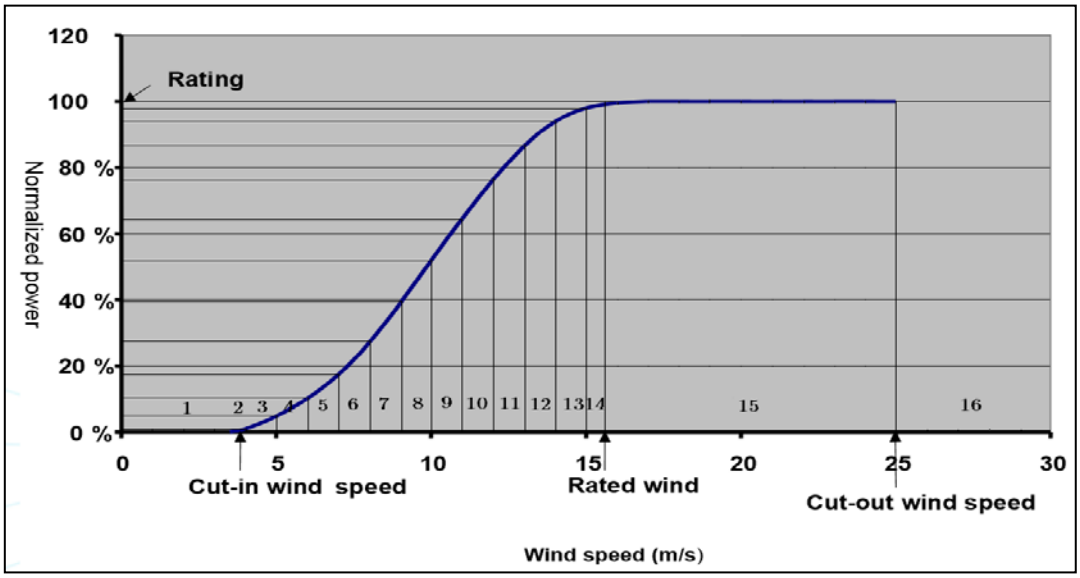

Figure 78: Wind speed sensitivity curve [31].

The wind speed sensitivity curve is divided into segments with 1 m/s per segment between the cut-in wind speed and rated wind speed. Wind speeds lower than the cut-in wind speed, rated wind speeds, and wind speeds higher than the cut-out wind speed are each represented by one segment. The previous figure displays the segment representation from 1 to 16. The wind speeds for each segment is given in Table 13.

Table 13: Wind speeds for segment 1-16 as illustrated in Figure 78.

Segment	1	2	3	4	5	6	7	8
Wind speed [m/s]	0-3,8	3,8-4	4-5	5-6	6-7	7-8	8-9	9-10
Probability (rounded)	0,131	0,013	0,072	0,079	0,084	0,084	0,082	0,077

Segment	9	10	11	12	13	14	15	16
Wind speeds [m/s]	10-11	11-12	12-13	13-14	14-15	15-15,6	15,6-25	25+
Probability (rounded)	0,070	0,0618	0,053	0,045	0,0366	0,01840	0,0921	0,0023

The wind speed sensitivity curve is compared with the Rayleigh distributions for a mean speed of 9 m/s, which are illustrated in the figure below:

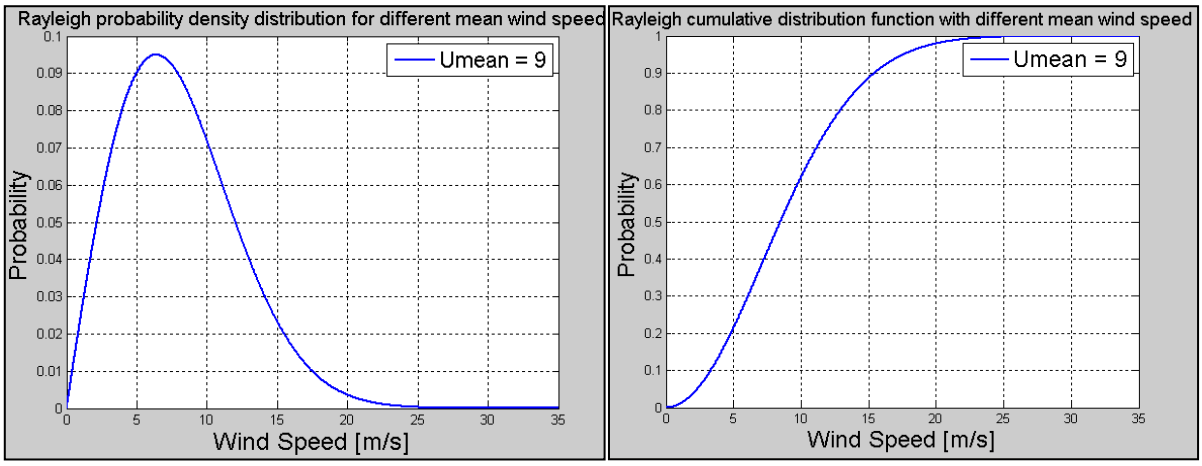

Figure 79: Rayleigh probability and cumulative distributions for a mean wind speed equal to 9 m/s.

Using MATLAB, the probability for each wind speed can be found. The probabilities for the different wind speeds are given in Table 13.

To simplify the simulations, it is assumed that each segment has a constant active power production. Since the goal in this section is mainly to calculate the difference in active power losses through the cables for two scenarios, some simplifications can be made without any major impacts on the results.

The wind power turbines are set to have a total rated power of 800 MW with the wind farm in P-Q control mode, and the offshore system is located 30 km from shore. In this operation, the voltages and current loading will be within their limits.

A complete table giving the active power productions, wind speeds, probabilities and mean values for losses in each segment is presented in Appendix 12.11.2.

The simulations are run for one hour. To calculate the annual production and losses in the cables in GWh, the active power losses in the simulations are multiplied with 365,2522*24 which is the average length of a year in number of days multiplied with the number of hours in each day. The active power production in the different segments and the appurtenant losses, both with and without the SVC, are illustrated in Figure 80 and Figure 81, respectively.

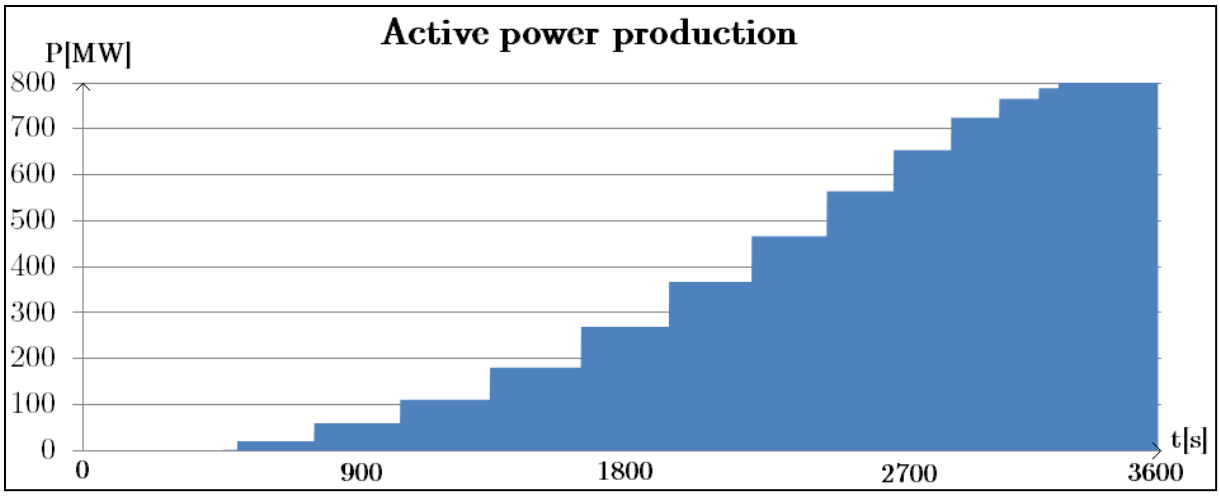

Figure 80: Active power production [MW].

The annual active power production in the system is calculated using the excel values extracted from the simulations in PowerFactory. It is assumed that the wind power turbines are in operation for the entire year. Average production is:

$$P_{avg} = 331{,}4482041 \approx 331{,}4\ \text{MW}$$

The total production during one year operation is:

$$\boldsymbol{P_{total\ one\ year}} = 331{,}4482041\text{MW} * 365{,}2522 * 24 = \mathbf{2{,}905}\ \boldsymbol{TWh}$$

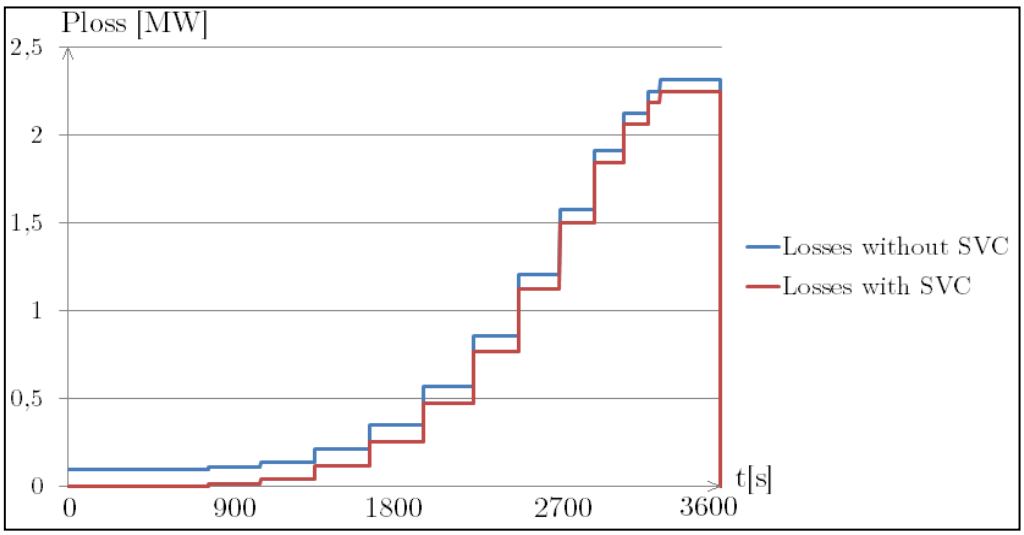

Figure 81: Losses [MW] with and without the SVC.

As illustrated in Figure 81, the losses are constantly higher for the simulations performed without any compensating devices. To make an estimation of the total losses both with and without the SVC, the average losses for each scenario are summarised. It is important to notice that the loss calculations are estimated only for the active losses in the transmission cables. At zero production, the losses are high

without the SVC. However, the estimation is performed with the extracted values from PowerFactory, so these losses are included in the calculations.

Average active power loss without the SVC:

$$P_{loss,avg} = 0{,}767194233 \approx 0{,}767\ MW$$

Total loss during one year operation:

$$\boldsymbol{P_{loss,total\ one\ year}} = 0{,}767194233MW * 365{,}2522 * 24 = \mathbf{6{,}725\ GWh}$$

With the SVC placed offshore, the average loss will be:

$$P_{loss,avg,SVC} = 0{,}680648521 \approx 0{,}681\ MW$$

The total loss for one year operation is:

$$\boldsymbol{P_{loss,total\ one\ year,SVC}} = 0{,}680648521 * 365{,}2522 * 24 = \mathbf{5{,}966\ GWh}$$

Total loss difference (displayed distributed over one year in Figure 82), estimated between the scenario with and without the SVC offshore for one year:

$$\boldsymbol{P_{loss,diff}} = 6{,}725GWh - 5{,}966GWh = \mathbf{0{,}759\ GWh}$$

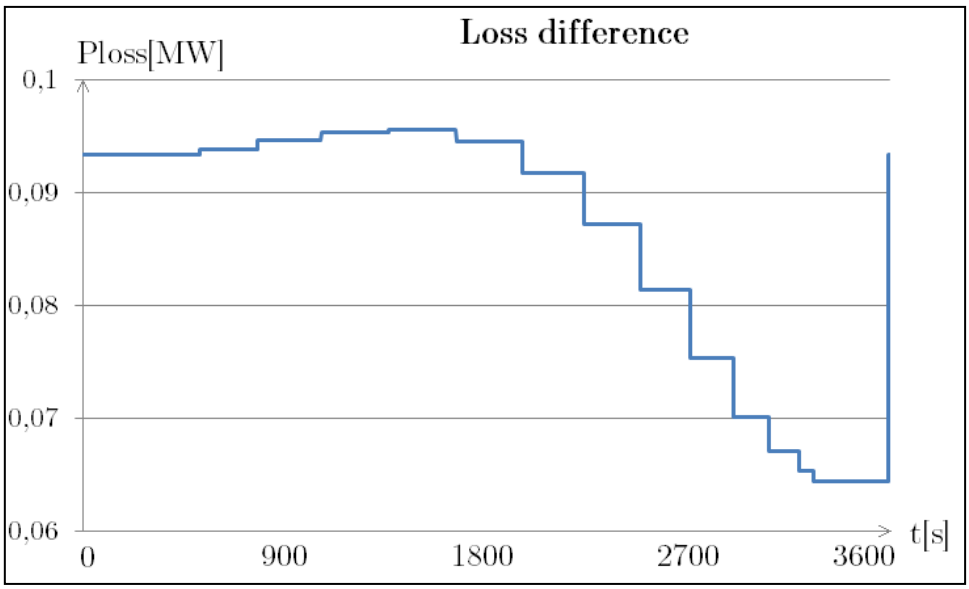

Figure 82: Loss difference [MW] between operation with and without SVC.

The losses with the SVC implemented are dependent on the voltage set point of the SVC. In Appendix 12.11.4 the reactive power consumed by the SVC is presented.

The total loss reduction by applying an SVC offshore for one year operation is estimated to be 0,759 GWh, with a annual production of 2,91 TWh. If the cable length was increased, the loss savings would increase accordingly.

Chapter 8

8 Discussion

From the simulated results, it can be concluded that an offshore location of the SVC provides the overall most beneficial solution for active power transmission from a wind farm to shore.

In this chapter, the results are analysed further. There are numerous ways to carry out simulations with the intention of testing the system performance with different strategies for placement of the SVC, control mode of the wind farm and the settings determined for the LTCs. System behaviour is addressed first. Next, the testing of various locations of the SVC with the wind farm operating in P-Q and P-V mode is discussed. Challenges concerning coordination between SVC and LTC, and how an SVC reduces system losses are discussed briefly. Finally, limitations and sources of error are reviewed.

Examination of System Behaviour

In order to ensure the reliability of the dynamic components applied, a comprehensive examination of their behaviour was performed. The results from testing system abilities of the VSC, LTC and SVC verified their expected performance. Deviations from the calculated theoretical values were insignificant, as presented in Section 7.1-7.3. The whole system was taken into consideration, and to examine the model thoroughly, different control strategies for the mentioned components were applied. Regulations presented in the grid codes, concerning voltage limits and reactive power capability, were followed in the model. However, some simplifying assumptions have been made for the purpose of comparing different control strategies. The voltages were assumed acceptable if they were within the range $0{,}9<U<1{,}05$ pu, and the maximum values of the reactive power capability for the SVC were set to +/- 50% of the active power production.

P-Q Control Mode of the Wind Farm

When the system behaviour was examined with the wind farm controlled in P-Q mode, the reactive power output was set to zero and the cable lengths varied from 20-100 km. The system was tested for three scenarios: without any compensating devices, with the SVC onshore, and with the SVC offshore. Load tap changers on the transformers were used if the voltages were outside the acceptable range. For P-Q control of the wind farm with a reactive power output set to zero, the produced reactive power in the cables flowed towards the main grid, because reactive power consumption offshore was impossible. The short overhead line connected to the main grid with low impedance only caused a minor voltage drop. Thus, the voltages in the rest of the system were accordingly low. As expected, the system performance was highly dependent on the cable length and the placement of the SVC.

- **Without reactive compensation**

Without any reactive power compensation, the current loading in the transmission cables was unacceptable for cable lengths larger than or equal to 40 km. The reactive power in the cables was proportional to the cable length, as theoretically expected (see Chapter 2), with only minor deviations. The consequence of increasing the cable length was an increase of the reactive power, which, without reactive compensating devices, led to current overload in the cables.

- **SVC onshore**

An SVC can consume or produce reactive power. Results show that an onshore location of the SVC was not favourable when the wind farm was in P-Q control mode. When the SVC consumed reactive power, the voltages declined slightly. The current in the cables, however, remained at approximately the same value. Reactive power consumption of the SVC decreased the reactive power flow in the overhead line towards the external grid. Reactive power production from the SVC had only a minor influence on the current through the transmission cables. When the SVC produced reactive power, the reactive power flowing towards the external grid increased. For 40 km cable lengths and longer, the condition of the system was unacceptable because of the high cable current.

- **SVC offshore**

With an offshore location of the SVC, the results improved significantly. Reactive power consumption of the SVC reduced the voltage levels and contributed to a more even distribution of the reactive power in the cables, thus reducing the onshore current. A feasible system operation was obtained for cable lengths up to 60 km. The active power losses increased with the cable length, but the SVC kept the cable current within an acceptable range for distances equal to, or lower, than 60 km.

P-V Control Mode of the Wind Farm

A different approach was used to compare operational strategies with the wind farm in P-V control mode. Four voltage set points of the wind farm were tested; 1,000 pu, 1,005 pu, 1,010 pu and 1,015 pu. Simulations were performed for maximum cable length with an acceptable operation for all voltage set points and for maximum cable length with feasible operation for at least one voltage set point. P-V control of the wind farm ensured stable and low voltages for all the simulations performed.

- **Without reactive compensation**

Results for cable lengths 26 and 54 km were presented. A voltage set point of 1,015 pu did not provide an acceptable state of operation for any of the cable lengths tested. With short cables, the production of reactive power in the wind farm increased above the maximum limits. Longer cables made the current too high. For other voltage set points, the maximum cable length presenting an acceptable state of operation was found to be 26 km. The lowest active losses were obtained with low voltage set points. Higher voltage set points caused the wind farm to produce reactive power, and thus also too high cable current. If the limit for acceptable reactive power

consumption in the wind farm was increased, longer cables would be possible. In order to test the system limitations, the cable length was increased to 54 km. For these cable lengths, only the scenario with a voltage set point equal to 1,005 gave a valid operation. The cable current was the limiting factor for the system.

- **SVC onshore**

The effect of placing an SVC onshore was minimal for the offshore system. Two different voltage set points for cable lengths of 26 km were tested. For these scenarios, only 8,5 % of the reactive power contributions from the SVC affected the offshore system. The main part of the SVC contributions was consumed from, or produced to, the main grid through the overhead line. The voltage at the bus was only marginally affected by the contributions from the SVC.

- **SVC offshore**

Results for cable lengths 35 and 66 km were presented. With the SVC placed offshore, longer cables were possible for all voltage set points. For 1,015 pu, the wind farm needed to produce a large amount of reactive power to keep the voltage at the given set point. This caused current overload in the cables for distances longer than 35 km, even with reactive power consumption in the SVC. For other voltage set points, there were no issues with the cable current at this length. Valid system operation for 66 km cables was only possible with a voltage set point of 1,005 pu. For this cable length, given a valid operation, the reactive power consumption for both the SVC and the wind farm was large. For higher voltage set points, the reactive power consumption offshore was not large enough to decrease the cable current sufficiently. For a voltage set point of 1,000 pu, the high reactive power consumption in the wind farm made it impossible for it to initialise. The current in the cables were highest on the offshore side, due to the reactive power consumption necessary for the wind farm to keep the voltages low.

Coordination Between the LTCs and the SVC

Coordination between the LTCs and the SVC was analysed to see if any problems could occur if they were activated close to each other. The voltages in the system were improved significantly with the SVC and the LTC working together. The load tap changer's influence on the reactive power contributions from the SVC was insignificant. The static var compensator was tested on both sides of the transformer, and the most beneficial solution was found when the SVC was located on the 33 kV side.

Annual Production and Cable Losses

Annual production and loss estimation was performed to investigate the effect of utilising an SVC in the system. A wind speed sensitivity curve was compared with a Rayleigh distribution to calculate the probability for different production levels. The annual production was estimated to be 2,91 TWh with a rated power of 800 MW and 30 km cable lengths. For this production, the gain of including an SVC offshore was

estimated to be 0,759 GWh in pure reduction of cable losses. If the cable lengths were to increase, the loss reduction by applying an SVC in the system would increase accordingly. This indicates that it can be economically favourable to introduce an SVC to the system, assuming reasonable costs of the component. For real-world offshore wind power, the average distance to shore in 2011 was 23,4 km [44]. Since the wind velocities are higher remote offshore than closer to shore, the gain in increased wind power production could make up for the costs of implementing an SVC into the system. However, the economic aspects of the system have not been examined in this thesis.

Sources of Error and Application of Theory

Reactive control theory, wind turbine theory and grid codes are very complex, and a real system is definitely even more complicated than the model utilised in this thesis. The real wind speeds are also less predictable and follow more complex patterns than those modelled in the simulations. However, it can be argued that the model is adequate, in spite of its limitations. For the purpose of analysing the behaviour of different strategies concerning reactive power and voltage control, the chosen limitations of the model would only have minor effect on the results when finding the most beneficial placement of the SVC. The theoretical foundation presented in this thesis was invaluable for making the right choices in the model developing process, and to find the right balance between simplification and a fair representation of reality. The theory has also been crucial for understanding and cross-checking results when interpreting the system behaviour. The simplifications done in this study should be fully comprehended and taken into account if the results are utilised for other purposes.

Chapter 9

9 Conclusion

In this Master's thesis, different operational strategies for reactive power and voltage control of offshore wind power production have been investigated. The conclusion from the simulations is that the most beneficial transmission strategy is an offshore placement of the SVC.

Simulations carried out have confirmed that the desired behaviour of the dynamic components applied for voltage control was achieved. Proportionality between reactive power produced by the cables and the cable length has been verified.

For operation of the wind farm in P-Q control mode, the cable current was high on the onshore side of the transmission cables, due to the produced reactive power in the cable itself. An onshore location of the SVC would not give a favourable operation. Without compensating devices, or with the SVC onshore, acceptable operation was only possible for cables shorter than 40 km. Consumption of reactive power with the SVC offshore allocated the reactive power flow in the cables more conveniently. In the scenario with the SVC offshore, the cable length ensuring a feasible state of operation could be longer than 60 km.

A more even distribution of reactive power in the cables was obtained with P-V operation since the wind farm could consume reactive power. For all the scenarios tested, the longest cables that preserved feasible operation were obtained with a voltage set point of the wind farm at 1,005 pu. Without any reactive compensation and the SVC onshore, the maximum cable length was 54 km. The longest cables possible with the SVC placed offshore were 66 km long.

Results indicate that coordination issues between the static var compensator and the load tap changers are negligible.

A rated power production of 800 MW leads to an annual production of 2,91 TWh. The loss reduction achieved by applying an SVC offshore was estimated to be 0,759 GWh, assuming a Rayleigh distribution of wind speeds and 9 m/s as mean wind speed.

The model utilised is a simplification of real-world conditions. Before the conclusions made are followed in the planning of real wind farms, additional studies should be conducted in order to confirm the results.

Chapter 10

10 Further Work

SVC, VSC and LTC technologies as reactive control mechanisms for active power transmission is a complex topic, and there are several aspects of the model design that can be improved through further work.

In this model an infinite voltage source with a voltage source converter has been used to represent the wind farm. For further development and utilisation of the model, a less deterministic structure, thereby representing a more complex wind turbine system could be considered for more realistic simulations. Wind power variations have in this thesis been simplified to step functions. More comprehensive data of real wind speeds from an existing site should also be inspected.

Other design philosophies for the whole system can be investigated to potentially find even better system modes of operation. The SVC could be tested in other locations, and utilising a STATCOM as a reactive power compensation device for comparison to the SVC could be interesting for further analysis. Additionally, simulations with other reactive power and voltage set points of the wind farm can be tested. The effect of implementing line drop compensation for the transformers can be analysed.

Economical aspects concerning reactive power compensation have not been taken into consideration in this thesis. For further analysis, it could be interesting to include economical aspects in order to attain a deeper understanding of the interconnection between investment costs, operating costs and electrical losses, as well as how these factors are prioritised in real decision making processes.

The grid code regulations utilised for simulations in this study, are simplified compared to the grid codes presented in Chapter 4. More comprehensive, long-term simulations with different minimum time-periods for operation of different voltage ranges, presented in Table 3, can be used for further work.

Chapter 11

11 References

[1] International Energy Agency. (2013 (accessed 10.11.2013)) Web page for http: IEA. [Online]. http://www.iea.org/media/freepublications/technologyroadmaps/foldout/WIND_Foldout.pdf

[2] Ocean Energy Council. (2013 (Accessed 10.11.2013)) Web page for Ocean Energy Council. [Online]. http://www.oceanenergycouncil.com/index.php/Offshore-Wind/Offshore-Wind-Energy.html#4

[3] T. B. Solvang, "Large-scale wind power integration in Nordland," Norwegian University of Science and Technology, Trondheim, Master thesis 2007.

[4] M. Marques and R. Castro, "Connection of Offshore Wind Parks: HVAC and HVDC-LCC links with STATCOM," IST - Technical University of Lisbon, Lisbon, IEEE 2011.

[5] P. K. M. Vormedal, "Voltage Source Converter Technology for Offshore Grids," Norwegian University of Science and technology, Trondheim, Master thesis 2010.

[6] J. Machowski, J. W. Bialek, and J. R. Bumby, *Power System Dynamics - Stability and Control*, Second Edition ed. West Sussex, United Kingdom: John Wiley & Sons Ltd., 2012.

[7] G. Bucea and H. Kent. (2007, Accessed 26.05.2014) contactenergy.co. [Online]. https://www.contactenergy.co.nz/web/pdf/our_projects/waikatowindfarm/june2008/R01_HMR_Connection_to_220kV_Main_Grid_Undergrounding_Study_Attachment1_Appendix7and8.pdf

[8] E. Ildstad, *TET 4160 - High Voltage Insulation Materials*. Trondheim, Norway: NTNU, 2012.

[9] GridOne. (2013, July (Accessed 04.11.2013)) http://gridone.us.com/. [Online]. http://gridone.us.com/2013/xlpe-insulated-power-cables-for-voltages-up-to-110kv/

[10] T. Toftevaag, "HVAC cable trasmission - equation and example," Norwegian University of Science and Technology, Trondheim, Memo for lectures in the course TET 4200 - Maritime and offshore power systems at NTNU 2013.

[11] R.N. Nayak, Y.K. Sehgal, and S. Sen, "EHV Transmission Line Capacity Enhancement through Increase in Surge Impedance Loading Level," Power Grid Corporation of India Ltd., New Dehli, IEEE 0-7803-9525-5, 2006.

[12] Norske Elektrisitetsverks Forening, "Kompensering i fordelingsnett," Oslo, Norway, 1983.

[13] C. L. Fortescue, "Power, Reactive Volt-Amperes, Power Factor," American Institute of Electrical Engineers, East Pittsburgh, USA, 2009 (1933).

[14] T. Toftevaag, "Wind power - Grid connection of wind farms," SINTEF Energy Research, Trondheim, Memo from course ELK-12 at NTNU 2013.

[15] M. Hadiya, "Case study of offshore wind farm integration to offshore oil and gas platforms as an isolated system - System Topologies, Steady State and Dynamic Aspect," Norwegian University of Science and Technology, Trondheim, Master thesis 2011.

[16] O. B. Fosso, "Reactive power and voltage control," Norwegian University of Science and Technology, Trondheim, Memo from course ELK-14 at NTNU 2013.

[17] P. Kundur, "Power System Stability and Control," McGraw-Hill, 1994.

[18] Siemens. (2011 , December(Accessed 13.10.2013)) Flexible AC Transmission Systems - What and Why. [Online]. http://electrical-engineering-portal.com/flexible-ac-transmission-system-what-and-why

[19] Siemens, "Benefits of FACTS for Transmission Systems," High Voltage Division, Erlagen, Germany, 2003.

[20] N. Mohan, T. M. Undeland, and W. P. Robbins, *Power Electronics*, Third Edition ed., Bill Zobrist, Ed. Danvers, United States of America: John Wiley & Sons, Inc., 2003.

[21] F. Blaaberg, M. Liserre, and K. Ma, "Power Electronics Converters for Wind Turbine Systems," IEEE, Aalborg, 2011.

[22] T. W. Shire, "VSC-HVDC based Network Reinforcement," Delft University of Technology, Delft, Master thesis 2009.

[23] P. Sørensen, A. D. Hansen, F. Iov, and F. Blaaberg, "Wind Farm Models and Control Strategies," Aalborg University, Aalborg, ISBN 87-550-3322-9/ISSN 0106-2840, 2005.

[24] E. L. Hannisdal, "Optimal Voltage Control of the Southern Norwegian Power Grid," Norwegian University of Science and Technology, Trondheim, Master thesis 2011.

[25] S. Rahmani, A. Hamani, K. Al-Haddad, and L. A Dessaint, "A Combination of Shunt Hybrid Power Filter and Thyristor-Controlled Reactor for Power Quality," École de Technologie Supérieure, Montréal, IEEE 2013.

[26] H. Saadat, *Power System Analysis*, Second Edition ed. Milwaukee, USA: McGraw-Hill, 2004.

[27] Boundless. (2014, Accessed februar 2014) Web page for Boundless. [Online]. https://www.boundless.com/physics/induction-ac-circuits-and-electrical-technologies/magnetic-flux-induction-and-faraday-s-law/transformers/

[28] M. Larsson, "Coordinated Voltage Control in Electrical Power Systems," Lund Institute of Technology, Lund University, Lund, Doctoral Dissertation 2000.

[29] J. F. Manwell, J. G. McGowan, and A.L Rogers, *Wind Energy Explained*, Second Edition ed., Anthony Rowe, Ed. Chichester, United Kingdom: John Wiley & Sons Ltd., 2009.

[30] A. Kalmikov, K. Dykes, and K. Araujo. (Accessed 2014) Web page for MIT, Wnid Power Fundamentals. [Online]. http://web.mit.edu/windenergy/windweek/Presentations/Wind%20Energy%20101.pdf

[31] T. Toftevaag, "ELK-12 Wind Power in the Norwegian Power System," Norwegian University of Science and Technology, Trondheim, Notes from the course ELK-12, automn 2013 at NTNU 2013.

[32] G. Özdemir. (2013 (accessed 23.04.2014), February) easywindenergy.blogspot.no. [Online]. http://easywindenergy.blogspot.no/2013/02/variable-speed-versus-fixed-speed.html

[33] EWEA. (2009, Accessed 23.04.14) Wind Energy The Facts. [Online]. http://www.ewea.org/fileadmin/ewea_documents/documents/publications/WETF/WETF.pdf

[34] E. C. Morgan, M. Lackner, R. M. Vogel, and L. B. Baise, "Probability Distributions for Offshore Wind Speeds," Dept. of Civil and Environmental Engineering, Tufts University, Massachusetts, Medford, Amherst, 2011.

[35] L. Caretto, "Use of Probability Distribution Functions for Wind," California

State University Northridge, California, 2010.

[36] G. L. Hunt, "Maine Offshore Wind Energy," School of Economics, University of Maine, Orono, 2009.

[37] M. S. Nielsen, "Monte Carlo Simulation of Power Systems with Wind Power," Norwegian University of Science and Technology, Trondheim, Master Thesis 2013.

[38] W. Bierbooms, "Offshore Wind Climate," Delft University Wind Energy Research Institute, Delft, Lecture in Course 0E5662 Offshore Wind Farm Design.

[39] Statnett SF, Responsible Øivind Rue, "Funksjonskrav i kraftsystemet," Oslo, Norway, 2012.

[40] ENTSO-E, "ENTSO-E Network Code for Requirements for Grid Connection Applicable to all Generators," European Commission (EC), Brussels, Belgium, 2012.

[41] DIgSILENT. (2013, Accessed 10.11.2013) Webpage for DIgSILENT (PowerFactory). [Online]. http://www.digsilent.de/index.php/products-powerfactory-basic_software_features.html#bottom

[42] DIgSILENT, "User's Manual," DIgSILENT, Gomaringen, PowerFactory User's Manual 2011.

[43] D. P. Kothari, K. C. Singal, and R. Ranjan, *Renewable Energy Sources and Emerging Technologies*, Second edition ed., Gosh and Asoke K., Eds. New Delhi, India: PHI Learning Private Limited, 2011.

[44] EWEA - The European Wind Energy Association, "The European offshore wind industry key 2011 trends and statistics," EWEA, 2012.

[45] G. Reed, J. Paserba, and et al., "The VELCO STATCOM-Based Transmission System Project," Mitsubishi Electric Power Products, Inc; Mitsubishi Electric Corporation; The Vermont Electric Power Co, Inc, Florida, IEEE 2001.

[46] C. Han, "Power System Dynamic Management with Advanced STATCOM and Energy Storage System," North Carolina State University, North Carolina, USA, 0549376380, 9780549376385, 2006.

[47] A.T. Holen and O. B. Fosso, "Kompendium TET4115 Power System Analysis," Norwegian University of Science and Technology, Trondheim, Compendium 2007.

[48] ABB, "XLPE Submarine Cable Systems: Attachment to XLPE Land Cable Systems," ABB, Sweden, User's Guide 2010.

[49] Georgia State University. (2000, August (Accessed 13.11.2013)) HyperPhysics - Resistivity and Temperature Coefficient at 20°C. [Online]. http://hyperphysics.phy-astr.gsu.edu/hbase/tables/rstiv.html

[50] Georgia State University. (2000, August (Accessed 12.11.2013)) HyperPhysics - Resistance: Temperature Coefficient. [Online]. http://hyperphysics.phy-astr.gsu.edu/hbase/electric/restmp.html

[51] SINTEF Energi AS, "Planleggingsbok for kraftnett," SINTEF, Trondheim, Technical data 2010.

[52] Mathworks. (2014, Accessed 25.04.14) Mathworks. [Online]. http://www.mathworks.se/help/physmod/sps/powersys/ref/abc_to_dq0transformation.html

[53] J. McCalley. (Accessed 25.04.14) Web page for Iowa State University. [Online]. http://www.google.no/url?sa=t&rct=j&q=&esrc=s&source=web&cd=14&sqi=2&ved=0CJEBEBYwDQ&url=http%3A%2F%2Fhome.eng.iastate.edu%2F~jdm%2Fwind%2FdqTransformation.ppt&ei=-1paU-zeMcKWyQPz_YCoBw&usg=AFQjCNGP1UYALRBuWtSZAXLDNysDD_NlBg&sig2=kc3gXFPKC_7x73kBb1ehyA

Chapter 12

12 Appendices

12.1 STATCOM

The STAtic Synchronous COMpensator, known as STATCOM, is a power electronic device which is a part of the FACTS devices. STATCOM has similar properties as a synchronous condenser, but without the rotating parts. During critical contingencies, it can provide fast voltage control by dynamic reactive compensation [45]. The reactive power flow between the grid and the STATCOM is given by Equation 2.23. Since the angle difference between the voltage source and the grid is 0°, the active voltage will be zero and the reactive power will be:

$$Q = \frac{V}{X}(E - V) \qquad 12.1$$

The basis of the STATCOM is a voltage source converter, which is described in Section 2.3.2. STATCOM is self commutated and transistor based, and one of the advantages using STATCOM instead of SVC is that the change in reactive output is not proportional to the voltage squared [16].

In addition to controlling the voltage and reactive compensation to the network, the STATCOM can also provide limited active power support to the network during transient conditions [4].

STATCOM basically consist of three parts; a Voltage Source Converter, a coupling reactor and a controller.

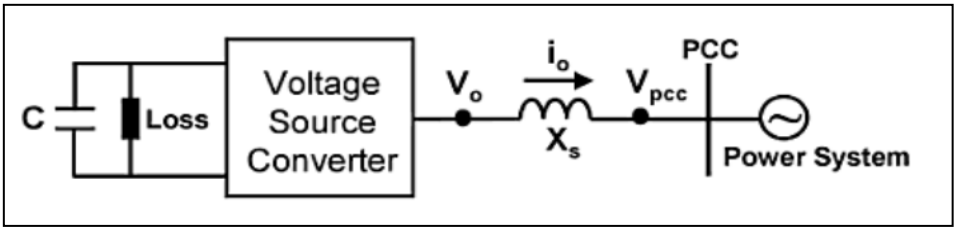

Figure 83: Single-line diagram of the Voltage Source Converter-based STATCOM [46].

The losses using a STATCOM are higher compared with SVC. At zero output, the loss is about 0,1-0,2% and 1% at full reactive output [46].

Table 14 shows a comparison between STATCOM and SVC for different characteristics [46].

Table 14: Comparison STATCOM and SVC [20].

Characteristics	**STATCOM**	**SVC**
Voltage support capability	Best	Good
Speed of support	Fastest	Fast
Footprint	Smallest	Small
Harmonic (without filter)	Small	Large
Loss	Low	Lower
Initial investment	High	Low
Maintenance cost	High	High
Technology lifecycle stage	Innovative	Maturity

12.2 Wind Turbine Control

12.2.1 Passive stall regulated turbines

Constant-speed, stall regulated wind turbines use twisted blades in a certain design which passively regulates the power production of the turbine. When the speed reaches its maximum, the twist in the blade will work as a break. This phenomenon is obtained by increasing the angle of attack as the wind speed increases, making the blade enter the stall region at high wind velocities. The only control required for a passive stall regulated turbine is the starting (soft-starter contactor) and stopping (break operation) based on wind speed or power criteria [29][31].

12.2.2 Active stall regulated turbines

Active stall regulated turbines use both the twisting of the blades as described in the passive stall regulated turbines and pitch control when the maximum power output is reached. As the wind moves towards high wind speeds, the blades break, but the maximum power output can be obtained for all wind speeds by pitching. Both the angle of attack and the drag increases when the power output is at its maximum and the wind speed is increasing.

12.2.3 Pitch regulated turbines

Pitch is achieved by rotating the blades around its own axis. Pitch controlled turbines use active rotor angle control to maximise the power coefficient in the wind speed up to rated value. When the wind speeds are above rated value, the power coefficient is reduced to maintain the maximum rated power output. The pitching is done by reducing the angle and turning the blade towards the wind [29][37].

As described above, two different methods of pitching is applied to regulate wind turbines. When the wind speed reaches approximately 15 m/s the pitching begins. The difference between passive stall and active pitch regulation is illustrated in the figure below.

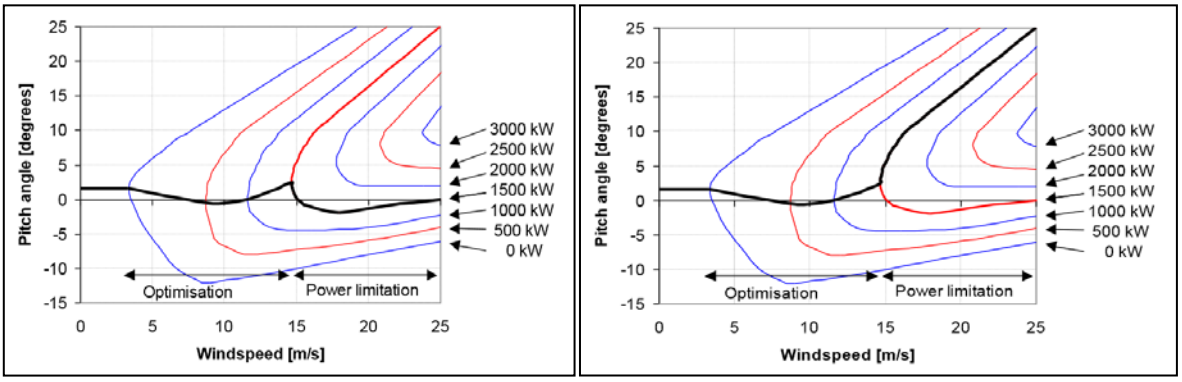

Figure 84: Pitch angle as a function of the rated power compared to different wind speed. Left graph: active stall. Right graph: active pitch [31].

A comparison of the power curves for a pitch regulated and a passive stall regulated turbine is illustrated in the following figure. When the rated power is obtained, the

stall regulated turbine is not able to keep the power output at the rated value, while the pitch regulated turbine follows the rated value until the cut-off wind speed. Power curves for passive stall and active pitch are presented as follows:

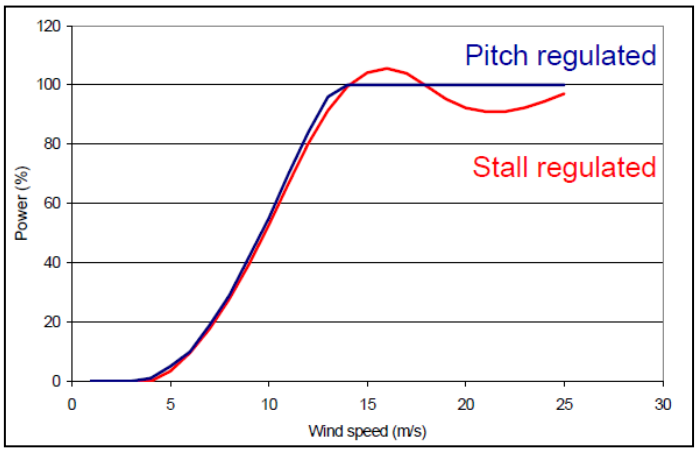

Figure 85: Power curves for passive stall regulated and active pitch regulated wind turbines [31].

12.3 Approximations for Deciding the Shape and Scale Factor

Both the shape factor (k) and the scale factor (c) are dependent of the mean wind speed ($\overline{U}$) and the standard deviation (σ_U). The following methods are collected from [29]. By applying Equation 3.18 for the Weibull distribution, the average velocity can be calculated:

$$\overline{U} = c \cdot \Gamma \cdot (1 - \frac{1}{k}) \tag{12.2}$$

Γ(x) is the gamma function, given by:

$$\Gamma(x) = \int_0^\infty e^{-t} t^{x-1}\, dt \tag{12.3}$$

From the Weibull distribution it can be shown that:

$$\sigma_U = \overline{U}^2 \cdot [\frac{\Gamma\left(1 + \frac{2}{k}\right)}{\Gamma\left(1 + \frac{1}{k}\right)} - 1] \tag{12.4}$$

From these equations, k and c can be calculated, but it is not a straightforward process. To make the calculation of these two parameters easier, some approximation methods have been developed.

1) Analytical/Empirical estimation of k and c

For 1≤k<10, k can be approximated by:

$$k = \left(\frac{\sigma_U}{\overline{U}}\right)^{-1{,}086} \tag{12.5}$$

By using Equation 12.2, c can be solved:

$$c = \frac{\overline{U}}{\Gamma(1 + \frac{1}{k})} \tag{12.6}$$

2) Empirical estimation of k and c

In the empirical estimation method, k is first found using Equation 12.2. Then it is possible to find c by applying the following approximation:

$$\frac{c}{\overline{U}} = (0{,}586 + \frac{0{,}433}{k})^{-\frac{1}{k}} \tag{12.7}$$

Several other approximations are used, but they will not be considered here.

12.4 Matlab Scripts Used for Figure 18 and Figure 20

12.4.1 Matlab script used for the Weibull probability density function

```
c = 12;
U = 0:0.00001:35;

k = 1.8;
p1=(k/c)*(U/c).^(k-1).*exp(-(U/c).^k);

k = 2.4;
p2=(k/c)*(U/c).^(k-1).*exp(-(U/c).^k);

k = 3.0;
p3=(k/c)*(U/c).^(k-1).*exp(-(U/c).^k);

figure
plot(U,p1,'r','LineWidth',2);
grid on
hold on
plot(U,p2,'b','LineWidth',2);
hold on
plot(U,p3,'c','LineWidth',2);
legend('k = 1,8', 'k = 2,4', 'k = 3,0')
title('Weibull probability density distribution for windspeed with different k values');
xlabel('Wind Speed [m/s]');
ylabel('Probability');
```

12.4.2 Matlab script used for the Weibull cumulative distribution function

```
c = 12;
U = 0:0.01:35;

k = 1.8;
F1=1-exp((-pi/4).*(U/c).^k);

k = 2.4;
F2=1-exp((-pi/4).*(U/c).^k);

k = 3.0;
F3=1-exp((-pi/4).*(U/c).^k);

figure
plot(U,F1,'r','LineWidth',2);
grid on
hold on
plot(U,F2,'b','LineWidth',2);
hold on
plot(U,F3,'c','LineWidth',2);
legend('k = 1,8', 'k = 2,4', 'k = 3,0')
title('Weibull cumulative distribution function for windspeed with different k values');
xlabel('Wind Speed [m/s]');
ylabel('Probability');
```

12.4.3 Matlab script used for the Rayleigh probability density function

```
U = 0:0.01:35;

Umean = 6,5;
p1=(pi/2)*(U/(Umean.^2)).*exp(-(pi/4)*(U/Umean).^2);

Umean = 8;
p2=(pi/2)*(U/(Umean.^2)).*exp(-(pi/4)*(U/Umean).^2);

Umean = 10.1;
p3=(pi/2)*(U/(Umean.^2)).*exp(-(pi/4)*(U/Umean).^2);

figure
plot(U,p1,'r','LineWidth',2);
grid on
hold on
plot(U,p2,'b','LineWidth',2);
hold on
plot(U,p3,'c','LineWidth',2);
legend('Umean = 6,5', 'Umean = 8,0', 'Umean = 10,1')
title('Rayleigh probability density distribution for windspeed with different values for mean
wind speed');
xlabel('Wind Speed [m/s]');
ylabel('Probability');
```

12.4.4 Matlab script used for the Rayleigh cumulative distribution function

```
U = 0:0.01:35;

Umean = 6.5;
F1=1-exp((-pi/4).*(U/Umean).^2);

Umean =8;
F2=1-exp((-pi/4).*(U/Umean).^2);

Umean = 10.1;
F3=1-exp((-pi/4).*(U/Umean).^2);

figure
plot(U,F1,'r','LineWidth',2);
grid on
hold on
plot(U,F2,'b','LineWidth',2);
hold on
plot(U,F3,'c','LineWidth',2);
legend('Umean = 6,5', 'Umean = 8,0', 'Umean = 10,1')
title('Rayleigh cumulative distribution function for windspeed with different values for mean
wind speed');
xlabel('Wind Speed [m/s]');
ylabel('Probability');
```

12.5 Power System Analysis

Power system analysis theory utilised for load flow calculations will be introduced in this section. There are several different methods that can be used for power system analysis, but the Newton-Raphson approach (explained in Section 12.5.2.1) is the most used.

12.5.1 Per unit system

The per-unit system (pu) is a frequently used approach when analysing a power system. Since the power system contains several voltage levels, issues comparing different values across voltage levels might arise. By applying the per-unit system, various different quantities such as power, voltage, current and impedance will be expressed as a fraction of the base quantities and the system will give a clear idea of these relative values. Regardless of whether the primary or secondary side is the reference, the per-unit values of the impedance, voltage and current of a transformer are the same. The formula used to transform the actual values to per-unit (pu) values are given by:

$$Quantity\ (pu) = \frac{actual\ quantity}{base\ value\ of\ quantity} \tag{12.8}$$

The direct formulas for apparent power, voltage, current and impedance in pu becomes:

$$S_{pu} = \frac{S}{S_B}, V_{pu} = \frac{V}{V_B}, I_{pu} = \frac{I}{I_B}\ and\ Z_{pu} = \frac{Z}{Z_B} \tag{12.9}$$

Minimum four base quantities are required to define a complete per-unit system. Usually, the three-phase apparent power S_B and the line-to-line voltage V_B are selected. The base current I_B and the base impedance Z_B are dependent on the base quantities of the apparent power and the voltage, and they need to obey the circuit laws. This gives:

$$I_B = \frac{S_B}{\sqrt{3}V_B} \tag{12.10}$$

$$Z_B = \frac{V_B/\sqrt{3}}{I_B} \tag{12.11}$$

To express the base impedance from the apparent power and the voltage, the formula for I_B is substituted into Z_B, which gives:

$$Z_B = \frac{(V_B)^2}{S_B} \tag{12.12}$$

Change of base:

The impedance of generators and transformers are generally expressed in per-unit based on their own ratings. By changing all the values in a common system base, the calculations become easier. If Z_{pu}^{old} is the per-unit impedance with the apparent power base S_{pu}^{old} and the voltage base V_{pu}^{old}, it is expressed by:

$$Z_{pu}^{old} = \frac{Z_{\Omega}}{Z_B^{old}} = Z_{\Omega} \frac{S_B^{old}}{\left(V_B^{old}\right)^2} \qquad 12.13$$

The new impedance expressed by the new apparent power base and voltage base becomes:

$$Z_{pu}^{new} = \frac{Z_{\Omega}}{Z_B^{new}} = Z_{\Omega} \frac{S_B^{new}}{(V_B^{new})^2} \qquad 12.14$$

By combining Equation 12.13 and 12.14, the relationship between the old and the new per-unit values can be expressed by:

$$Z_{pu}^{new} = Z_{pu}^{old} \frac{S_B^{new}}{S_B^{old}} \cdot \left(\frac{V_B^{old}}{V_B^{new}}\right)^2 \qquad 12.15$$

If the voltage levels are the same, the expression becomes:

$$Z_{pu}^{new} = Z_{pu}^{old} \frac{S_B^{new}}{S_B^{old}} \qquad 12.16$$

12.5.2 Nodal classification and power system analysis equations

Power flow equations and power systems used by PowerFactory determines the voltage magnitude (V) and the voltage angle (δ) of all the nodes, together with the active power (P) and reactive power (Q) on branches, when the load flow calculations are determined. Depending on the node type, the nodes are represented by two of these quantities. There are four types of nodal classifications which are generally applied in power flow calculations. These four classification types are also represented in PowerFactory simulation software. These node types are:

- P-V nodes: active power and voltage specified. Typical components representing these nodes are generators and synchronous condensers.
- P-Q nodes: active and reactive power specified. Usually represents loads and machines with fixed values.
- Slack nodes: voltage magnitude and angle are fixed.
- Device nodes: nodes with different control conditions like HVDC converters and SVSs.

The general power flow equations determining the active and reactive power from bus i to bus j are given by:

$$P_{ij} = Y_{ij}U_iU_j\cos(\delta_i - \delta_j - \theta_{ij}) \quad 12.17$$
$$Q_{ij} = Y_{ij}U_iU_j\sin(\delta_i - \delta_j - \theta_{ij}) \quad 12.18$$

12.5.2.1 Newton-Raphson method

The equations used to calculate and analyse the parameters in the network model are the Newton-Raphson current equations and the Newton-Raphson power equations. These methods are both solved iteratively. PowerFactory also uses an outer loop after the Newton-Raphson iterations converge to increase/decrease discrete taps, switchable shunts and limit/release synchronous machines with respect to reactive power limits. To determine the new network operating point, Newton-Raphson load flow is repeated [42].

The calculations using Newton-Raphson are described in five steps below:

1. Initial values

First the initial values must be defined. It is normal to use $U_{i(0)}$=1,0 pu and $\delta_{i(0)}$=0°.

The initial values for P and Q are found by using the power flow equations. These equations give the injected power into bus i:

$$P_i = \sum_{j=1}^{n} Y_{ij}U_iU_j\cos(\delta_i - \delta_j - \theta_{ij}) \quad 12.19$$
$$Q_i = \sum_{j=1}^{n} Y_{ij}U_iU_j\sin(\delta_i - \delta_j - \theta_{ij}) \quad 12.20$$

To be able to solve these equations, the admittance matrix y needs to be found. In this matrix, Y_{ij} is the magnitude of the value at position ij in the matrix and ϑ_{ij} is the angle at the same position.

2. Mismatch

In this section the specified initial values for P_{spec} and Q_{spec} are corrected by adding the values found in the previous section.

$$\Delta P_{i(0)} = P_{i,spec} - P_{i(0)} \quad 12.21$$
$$\Delta Q_{i(0)} = Q_{i,spec} - Q_{i(0)} \quad 12.22$$

3. Jacobian elements

The Jacobian elements are the values for the active and reactive power from the load flow equations derived by the voltage and the voltage angle:

$$J = \begin{bmatrix} \frac{\partial P_i}{\partial \delta_i} & \frac{\partial P_i}{\partial U_i} \\ \frac{\partial Q_i}{\partial \delta_i} & \frac{\partial Q_i}{\partial U_i} \end{bmatrix} \quad 12.23$$

4. Jacobian equations

The modified values for the voltages and the angles are calculated in this section.

$$\begin{bmatrix} \Delta U_{i(0)} \\ \Delta \delta_{i(0)} \end{bmatrix} = [J]^{-1} \begin{bmatrix} \Delta P_{i(0)} \\ \Delta Q_{i(0)} \end{bmatrix} \quad 12.24$$

5. New values

New values are found by adding the modified values to the old values.

$$\Delta U_{i(1)} = U_{i(0)} + \Delta U_{i(0)} \quad 12.25$$

$$\Delta \delta_{i(1)} = \delta_{i(0)} + \Delta \delta_{i(0)} \quad 12.26$$

If the difference between the iterations is too large, even more iterations need to be performed [26][47]. The simplified power flow iteration procedure can be described by the following flow-chart.

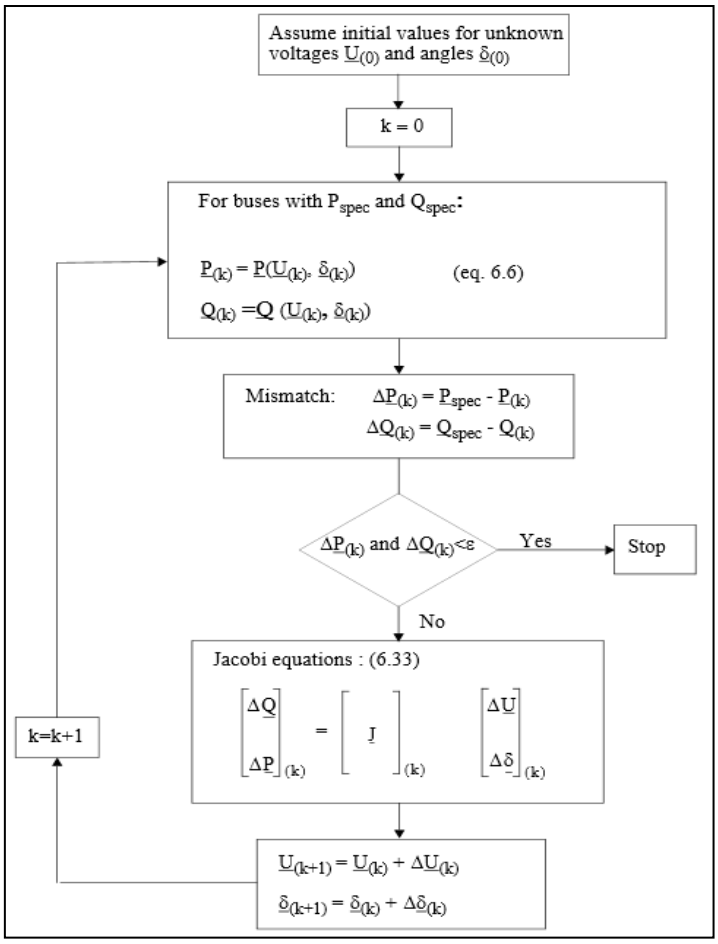

Figure 86: Flow-chart describing the power flow iteration procedure[47]

12.5.2.2 Sensitivity analysis

The sensitivity of the relationship between the active power at the voltage angle and magnitude shows how sensitive the active power is when then angle or the magnitude of the voltage is modified. Typically in the main grid, the value of the reactance is much bigger than the value of the resistance. Normally $\sin(\delta_i - \delta_j) \ll \cos(\delta_i - \delta_j)$, which can contribute to the following observation:

$$\frac{\partial P_i}{\partial \delta_i} \gg \frac{\partial P_i}{\delta U_i} \qquad 12.27$$

When r≪x, typically for transmission, it can be observed that the real power is much more sensitive to the voltage angle than the voltage magnitude. The reactive power is, on the other hand, more sensitive to voltage magnitude than to voltage angles as in the following inequality describes:

$$\frac{\partial Q_i}{\partial \delta_i} \ll \frac{\partial Q_i}{\delta U_i} \qquad 12.28$$

These differences in sensitivities used in the Jacobian matrix makes specific iteration schemes of the power flow equations, and takes advantage of the decoupling between real and reactive power. [47].

12.6 Data Sheet for Given Cable Parameters

10-90 kV XLPE 3-core cables		
Cross section mm²	Copper conductor	Aluminium conductor
	A	A
95	300	235
120	340	265
150	375	300
185	420	335
240	480	385
300	530	430
400	590	485
500	655	540
630	715	600
800	775	660
1000	825	720

100-300 kV XLPE 3-core cables		
Cross section mm²	Copper conductor	Aluminium conductor
	A	A
300	530	430
400	590	485
500	655	540
630	715	600
800	775	660
1000	825	720

Figure 87: Current rating for three-core submarine cables with steel wire armour [48].

Three-core cables, nominal voltage 30 kV (Um = 36 kV)										
70	9.6	8.0	28.0	16	100.6	16.9	18.2	0.16	0.9	0.46
95	11.2	8.0	29.6	16	104.0	17.7	19.5	0.18	1.0	0.44
120	12.6	8.0	31.0	16	107.0	18.4	20.7	0.19	1.0	0.42
150	14.2	8.0	32.6	16	110.5	19.3	22.1	0.21	1.1	0.41
185	15.8	8.0	34.2	16	114.0	20.1	23.6	0.22	1.2	0.39
240	18.1	8.0	36.5	16	118.9	21.4	25.9	0.24	1.3	0.38
300	20.4	8.0	38.8	16	123.9	22.6	28.2	0.26	1.4	0.36
400	23.2	8.0	41.6	16	129.9	24.6	32.0	0.29	1.6	0.35
500	26.2	8.0	45.0	16	137.3	26.7	36.0	0.32	1.7	0.34
630	29.8	8.0	48.6	16	145.1	29.2	40.9	0.35	1.9	0.32
800	33.7	8.0	52.5	16	154.4	32.2	47.2	0.38	2.1	0.31

Figure 88: Technical data for XLPE submarine cable systems - Three-core cables with copper wire screen used for the 33 kV cables [48].

Three-core cables, nominal voltage 275 kV (Um = 300 kV)										
500	26.2	26.0	81.6	2.9	229.0	75.3	84.7	0.14	6.8	0.44
630	29.8	24.0	81.2	3.0	228.0	77.0	88.9	0.16	7.7	0.42
800	33.7	24.0	85.1	3.1	237.0	82.5	97.6	0.17	8.3	0.40
1000	37.9	24.0	89.3	3.1	247.0	87.4	106.3	0.18	9.0	0.39

Figure 89: Technical data for XLPE submarine cable systems - Three-core cables with copper wire screen used for the 300 kV cables [48].

12.7 Calculations for the Cables and Overhead Line

All the parameters calculated in this section are based on the values given in Appendix 12.6.

12.7.1 Cables connecting the turbines to the transformer station

First, the current rating I_{rated} was found for each cable:

$$\boldsymbol{I_{rated}} = \frac{S_{rated}}{V_{rated}\sqrt{3}} = \frac{1000\ MVA/100}{33\ kV\sqrt{3}} = \boldsymbol{174,955A}$$

I_{rated} is the current rating for this value, i.e. the closest value higher than 174,955A for the 10-90 kV XLPE three-core cables.

The current rating found in this table was 300A, which gives a cross-section of 95 mm^2. The Rated current implemented in the simulation model for this cable is:

$$\boldsymbol{I_{rated,50\ cables}} = I_{rated} * 50 = \boldsymbol{8,748\ kA}$$

Then the calculations for the resistance r, inductance L and capacitance C per km was calculated [49] [50].

$$\boldsymbol{r_{50\ cables}} = \frac{\rho L}{A * 50} k = \frac{1{,}68 * 10^{-8}\Omega m}{95 * (10^{-3})^2 m^2 * 50} * 1000 * (1 + 0{,}003862 * (90 - 20)$$
$$= \boldsymbol{0,00493\frac{\Omega}{m}}$$

Where $k = [1 + k_t \Delta t]$

$$\boldsymbol{L_{50cables}} = \frac{L_{one\ cable}}{50} = \frac{0{,}44mH/km}{50} = \boldsymbol{0,008\frac{mH}{km}}$$

$$\boldsymbol{C_{50\ cables}} = C_{one\ cable} * 50 = 0{,}18\frac{\mu F}{km} * 50 = \boldsymbol{9\frac{\mu F}{km}}$$

The length of this cable was chosen to be two kilometers.

12.7.2 Long cables connecting the offshore system to shore

To be able to transfer as much current as possible, it was chosen to use the thickest cable with a cross-section area of 1000 mm^2. This area gave a current rating of 825 A.

$$\boldsymbol{r} = \frac{\rho L}{A} k = \frac{1{,}68 * 10^{-8}\Omega m}{1000 * (10^{-3})^2 m^2} * 1000 * (1 + 0{,}003862 * (90 - 20)) = \boldsymbol{0,021342\frac{\Omega}{km}}$$

$$\boldsymbol{C = 0,18\frac{\mu F}{km}}$$

$$\boldsymbol{L = 0,39\frac{mH}{km}}$$

The length of these cables is varying from 10-50 km, with a step size of 10 km.

12.7.3 Overhead line values

300 kV overhead line (duplex)

Type	Cu ekv.	R [Ω/km]	X [Ω/km]	C_d [nF/km]	R_0 [Ω/km]	X_0 [Ω/km]	C_j [nF/km]	I_{th} [A]	Mastekonfigurasjon
381-AL1/62-ST1A	2x240	0,039	0,318	11,632	0,212	0,742	8,588	2284	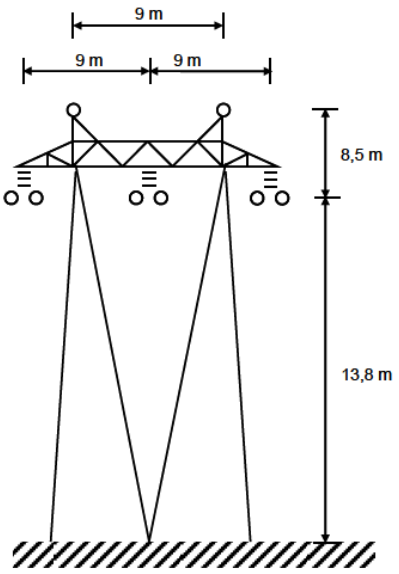
402-AL1/52-ST1A	2x253	0,037	0,318	11,645	0,21	0,742	8,595	2354	
476-AL1/78-ST1A	2x300	0,031	0,314	11,769	0,204	0,739	8,662	2640	
525-AL1/68-ST1A	2x329	0,029	0,313	11,813	0,202	0,738	8,686	2800	
565-AL1/72-ST1A	2x354	0,027	0,312	11,86	0,2	0,737	8,711	2918	
606-AL1/77-ST1A	2x380	0,025	0,311	11,902	0,198	0,735	8,734	3042	
645-AL1/82-ST1A	2x405	0,024	0,31	11,943	0,197	0,734	8,756	3178	
766-AL1/97-ST1A	2x481	0,02	0,307	12,057	0,193	0,732	8,816	3556	
806-AL1/102-ST1A	2x506	0,019	0,307	12,091	0,192	0,731	8,834	3662	

Figure 90: Values implemented for the overhead line [51].

The overhead line with the short-circuit impedance is one kilometre long.

12.8 PowerFactory Model of the PV Controller

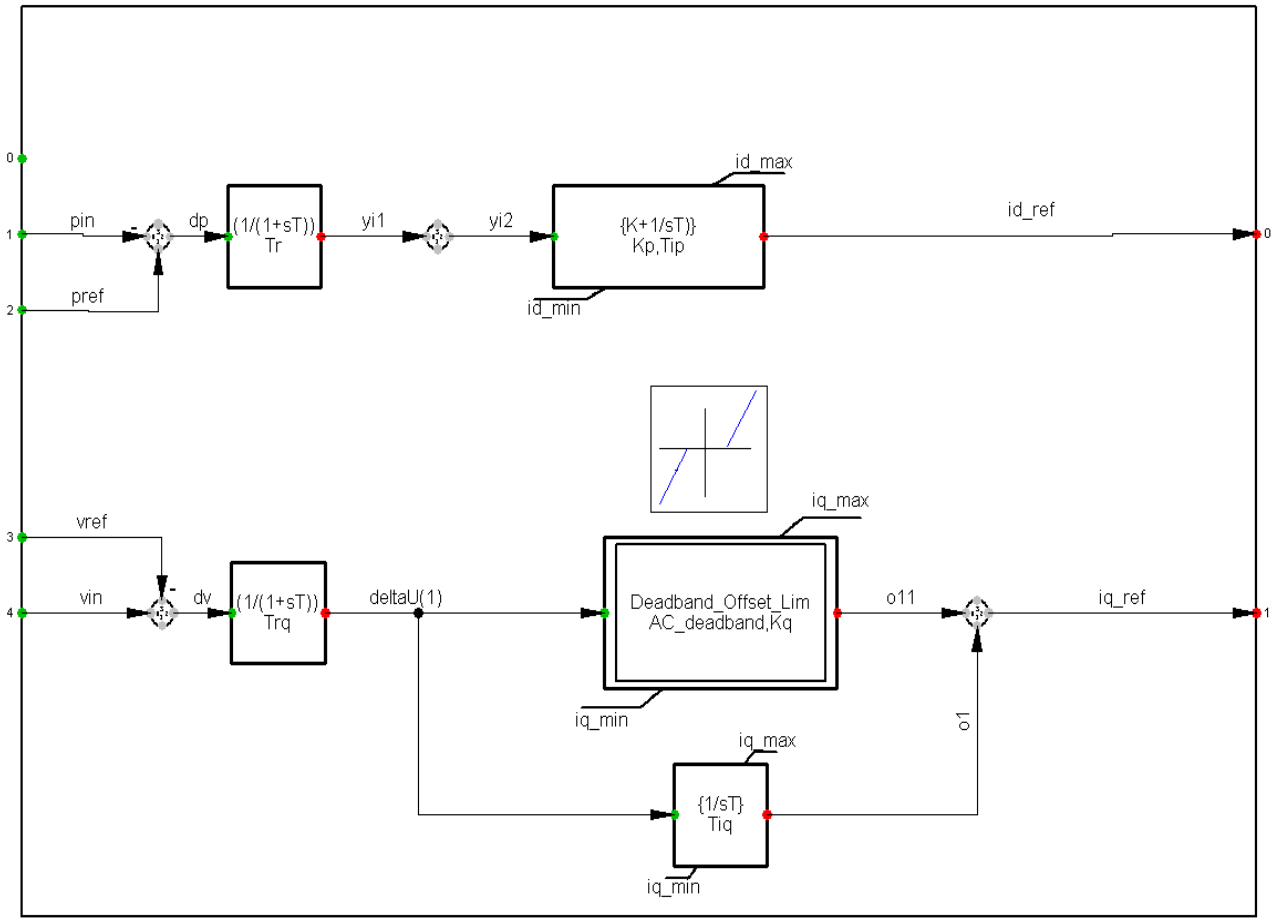

Figure 91: The PV controller used in the PowerFactory model.

12.9 PowerFactory Model of the SVC

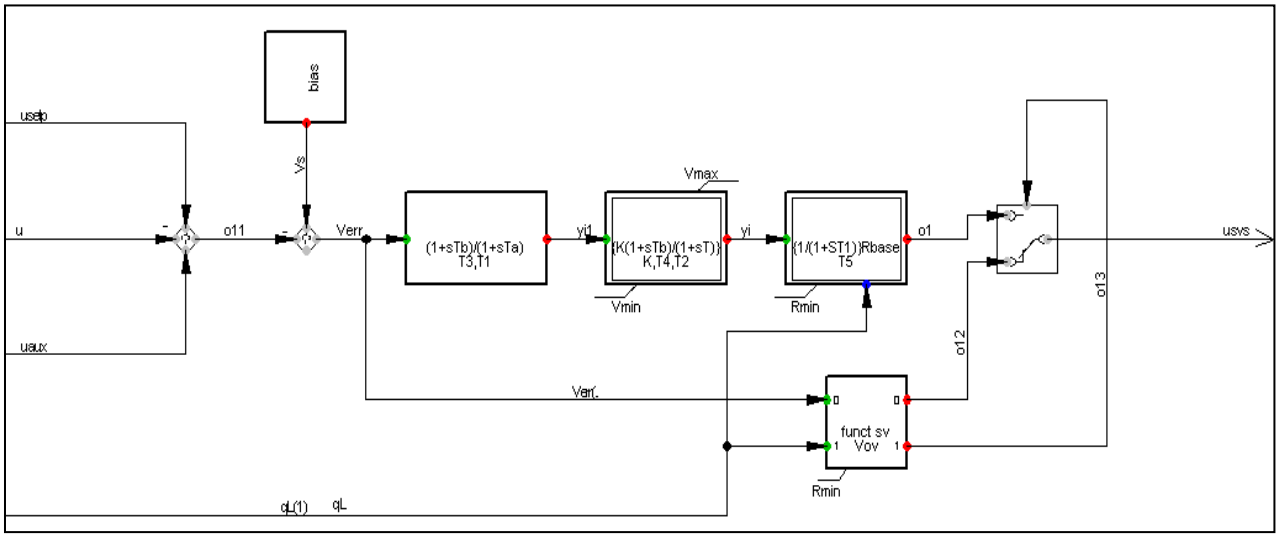

Figure 92: The control system of the SVC utilised in the PowerFactory model.

12.10 Park Transformation

In the PowerFactory model made in this thesis, d-q components are applied in the control system of the voltage source converter. The Park transformation block (see Figure 93) converts the three phase sinusoidal signal into quantities in a two-axis rotating reference frame consisting of a direct axis, a quadratic axis and a zero sequence. The three phase sinusoidal signal is represented by the phases a, b and c.

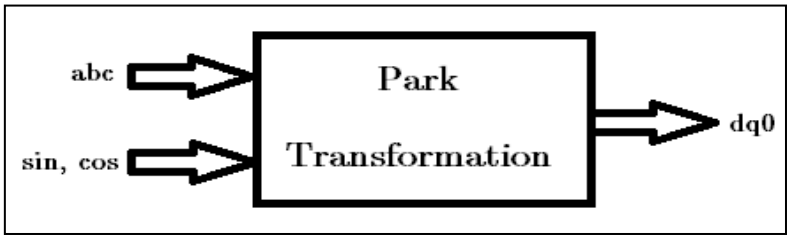

Figure 93: Park transformation block.

By solving the set of equations in the following matrix, Park transformation can be carried through:

$$\begin{bmatrix} i_q \\ i_d \\ i_0 \end{bmatrix} = \frac{2}{3}\begin{bmatrix} \sin(\omega t) & \sin(\omega t - \frac{2\pi}{3}) & \sin(\omega t + \frac{2\pi}{3}) \\ \cos(\omega t) & \cos(\omega t - \frac{2\pi}{3}) & \cos(\omega t + \frac{2\pi}{3}) \\ \frac{1}{2} & \frac{1}{2} & \frac{1}{2} \end{bmatrix}\begin{bmatrix} i_a \\ i_b \\ i_c \end{bmatrix} \quad 12.29$$

The solution of this matrix gives the following equations:

$$i_q = \frac{2}{3}(i_a \sin(\omega t) + i_b \sin\left(\omega t - \frac{2\pi}{3}\right) + i_c \sin(\omega t + \frac{2\pi}{3}) \quad 12.30$$

$$i_d = \frac{2}{3}(i_a \cos(\omega t) + i_b \cos\left(\omega t - \frac{2\pi}{3}\right) + i_c \cos(\omega t + \frac{2\pi}{3}) \quad 12.31$$

$$i_0 = \frac{1}{3}(i_a + i_b + i_c) \quad 12.32$$

The same transformation procedure can be applied for the voltage, substituting voltages for the currents. The main advantage by using Park transformed quantities is that time-varying inductances are allowed to be eliminated by referring to the stator and rotor quantities to a fixed or rotating reference frame. i_d and i_q represents the two DC currents flowing in the two equivalent rotor windings, where the q-windings are directed on the same winding as the field winding and the d-windings are directed on the quadratic axis. The magnitude and angle of the currents can be found using [52][53]:

$$|i_1| = \sqrt{i_q^2 + i_d^2} \quad 12.33$$

$$\angle i_1 = atan\left(\frac{i_q}{i_d}\right) \quad 12.34$$

12.11 Results

The following figures gives the model made in PowerFactory with various locations of the SVC.

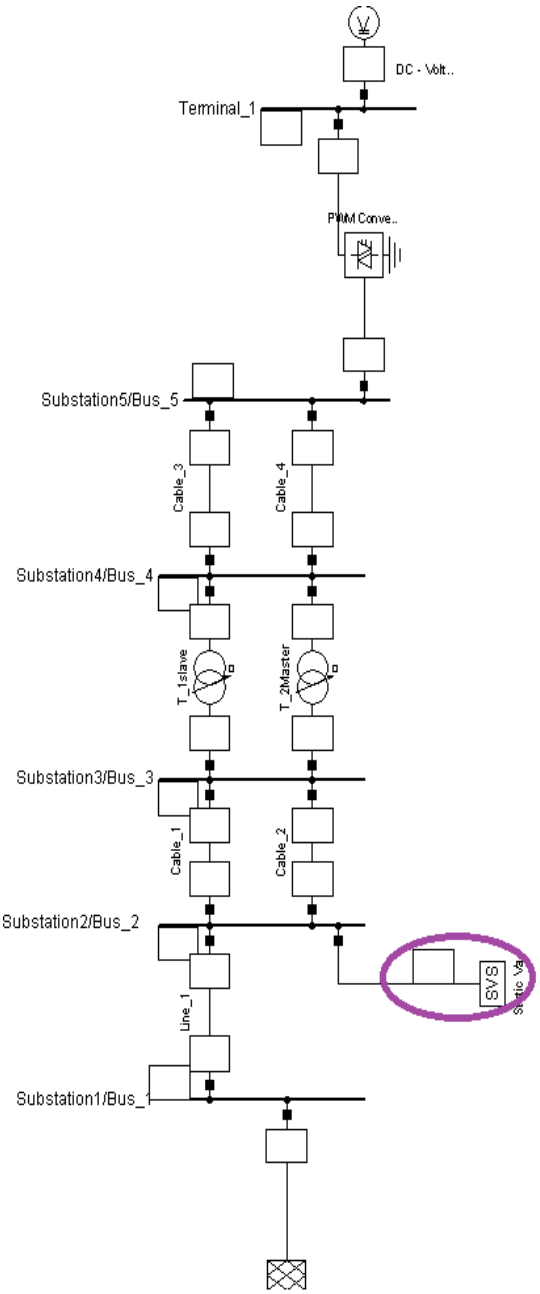

Figure 94: System model used in PowerFactory with the SVC placed onshore.

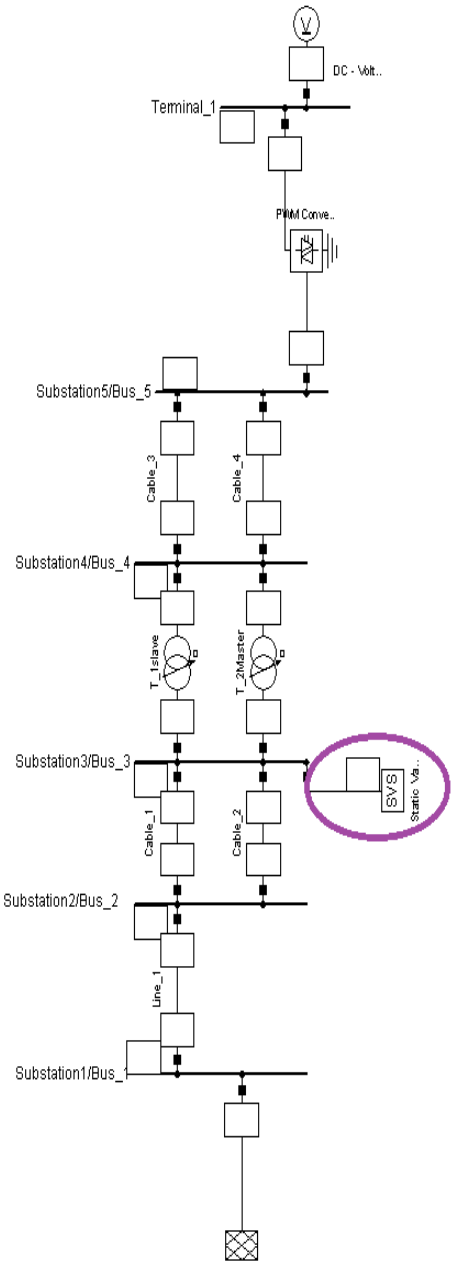

Figure 95: System model used in PowerFactory with the SVC placed offshore.

12.11.1 P-Q control of the VSC

12.11.1.1 Base case scenario

Cable length: 20 km

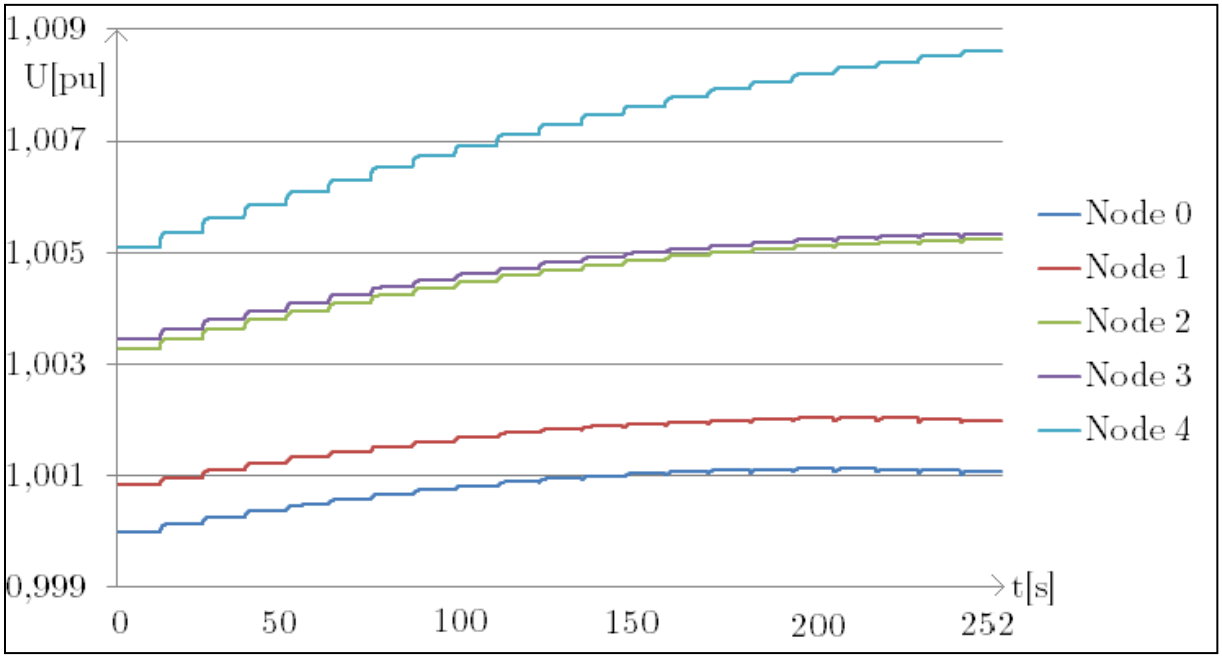

Figure 96: Voltages in the system for 20 km cables in base case.

12.11.1.2 SVC located onshore

Cable length: 100 km

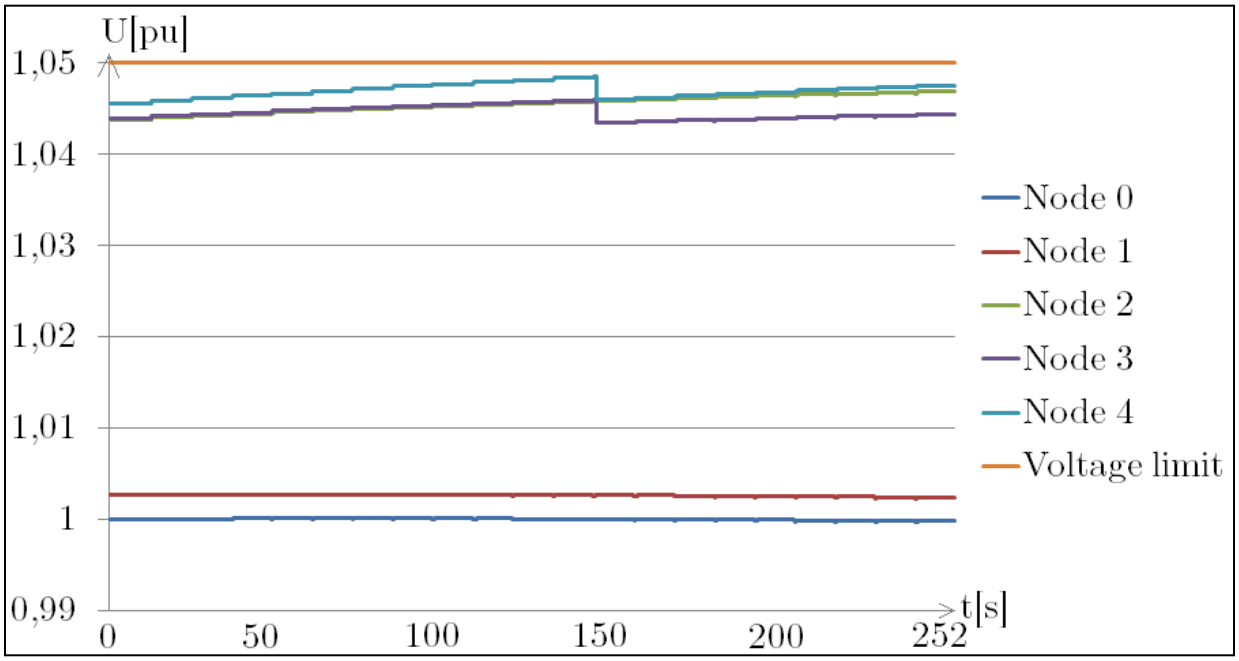

Figure 97: Voltages with the LTCs activated and the SVC onshore for 100 km cable length.

12.11.1.3 SVC placed offshore

Cable length: 40 km

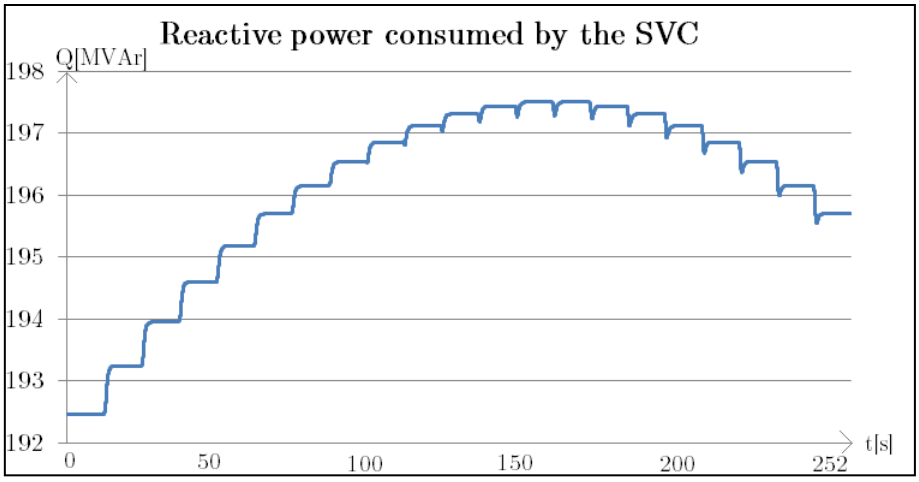

Figure 98: Reactive power consumed by the SVC offshore for 40 km long cables.

Cable length: 60 km

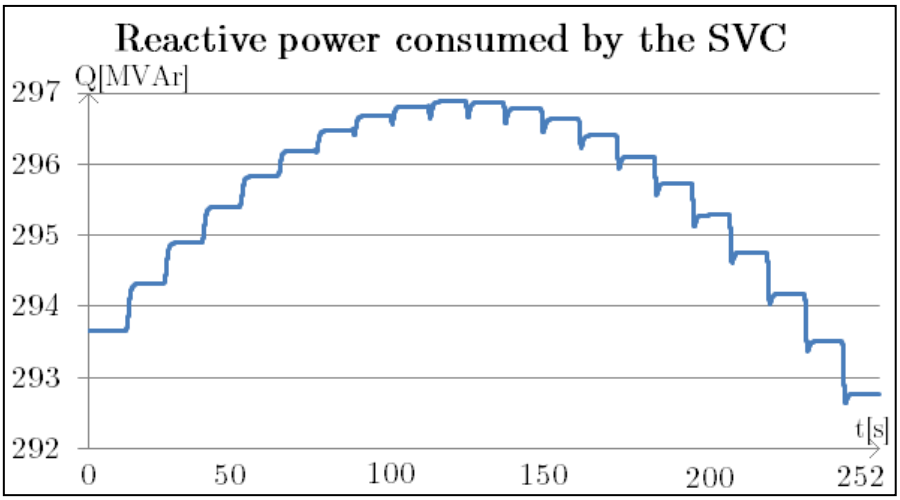

Figure 99: Reactive power consumed by the SVC offshore for 60 km long cables.

12.11.2 P-V control of the VSC

12.11.2.1 Base case

Cable length: 54 km

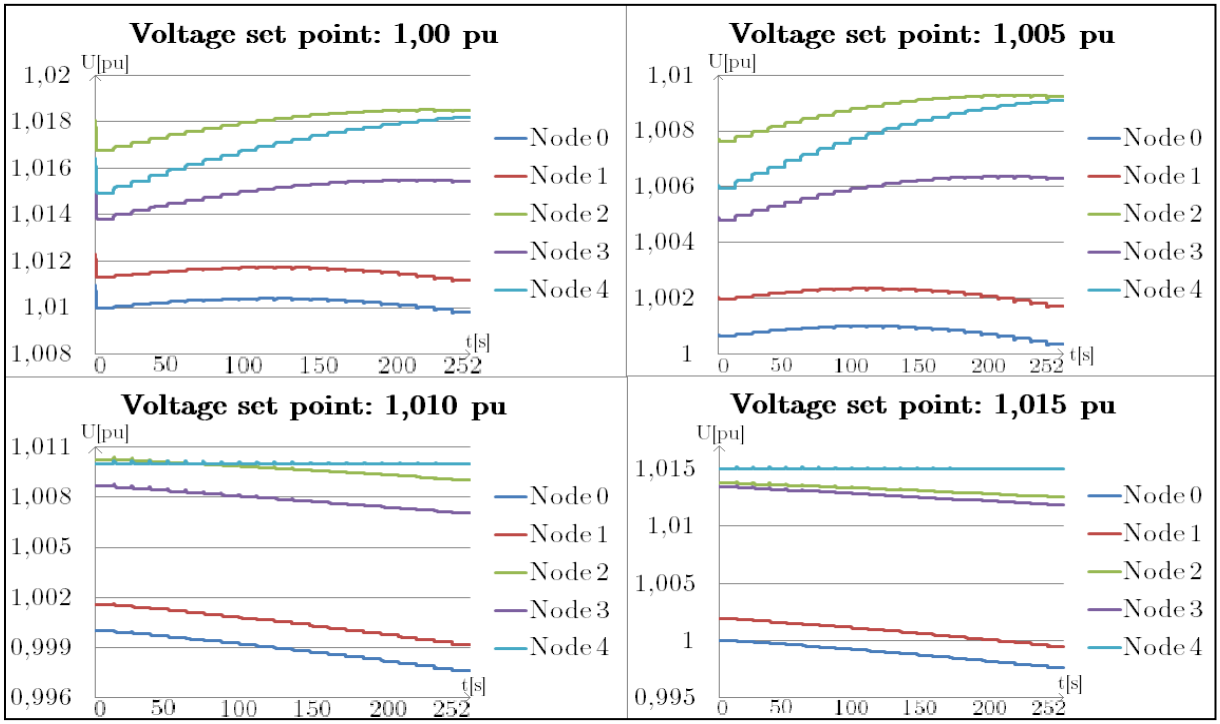

Figure 100: Voltages in the base case scenario with different voltage set points of the wind farm. Cable length: 54 km.

12.11.3 Coordination between the LTC and the SVC

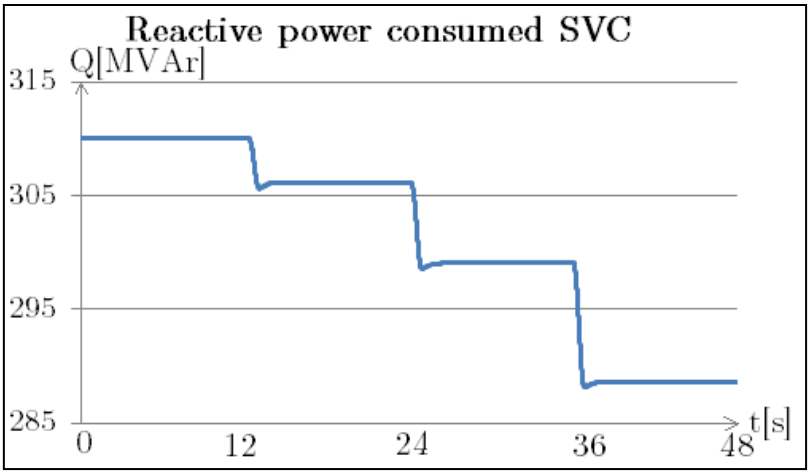

Figure 101: Reactive power consumed with the SVC offshore without the LTC.

12.11.4 Annual production and cable losses

Table 15: Overview of the wind speed, probability, active power production and losses for each operational segment.

Segment	1	2	3	4	5	6	7	8
Wind speed [m/s]	0-3,8	3,8-4	4-5	5-6	6-7	7-8	8-9	9-10
Probability (rounded)	0,131	0,013	0,072	0,079	0,084	0,084	0,082	0,077
Active power production [MW]	0	1,6	20	59,2	110,4	180,4	269,2	366,8
Average loss without SVC [MW]	0,103	0,103	0,105	0,115	0,144	0,211	0,341	0,543
Average loss with SVC [MW]	0,002	0,002	0,004	0,014	0,043	0,111	0,248	0,459

Segment	9	10	11	12	13	14	15	16
Wind speeds [m/s]	10-11	11-12	12-13	13-14	14-15	15-15,6	15,6-25	25+
Probability (rounded)	0,070	0,0618	0,053	0,045	0,0366	0,01840	0,0921	0,0023
Active power production [MW]	466,4	564	653,2	724	765,2	788,4	800	0
Average loss without SVC [MW]	0,813	1,140	1,494	1,813	2,015	2,133	2,194	0,103
Average loss with SVC [MW]	0,741	1,082	1,450	1,779	1,987	2,108	2,171	0,002

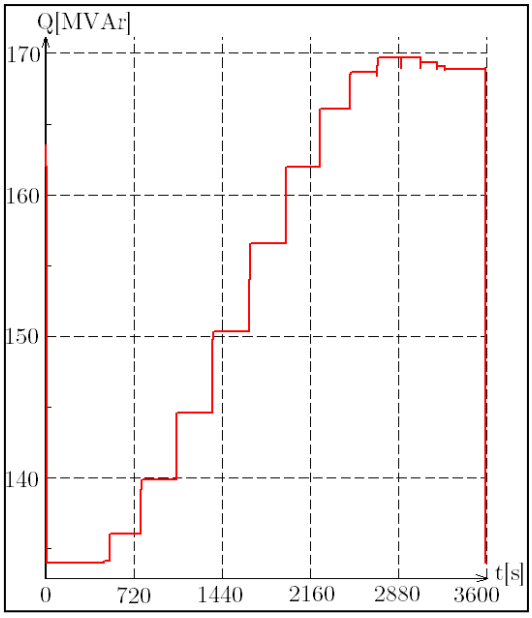

Figure 102: Reactive power consumed by the SVC offshore for annual loss calculations.